Brain-Computer Interface for Position Control of a Neuro-Prosthetic Artificial Limb

A Thesis

submitted in partial fulfilment of the requirements for

the Degree of

Master of Technology in Intelligent Automation and Robotics

in the Faculty of Engineering & Technology

Jadavpur University

May 2024

By

Deblina Pathak

Registration No: 160227 of 2021-2022

Examination Roll No: M6IAR24009

Under the Guidance of

Prof. Amit Konar

Department of Electronics & Telecommunication Engineering

Jadavpur University

Kolkata-700032

India

FACULTY OF ENGINEERING AND TECHNOLOGY

JADAVPUR UNIVERSITY

CERTIFICATE

This is to certify that the dissertation entitled "**Brain-Computer Interface for Position Control of a Neuro-Prosthetic Artificial Limb**" has been carried out by **Deblina Pathak** (University Registration No: 160227 of 2021-2022, Examination Roll No: M6IAR24009) under my guidance and supervision and accepted in partial fulfilment of the requirement for the Degree of Master of Technology in Intelligent Automation and Robotics. The research results presented in the thesis have not been included in any other paper submitted for the award of any degree to any other University or institute.

_____

Prof. Amit Konar (Supervisor)
Dept. of Electronics & Telecommunication Engineering
Jadavpur University

_____

Prof. Manotosh Biswas
Head of Department
Electronics & Telecommunication Engineering
Jadavpur University

_____

Prof. Dipak Laha
Dean, Faculty Council of Engineering and Technology
Jadavpur University

FACULTY OF ENGINEERING AND TECHNOLOGY

JADAVPUR UNIVERSITY

CERTIFICATE OF APPROVAL

The forgoing thesis is hereby approved as a creditable study of a Master of Technology subject and presented in a manner satisfactory to warrant acceptance as prerequisite to the degree for which it has been submitted. It is understood that by this approval the undersigned do not necessarily endorse or approve any statement made, opinion expressed or conclusion drawn there in but approve the thesis only for which it is submitted.

Final examination for evaluation of the thesis.

_____

Signature of Examiner

_____

Signature of Supervisor

FACULTY OF ENGINEERING AND TECHNOLOGY

JADAVPUR UNIVERSITY

DECLARATION OF ORIGINALITY AND COMPILANCE OF ACADEMIC THESIS

I hereby declare that this thesis entitled "**Brain-Computer Interface for Position Control of a Neuro-Prosthetic Artificial Limb**" contains literature survey and original research work by the undersigned candidate, as part of her Degree of Master of Technology in Intelligent Automation & Robotics.

All information has been obtained and presented in accordance with academic rules and ethical conduct.

I also declare that, as required by these rules and conduct, I have fully cited and referenced all materials and results that are not original to this work.

Name: DEBLINA PATHAK

Examination Roll No: M6IAR24009

Thesis Title: Brain-Computer Interface for Position Control of a Neuro-Prosthetic Artificial Limb

_____

Signature of the Candidate

ACKNOWLEDGEMENTS

I would like to seize this moment to extend my appreciation to all those who provided me with unwavering support during my coursework. I am deeply grateful for their invaluable mentorship, constructive feedback, and kind counsel throughout this journey.

I would like to express my earnest gratitude and heartfelt indebtedness to my advisor, Prof. Amit Konar, Department of Electronics and Telecommunication Engineering, for the privilege and the pleasure, of allowing me to work under him towards my Degree of Master of Technology in Intelligent Automation and Robotics. This work would not have been materialized, without his whole-hearted help and support. Throughout the journey of my thesis, he has been a constant source of inspiration, guiding me to overcome obstacles and navigate the challenges not only in my studies but also in my personal life. I sincerely thank my supervisor, particularly for all the faith he had in me.

I am deeply honoured to extend my heartfelt gratitude to Miss Sayantani Ghosh and Dr. Arnab Rakshit for their unconditional help, support, and valuable advices. I would also like to express my sincere respect to Prof. Manotosh Biswas, the Head of the Department of Electronics & Telecommunication Engineering at Jadavpur University, Prof. Pratyusha Rakshit, Prof Sheli Sinha Chaudhuri.

I am indebted to my classmates and friends for their constant support and good wishes and supporting me in a number of ways.

Finally, I would like to express my utmost respect and gratitude to my beloved parents, Dr. Manas Kumar Pathak and Mrs Archana Pathak as well as my younger brother Archisman for encouraging me to pursue this course and providing love, support, trust and guidance throughout my journey. Additionally, I would like to pay my respect to my late grandfather, Late Nalini Ranjan Pathak. Though he is no longer with us, his guidance and blessings have always remained in my heart, serving as a guiding light in my endeavours. I am truly blessed to have such a loving and supportive family.

LIST OF CONTENTS

CERTIFICATE i

CERTIFICATE OF APPROVAL ii

DECLARATION OF ORIGINALITY AND COMPILANCE OF ACADEMIC THESIS iii

ACKNOWLEDGEMENTS iv

CONTENTS v

LIST OF FIGURES vi

LIST OF TABLES vii

ABSTRACT viii

LITERATURE SURVEY x

CHAPTER 1 1

- **1.1 Introduction** 1
- **1.2 What is Brain-Computer Interfacing (BCI)?** 2
- **1.3 Types of BCI** 5
- **1.4 Examples of specific BCI technologies and their applications** 7
- **1.5 Commonly used Signals in EEG-BCI System** 8
- **1.6 Closed-Loop Position Control Using MI signals** 13
- **1.7 Generic Approach of Designing a Closed-loop BCI Framework** 18
- **1.8 Modules of Closed-Loop Brain-Computer Interface System** 21
- **1.9 State-of-the-art BCI-based Control Schemes** 36

CHAPTER 2 49

- **2.1 Introduction** 49
- **2.2 System Overview** 51
- **2.3 MI/ErrP Classification** 54
- **2.4 Modelling of the Proposed Brain-Actuated Speed Controller** 55
- **2.5 Analysis of Stability Margin of the Proposed Controllers** 59
- **2.6 Experiments and Results** 61

CHAPTER 3 68

- **3.1 Design of the Brain-Actuated Speed Modulator** 68
- **3.2 Matlab Simulink** 73
- **3.3 Simulink Model** 74
- **3.4 Output Plots** 75

CHAPTER 4 77

- **4.1 Future Directions and Innovations**

REFERENCES 80

LIST OF FIGURES

CHAPTER 1:

Figure 1.1: BCI system, with stimulus and response	**2**
Figure 1.2: Schematic Diagram of a Closed-loop BCI system	**3**
Figure 1.3: Different signals used in BCI along with their waveform shape and origin	**4**
Figure 1.4: Figure showing multiple traces of motor-imagery brain signal with the dotted lines. The grand average is marked with a solid line	**9**
Figure 1.5: Figure showing multiple trials of Error Related Potential (ErrP) brain patterns in dotted lines. The grand average of the trials is shown with the solid line.	**10**
Figure 1.6: Figure showing P300 brain patterns in the dotted lines. The grand average of (the trials is marked with a solid line).	**11**
Figure 1.7: Figure showing SSVEP brain patterns in the dotted lines. The grand average of the trials is marked with a solid line.	**12**
Figure 1.8: Types of brain signals used in BCI.	**13**
Figure 1.9: The closed-loop system based on brain stimulation with feedback	**14**
Figure 1.10: BCI-based complete position control scheme in 2D workspace.	**16**
Figure 1.11: BCI-based position control of a robot arm in 3D workspace.	**17**
Figure 1.12: Complete closed-loop system of BCI-based position control of a robot arm in 3-D space.	**17**
Figure 1.13: Schematic representation of Closed-loop BCI Framework 1	**20**
Figure 1.14: Schematic representation of Closed-loop BCI Framework 2	**20**
Figure 1.15: Schematic representation of Closed-loop BCI Framework 3	**21**
Figure 1.16: Schematic representation of Closed-loop BCI Framework 4	**21**
Figure 1.17: Schematic diagram of BCI-based control strategy proposed by Tariq et al	**37**
Figure 1.18: Schematic diagram of BCI-based control strategy proposed by Liu et al.	**37**
Figure 1.19: Schematic diagram of BCI-based control strategy proposed by Xu et al.	**39**
Figure 1.20: Schematic diagram of the BCI strategy proposed by Mao et al.	**43**

CHAPTER 2:

Figure 2.1: Motor on-off control by MI and ErrP signals	**51**
Figure 2.2: Schematic diagram of the 2-loop position control system	**54**
Figure 2.3: Brain Actuated Speed Modulator Model	**56**
Figure 2.4: Timing diagram of zero-crossing sensitive speed modulator	**61**
Figure 2.5: a) Block diagram of the proportional-type modulation system, **b)** Root locus for proportional type speed modulation with K = 0.3	**62**
Figure 2.6: (a) Block diagram of the zero-crossing sensitive speed modulation system, **(b)** Root locus for zero-crossing sensitive speed modulation system with $V_0 = 2$	**63**
Figure 2.8: (a) Lab-developed model of a 2-link robot arm, **(b)** Single-link position control using motor M_1	**64**
Figure 2.9: Photograph of the experimental setup for 3-link Position Control	**64**

CHAPTER 3:

Figure 3.1: Brain actuated speed modulator model	**69**
Figure 3.2: An example of the speed modulation with respect to positional error	**69**
Figure 3.3: Root Locus plot of the proposed model	**73**
Figure 3.4: Simulink Model	**74**
Figure 3.5: Step Parameters	**74**
Figure 3.6: Reference Angular Velocity Vs Time	**75**
Figure 3.7: Angular Position Vs Time	**75**
Figure 3.8: Calculated Angular Velocity Vs Time	**76**

LIST OF TABLES

Table Name	Page No
Table 1 List of features extracted from the EEG signals	66
Table 2 Classification accuracy in the training and the test phase	67
Table 3 Comparative controller performance analysis	68

ABSTRACT

Brain Computer Interface (**BCI**), sometimes called a **Brain Machine interface** (**BMI**), is a direct communication link between the brain's electrical activity and an external device, most commonly a computer or robotic limb, bypassing traditional neuromuscular routes. BCIs are often directed at researching, mapping, assisting, augmenting, or repairing human cognitive or sensory-motor functions. They are often conceptualized as a human–machine interface that skips the intermediary of moving body parts although they also raise the possibility of erasing the distinction between brain and machine.

Brain-Computer Interface (BCI) technology has emerged as a revolutionary approach for controlling neuroprosthetic devices, offering a new lease of functional independence to individuals with severe motor impairments. Sophisticated signal processing and machine learning algorithms decode these signals into precise control commands, facilitating intuitive and responsive prosthetic movement.

Current research focuses on enhancing the accuracy, reliability, and usability of BCI-controlled neuroprosthetics. Innovations in high-resolution signal acquisition, noise reduction, and real-time processing are critical to improving system performance. Integrating sensory feedback mechanisms, such as haptic feedback, is a promising area of development, aimed at providing users with real-time information about the prosthetic's interaction with the environment. This feedback is crucial for tasks requiring fine motor control and can significantly enhance the user experience by making the control of the prosthetic arm more natural and intuitive.

Personalization and adaptability of BCI systems are also key research areas, with adaptive algorithms that learn and adjust to the user’s unique neural patterns over time. The development of wireless and wearable BCI devices aims to increase mobility and ease of use, making these systems more practical for everyday applications. Additionally, interdisciplinary collaboration among neuroscientists, engineers, and clinicians is essential to advance the field, along with addressing ethical and regulatory considerations related to data privacy, user consent, and long-term impacts.

This Thesis presents a 2-loop architecture of brain-actuated position control system of a robot arm, realized with a Takagi-Sugeno type fuzzy speed modulator placed in the outer loop and a traditional speed-controller placed in the inner loop.

Chapter 1 provides a detailed review on the Brain-Computer Interface (BCI) technology. It begins with a classification BCI-based controllers, and gradually explores different types of standard BCI system along with their control policies. The different modules of a closed-loop BCI are discussed in brief with their current state-of-the-art approaches. It also provides an outline of the electroencephalography (EEG)-based brain signals commonly used in closed-loop BCI-based robot control tasks.

Chapter 2 provides a 2-loop position control scheme is proposed here with an outer loop for position control of the motor and the inner loop for speed-setting of a robotic limb. Three distinct models of brain-actuated speed-setting with possible control policies and stability analysis are presented. The analysis reveals that *Takagi–Sugeno* type fuzzy control yields the best results. Additionally, cognitive load is also reduced significantly as the user needs to generate error-related potential once only to identify the position of the targeted object he needs to translate. Traditional BCI-based position control schemes utilize acquired motor imagery signals of the subject for motor actuation and error-related potential signals to detect positional overshoots. The positional overshoot results in steady-state positional error. Current BCI research attempts to reduce steady-state errors at the cost of high cognitive load of the subjects. The motivation here is to reduce the steady-state positional error without enhancing cognitive load of the subjects.

Chapter 3 provides the designing of Brain-Actuated Speed Modulator along with the corresponding Simulink Models and plots. Finally, **Chapter 4** ends with a brief conclusion along with future scope and innovations.

The future scope of BCI-based neuroprosthetic control is vast, with the potential to significantly enhance the quality of life for individuals with disabilities. By continuing to refine the technology and addressing current challenges, BCIs can offer more precise, intuitive, and accessible solutions for neuroprosthetic control, paving the way for broader adoption and improved outcomes in clinical and everyday settings.

LITERATURE SURVEY

A **Brain-Computer Interface (BCI)** is a technology that allows direct communication between the brain and an external device. BCIs are often aimed at assisting, augmenting, or repairing human cognitive or sensory-motor functions. They have various applications, including medical, military, gaming, and other fields.

BCI was historically envisioned as a potential technology for augmenting/replacing existing neural rehabilitations or serving assistive devices controlled directly by the brain (*Vidal, 1973; Birbaumer et al., 1999; Alcaide-Aguirre et al., 2017; Shahriari et al., 2019*). The first systematic attempt to implement an electroencephalogram (EEG)-based BCI was made by *J. J. Vidal* in *1973*, who recorded the evoked electrical activity of the cerebral cortex from the intact skull using EEG (*Vidal, 1973)*, a non-invasive technique first studied in humans invented by *Berger (1929).* Another early endeavour to establish direct communication between a computer and the brain of people with severe motor impairments had utilized P300, an event related brain potential (*Farwell and Donchin, 1988*). As an alternative to conventional therapeutic rehabilitation for motor impairments, BCI technology helps to artificially augment or re-excite synaptic plasticity in affected neural circuits. By exploiting undamaged cognitive and emotional functions, BCI aims at re-establishing the link between the brain and an impaired peripheral site (*Vansteensel et al., 2016*). However, the research applications of BCI technology evolved significantly over the years, including brain fingerprinting for lie detection (*Farwell et al., 2014*), detecting drowsiness for improving human working performances (*Aricò et al., 2016; Wei et al., 2018*), estimating reaction time (*Wu et al., 2017b*), controlling virtual reality (*Vourvopoulos et al., 2019*), quadcopters (*LaFleur et al., 2013*) and video games (*Singh et al., 2020*), and driving humanoid robots (*Choi and Jo, 2013; Spataro et al., 2017*).

Key Components of a Brain-Computer Interface (BCI) System

1. **Signal Acquisition:-**

    - **Electroencephalography (EEG):-**Measures electrical activity on the scalp.
    - **Electrocorticography (ECoG):-**Measures electrical activity from the cortical surface.
    - **Functional Magnetic Resonance Imaging (fMRI):-**Measures brain activity by detecting changes associated with blood flow.

- **Near-Infrared Spectroscopy (NIRS):-**Measures brain activity by monitoring blood oxygenation levels.
- **Intracortical Neurons:-**Measures activity directly from neurons via implanted electrodes.

2. **Signal Processing:-**

- **Preprocessing:-**Removing noise and artifacts from the signals.
- **Feature Extraction:-**Identifying relevant patterns or features in the brain signals.
- **Feature Translation:-**Converting the extracted features into commands that can be understood by the external device.

3. **Application Interface:-**

- **Output Device:-**Could be a computer cursor, a robotic limb, a wheelchair, or other devices that the BCI system controls.
- **Feedback Mechanism:-**Provides real-time feedback to the user to adjust and improve control.

Applications of BCIs

1. **Medical Applications:-**

- **Neuroprosthetics:-**Restoring function for individuals with paralysis or limb loss.
- **Communication Devices:-**Helping individuals with severe motor disabilities to communicate.
- **Rehabilitation:-**Assisting in the rehabilitation of stroke patients.

2. **Non-Medical Applications:-**

- **Gaming and Entertainment:-**Enhancing immersive experiences.
- **Smart Home Control:-**Allowing individuals to control home appliances using their thoughts.
- **Education and Training:-**Enhancing learning experiences through brain-based feedback.

3. **Research:-**

- Understanding brain function and the neural basis of cognition and behaviour.
- Investigating neurological and psychiatric conditions.

BCI in Neuroprosthetics

Neuroprosthetics is an area of neuroscience concerned with neural prostheses i.e. using artificial devices to replace the function of impaired nervous systems and brain-related problems ,sensory or other organs (bladder, diaphragm, etc).As of December 2010, cochlear implants had been implanted as neuroprosthetic devices in some 736,900 people worldwide. Other neuroprosthetic devices aim to restore vision, including retinal implants. The first neuroprosthetic device, however, was the pacemaker.

The terms are sometimes used interchangeably. Neuroprosthetics and BCIs seek to achieve the same aims, such as restoring sight, hearing, movement, ability to communicate, and even cognitive function. Both use similar experimental methods and surgical techniques. Position control of a neuroprosthetic limb involves using brain signals to precisely control the movements and positioning of a prosthetic limb. This requires several components working together seamlessly: signal acquisition from the brain, signal processing, translation into commands, and control of the prosthetic limb.

Components and Process

1. **Signal Acquisition:-**
    - **Electroencephalography (EEG):-**Non-invasive method using electrodes placed on the scalp to measure brain activity.
    - **Intracortical Electrodes:-**Invasive method where electrodes are implanted directly into the brain to capture neuronal activity with high precision.
2. **Signal Processing:-**
    - **Preprocessing:-**Filtering out noise and artifacts from the raw brain signals to ensure clean data.
    - **Feature Extraction:-**Identifying and extracting relevant features from the brain signals that correlate with intended movements.
    - **Pattern Recognition:-**Using machine learning algorithms to classify these features and predict the user's intended movement.

3. **Command Translation**:-

    - Translating the processed brain signals into specific commands that the neuroprosthetic limb can understand. This involves mapping the brain activity patterns to corresponding movements of the limb (e.g., hand grasp, arm lift).

4. **Control Algorithms:-**

    - **Proportional-Derivative (PD) Control:-**A control strategy where the position of the prosthetic limb is adjusted based on the difference between the desired position and the current position.
    - **Adaptive Control:-**Adjusts control parameters in real-time based on feedback to improve performance.
    - **Machine Learning-Based Control:-** Utilizes learning algorithms to continuously improve the accuracy of the limb's movements based on user feedback.

5. **Feedback Mechanism:-**

    - **Visual Feedback:-**The user observes the limb's movements and adjusts their thoughts accordingly.
    - **Sensory Feedback:-** Advanced systems may include sensors on the prosthetic limb to provide tactile feedback to the user, improving control and intuitiveness.

Neuroprosthethic Artificial Limb

A neuroprosthetic artificial limb is an advanced prosthetic device that is controlled by brain signals, enabling individuals with limb loss or paralysis to perform movements and tasks with a high degree of precision and naturalness. This involves a complex integration of neuroscience, bioengineering, robotics, and signal processing technologies.

Key Components of Neuroprosthetic Artificial Limb

1. **Brain-Computer Interface (BCI) System:-**

    - **Signal Acquisition:-**Methods such as EEG, ECoG, or implanted electrodes capture neural signals.
    - **Signal Processing:-** Extracts meaningful features from the raw brain signals.
    - **Command Translation:-**Converts neural signals into control commands for the prosthetic limb.

2. **Prosthetic Limb Hardware:-**

    - **Actuators and Motors:-**Provide movement and control for the artificial limb.
    - **Sensors:-**Measure force, position, and sometimes temperature, providing feedback to the user.
    - **Materials:-**Lightweight, durable materials to construct the limb for ease of use and comfort.

3. **Control Algorithms:-**

    - **Proportional-Derivative (PD) Control:-**Ensures smooth and accurate movements.
    - **Adaptive Control:-**Adjusts control parameters in real-time based on feedback.
    - **Machine Learning Algorithms:-**Continuously improve control accuracy based on user interactions.

4. **Feedback Systems:-**

    - **Visual Feedback:-**User monitors limb movements visually.
    - **Haptic Feedback:-**Sensors on the limb provide tactile sensations to the user.
    - **Auditory Feedback:-**Sound cues to indicate successful movement or action.

Steps in Position Control of a Neuroprosthetic Limb

1. **Calibration:-**

    - The system is calibrated with the user by having them perform specific movements while the brain signals are recorded. This helps in creating a model that maps brain activity to limb movements.

2. **Real-Time Signal Acquisition and Processing:-**

    - Brain signals are continuously acquired and processed in real-time to extract relevant features and predict intended movements.

3. **Command Generation and Execution:-**

    - The processed signals are translated into control commands that are sent to the prosthetic limb's actuators, causing the limb to move accordingly.

4. **Feedback and Adjustment:-**

    - The system provides feedback to the user, who can then adjust their mental strategies to improve control. This feedback loop is crucial for fine-tuning the movements and achieving precise control.

Functional Workflow

1. **Signal Acquisition and Preprocessing:-**

    - Brain signals are captured through non-invasive (e.g., EEG) or invasive (e.g., intracortical electrodes) methods.
    - Noise and artifacts are filtered out to obtain clean signals.

2. **Feature Extraction and Pattern Recognition:-**

    - Relevant features (e.g., specific brainwave patterns) are extracted from the processed signals.
    - Machine learning algorithms classify these patterns to predict the user's intended movements.

3. **Command Generation:-**

    - Classified patterns are translated into specific commands that the prosthetic limb can execute.
    - Commands are sent to the prosthetic limb's actuators to perform the intended movements.

4. **Movement Execution and Feedback:-**

    - The prosthetic limb moves according to the received commands.
    - Feedback from the limb's sensors (e.g., force, position) is sent back to the user, allowing them to make adjustments.

Applications

1. **Restoring Mobility:-**

    - Enables individuals with amputations or paralysis to regain the ability to perform daily tasks, such as grasping objects, walking, or typing.

2. **Rehabilitation:-**

    - Used in therapeutic settings to help patients recover motor functions after neurological injuries, such as stroke.

3. **Research and Development:-**

    - Enhances understanding of neural control of movement and aids in the development of more advanced neuroprosthetic technologies.

Challenges and Solutions

1. **Signal Quality and Stability**:-

    - **Challenge:-**Neural signals can be noisy and unstable over time.
    - **Solution:-**Use advanced signal processing techniques and adaptive algorithms to maintain signal quality.

2. **Latency:-**

    - **Challenge:-**Delays between brain signal generation and limb movement can hinder natural control.
    - **Solution:-**Optimize hardware and software to minimize latency.

3. **User Training and Adaptation:-**

    - **Challenge:-**Users need time to learn how to control the prosthetic limb effectively.
    - **Solution:-**Develop intuitive interfaces and provide comprehensive training programs.

4. **Invasiveness and Safety:-**

    - **Challenge:-**Invasive methods (e.g. implanted electrodes) pose surgical risks.
    - **Solution:-**Develop less invasive methods and enhance safety protocols for invasive procedures.

5. **Ethical and Privacy Concerns:-**

    - **Challenge:-**Protecting user data and ensuring ethical use of neuroprosthetic technologies.
    - **Solution:-**Implement robust data protection measures and ethical guidelines.

Future Directions

1. **Improved Non-Invasive Interfaces:-**

    - Development of more effective non-invasive methods for capturing brain signals, such as advanced EEG caps.

2. **Integration with Advanced AI:-**

    - Leveraging artificial intelligence to improve the accuracy and adaptability of neuroprosthetic limbs.

3. **Enhanced Sensory Feedback:-**

    - Developing more sophisticated haptic feedback systems to provide users with a more natural sense of touch and proprioception.

4. **Miniaturization and Portability:-**

    - Making neuroprosthetic systems more compact and portable for everyday use.

5. **Long-Term Stability and Biocompatibility:-**

    - Ensuring that implanted components are stable and biocompatible over long periods.

BCIs hold tremendous potential for transforming many aspects of human life, from medical care to daily living activities, and continuous advancements in technology and research are driving this field forward. Neuroprosthetic artificial limbs represent a significant advancement in prosthetic technology, offering individuals with limb loss or paralysis the potential to regain functional independence. By addressing various challenges discussed above and continuously improving the technology, the position control of neuroprosthetic limbs can significantly enhance the quality of life for individuals with limb loss or paralysis. Continuous improvements in neuroscience, bioengineering, and AI are driving this field forward, promising even more sophisticated and user-friendly solutions in the future.

CHAPTER 1

REVIEW ON BRAIN COMPUTER INTERFACE

1.1 Introduction

Human brain comprises several trillions of neurons connected in tandem and parallel to serve as the basic infrastructure of knowledge/information processing. Although the complete picture of brain functionality remained a mystery to this date, there remains evidence of local processing of signals pertaining to perception, memory and learning, and motor control and coordination by specific regions/lobes of the brain. It is noted that neurons engaged in processing different cognitive tasks had evolutions over several decades to specialize themselves in handling the selected tasks. For instance, neurons responsible for processing olfactory signals usually have long axonal lengths to carry messages to the olfactory bulbs from the receptor end [1]. In contrast, the neurons participating in memory tasks are relatively small in length to carry messages for storing in the Long-Term Memory (LTM) from the Working Memory (WM) [2]. The motor cortex in the human brain takes the responsibility to generate the necessary commands for voluntary actuation and/or control of the motor actions intended by the subject. The Parietal lobe also has an important role in planning the intended motor action. In fact, there exists coordination between the Parietal lobe and the motor cortex to plan and execute a motor task [3]. In the present research, we emphasize greatly the decoding of motor actions. Such decoding is needed to execute the intended motor task by an artificial robotic limb. Several strategies of BCI-based motor control are available in the literature. We would discuss them in detail in a subsequent section. Capturing the motor planning and motor execution requires brain-signal acquisition equipment. Different modalities of brain signal/image acquisition techniques are available in the literature. A few of these that deserve mentioning include electroencephalography (EEG), functional Magnetic Resonance Imaging (f-MRI), Positron Emission Tomography (PET),

functional Near Infrared Spectroscopy (f-NIRS) and Electrocorticography (ECOG). EEG is preferred to other brain signal/image acquisition devices for its excellent temporal response, portability, and low cost, and above all its non-invasive characteristics. In this thesis, we would restrict ourselves to examining the response of BCI-driven motor activations using the EEG modality.

1.2 What is Brain-Computer Interfacing (BCI)?

Brain-Computer Interfacing (BCI) refers to interfacing the human/animal brain with a computer, bypassing the muscular pathways of communication, to understand and decode brain activity by the computer. The primary contribution of this technology lies in the field of rehabilitation and mainly focuses on controlling robotic prostheses with mental commands. However, there are other valuable contributions also, such as the development of a BCI-based virtual keyboard [4][5], wheelchair control [6][7], BC1-based gaming [8][9], etc. The use of BCI in rehabilitation was designed to enhance the quality of life for individuals experiencing various conditions, including complete or partial paralysis, motor difficulties associated with locked in syndrome, cerebral palsy Amyotrophic Lateral Sclerosis (ALS), amputations, and cranium trauma.

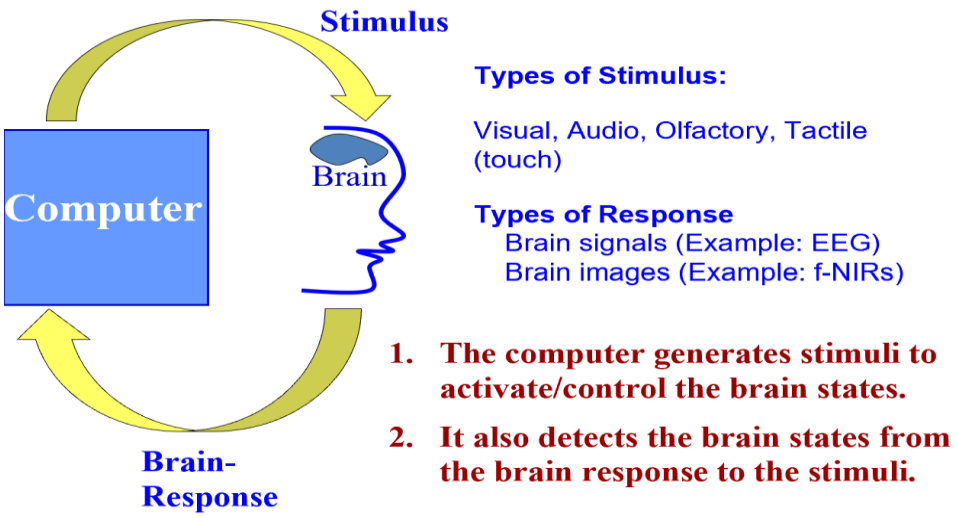


Figure 1.1: BCI system, with stimulus and response

BCI systems are of 2 common types: Open-loop systems and Closed-loop systems. In an open-loop BCI, the subject either by being stimulated externally or by mentally imagined cognitive tasks releases certain brain signals, which are used up by the associated system as open-loop control signals/commands. These open-loop control signals/commands may activate a relay or a switch to perform the desired task. In the open-loop system, the external state of the controlled agent does not influence the current brain state of the subject.

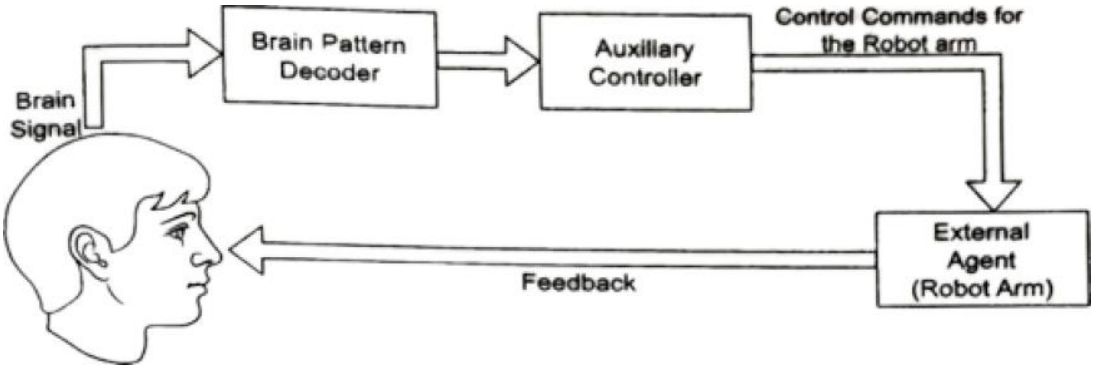


Figure 1.2: Schematic Diagram of a Closed-loop BCI system

In a closed-loop BCI, a feedback measure of the targeted action is generated by suitable sensors to offer necessary feedback to the subject to assist him in moderating his decisions to release necessary brain-actuated commands in the next time slot. Hence the control action of the human subject is influenced by the present state of the external device. As an example, a subject controlling a robotic arm receives visual feedback about the position of the end-effector in a closed-loop system. Such feedback establishes a both-way communication between the human and the external agent, which is proven to be highly useful to treat severe neurological disorders like depression, epilepsy, Parkinson's disease, and obsessive-compulsive disorder (OCD) by stimulating a part of the brain based on feedback.

Apart from medical use, the neuro-feedback signal has also got widespread usage in robotic prosthesis control as it enables the human subject to determine how well he/she can control the robot and reach the desired target and participate in the task interactively. It also enables them to take corrective action in case an error occurs. The additional information in terms of the feedback signal has the capability to alter the brain state of the human subject to

achieve the desired performance. A schematic overview of a general closed-loop system is given in Figure 1.2.

Literature shows that various types of feedback have been used to provide additional information about the external agent to the operating subject. Such feedback includes visual feedback, vibrotactile feedback, electrical or magnetic stimulation, and optogenetic and sonogenetic feedback. Among them, visual feedback is the simplest yet powerful form of feedback, hence the current thesis considers visual feedback for designing the closed-loop Brain-machine Interface. The visual feedback is incorporated into the system through different modalities like P300, SSVEP, and ErrP brain patterns, which are utilized here to design the brain-actuated controller to actuate the robot arm with the user intent.

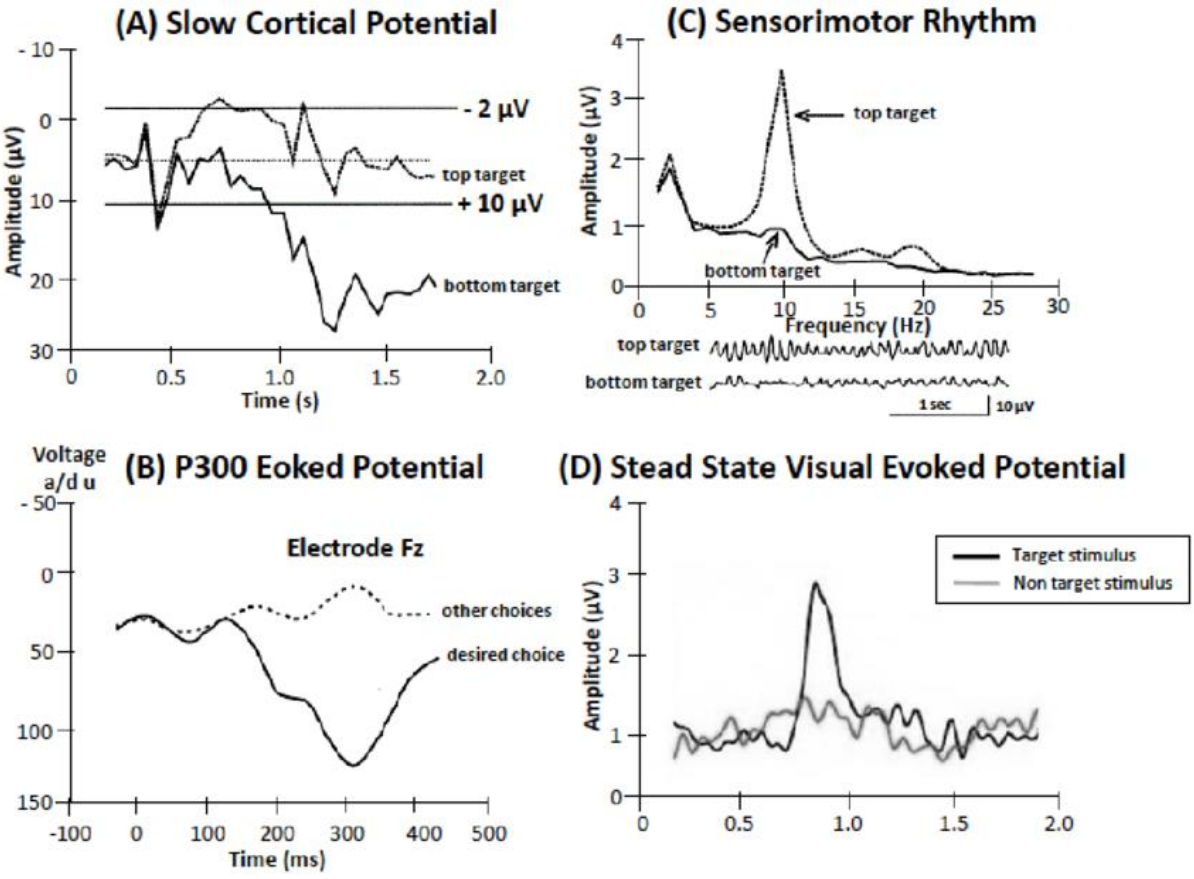


Figure 1.3: Different signals used in BCI along with their waveform shape and origin.

1.3 Types of BCI

Brain-Computer Interfaces (BCIs) can be classified based on several criteria, including the type of signal acquisition method, the application, the direction of communication (input/output), and the level of invasiveness.

Here are the main types of BCIs:

1.3.1 Based on Signal Acquisition Method

1. **Electroencephalography (EEG):-**

   - **Non-invasive:** Uses electrodes placed on the scalp to measure electrical activity of the brain.
   - **Applications:** Communication aids, gaming, neurofeedback, rehabilitation.

2. **Magnetoencephalography (MEG):-**

   - **Non-invasive:** Measures magnetic fields produced by neural activity.
   - **Applications:** Research applications, some clinical uses.

3. **Functional Magnetic Resonance Imaging (fMRI):-**

   - **Non-invasive:** Measures brain activity by detecting changes in blood flow.
   - **Applications:** Research, some clinical applications, understanding brain functions.

4. **Near-Infrared Spectroscopy (NIRS):-**

   - **Non-invasive:** Uses infrared light to measure brain activity by monitoring blood oxygenation.
   - **Applications:** Research, brain-computer communication.

5. **Electrocorticography (ECoG):-**

   - **Partially invasive:** Electrodes are placed on the surface of the brain, under the skull.
   - **Applications:** Medical research, epilepsy monitoring, advanced neuroprosthetics.

6. **Intracortical Neuron Recording:-**

   - **Invasive:** Electrodes are implanted directly into the brain tissue to record neuronal activity.
   - **Applications:** Advanced neuroprosthetics, deep brain research

1.3.2 Based on Application

1. **Communication BCIs:-**
    - Enables individuals with severe motor impairments to communicate by translating brain signals into text or speech.
    - Examples: P300 speller, motor imagery-based communication systems.
2. **Control BCIs:-**
    - Allows users to control external devices such as computers, wheelchairs, or robotic arms.
    - Examples: EEG-based cursor control, robotic limb control.
3. **Therapeutic BCIs:-**
    - Used for rehabilitation purposes, particularly for stroke or spinal cord injury recovery.
    - Examples: BCIs for motor rehabilitation, neurofeedback systems.
4. **Entertainment BCIs:-**
    - Used in gaming and virtual reality to enhance user experience.
    - Examples: BCI-controlled video games, VR environments.
5. **Research BCIs:-**
    - Employed in neuroscience and psychology research to understand brain function and cognition.
    - Examples: BCIs used in cognitive neuroscience studies, brain mapping.

1.3.3 Based on Direction of Communication

1. **Active BCIs:-**
    - Require active, conscious effort from the user to generate brain signals.
    - Examples: Motor imagery BCIs, P300-based BCIs.
2. **Reactive BCIs:-**
    - Respond to specific stimuli without requiring active user effort, relying on brain's automatic responses.

- Examples: Steady-state visual evoked potentials (SSVEP) BCIs, auditory evoked potentials.

3. **Passive BCIs:-**

- Monitor brain activity without any direct intent to control, often used for assessing cognitive or emotional states.
- Examples: BCIs for monitoring workload or attention, affective computing.

1.3.4 Based on Level of Invasiveness

1. **Non-Invasive BCIs:-**

- No surgery required, electrodes placed on the scalp or use external devices.
- Examples: EEG, MEG, NIRS.

2. **Partially Invasive BCIs:-**

- Requires minor surgery, electrodes placed on the surface of the brain but not penetrating brain tissue.
- Examples: Electrocorticography (ECoG).

3. **Invasive BCIs:-**

- Requires surgery to implant electrodes directly into brain tissue.
- Examples: Intracortical neuron recording, deep brain stimulation (DBS).

1.4 Examples of specific BCI technologies and their applications

1. **EEG-Based BCIs:-**

- **Motor Imagery BCI:** Users imagine specific movements to control devices. Used in rehabilitation and control of prosthetic limbs.
- **P300 Speller:** Utilizes the P300 wave, an event-related potential elicited in the brain's parietal lobe, to help users select letters or commands. Used for communication by individuals with severe motor disabilities.
- **SSVEP BCI:** Based on brain's response to visual stimuli flickering at different frequencies. Used for controlling computer interfaces and devices.

2. **MEG-Based BCIs:-**

- Primarily used in research due to its high spatial resolution in mapping brain activity. Useful in understanding complex neural networks and brain functions.

3. **fMRI-Based BCIs:-**

    - Applied in neurofeedback and research to understand brain activity patterns associated with specific tasks or stimuli. Limited use in real-time applications due to the size and cost of the equipment.

4. **NIRS-Based BCIs:-**

    - Used for communication and control applications, especially where portability is important. Offers a compromise between non-invasiveness and signal quality.

5. **ECoG-Based BCIs:-**

    - Provides higher signal quality than non-invasive methods and is used in clinical settings for monitoring and controlling epileptic seizures, as well as in advanced neuroprosthetics.

6. **Intracortical BCIs:-**

    - Offers the highest signal fidelity and used in cutting-edge neuroprosthetic applications, allowing for precise control of robotic limbs. These BCIs have been successfully used in research projects to help paralyzed individuals control robotic arms with high precision.

1.5 Commonly used Signals in EEG-BCI System

There exist quite a few brain signals which are used to design different BCI-based systems, among them Motor Imagery (MI) signal, P300, ErrP, and Steady-state visual Evoked potentials are widely used in EEG-based BCI systems for their high detection accuracy through EEG. Figure 1.3 provides a ready reference of the commonly used BCI signals and their origin and shape.

A details description of the signals is given below.

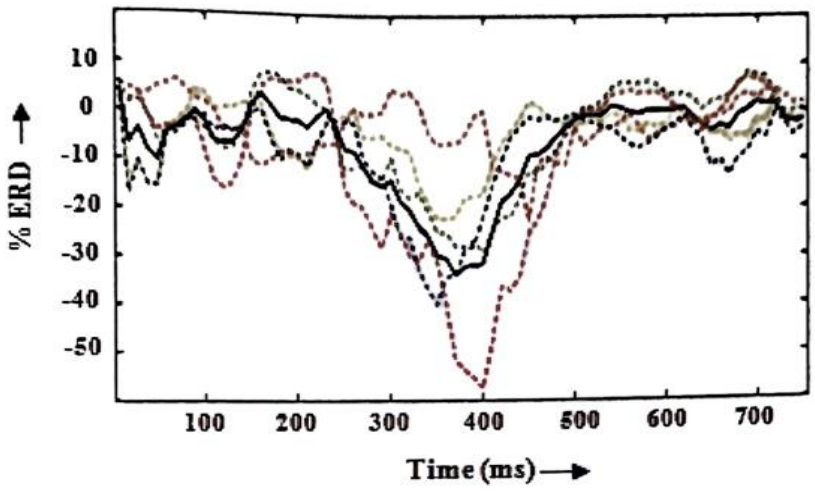
1.5.1 Motor Imagery Signal

When a person undertakes imagination about the movement of his voluntarily controllable body parts/organs, such as upper and lower limbs, jaws, etc., the process is referred to as motor imagination, and the imagined item is often called motor imagery (MI). On the other hand, when a person executes the movement of his voluntarily controllable organs, the process is referred to as motor execution (ME). It is apparent from the BCI literature

[10] that during both motor imagination and execution phases, the human brain releases a specialized Event-Related Potential (ERP), which primarily has two main temporal segments. The first component, called Event-Related De-Synchronization (ERD), which lies in the Rolandic Mu band (8-12 Hz) and beta band (13-19 Hz) appears on-screen as a waveform of gradually diminishing amplitude. The ERD originates in the Parietal lobe during motor imagination with a peak at the $\mathbf{P_z}$ electrode and also from the Motor Cortex region during the motor execution phase with a peak at $\mathbf{C_z}$ electrode.

The second segment, called Event Related Synchronization (ERS) signal, which appears in the beta band (13-18 HZ), originates from the motor cortex (Parietal lobe) and is released after motor execution (imagination) is stopped. The ERS signal exhibits a gradually increasing power until the previous power level that appeared before the occurrence of ERD is restored. The ERD-ERS together looks like a v-type of signal with a peak at the left motor cortex for the Right-Hand Motor Imagery or Execution (RHMI or RHME) and a peak at the Right Motor Cortex for the Left-Hand Motor Imagery or Execution (LHME). This is due to the inherent contra-lateral connection between our brain and the body. In most of the BCI literature that employs ERD/ERS signals, MI/ME are undertaken for open-loop control of an external device, such as a robotic car [11][12][13], artificial robotic link [14], and the like. In recent times, researchers have shown keen interest to develop closed-loop position control applications for a robot arm by employing one additional signal along with ERD/ERS.

Figure 1.4: Figure showing multiple traces of motor-imagery brain signal with the dotted lines. The grand average is marked with a solid line.



1.5.2 ErrP Signal

In a BCI-based robotic device control application, the additional signal used in conjunction with ERD/ERS is Error-Related Potential (ErrP) and P300. The ErrP signal is used to detect the occurrence of a positional overshoot around a given target position. The subjects are expected to liberate ErrP signal when they observe any person or a robotic device committing any error or they themselves commit any error. The signal can be thought of as the response of the brain to an erroneous action.

The ErrP brain signal is characterized by the occurrence of Error Related negativity followed by Error Related Positivity (Pe). ERN [15] is a sharp negative going peak that is generated around 50-100ms after the subject observes/commits any error. On the other hand, Error Related Positivity is a positive going peak that appears right after the ERN [16].

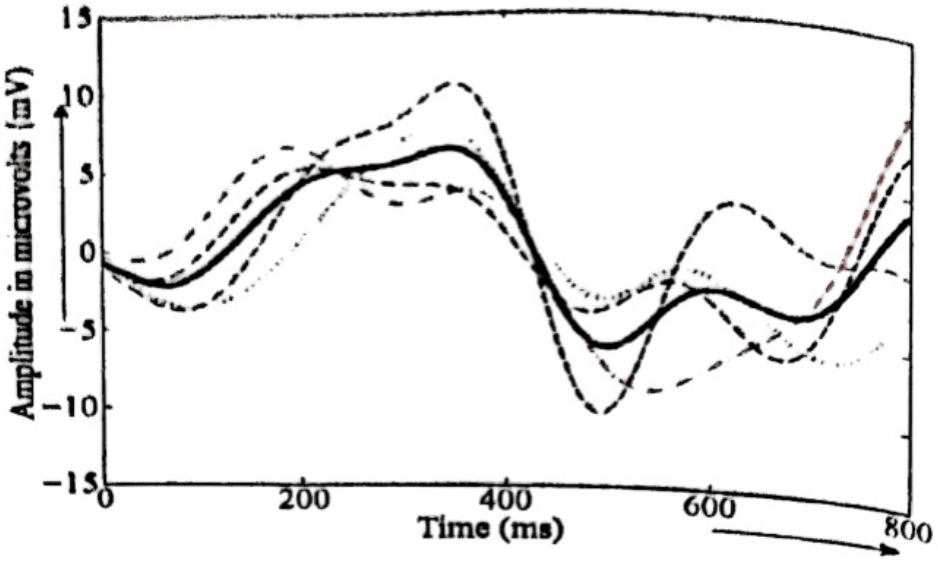


Figure 1.5: Figure showing multiple trials of Error Related Potential (ErrP) brain patterns in dotted lines. The grand average of the trials is shown with the solid line.

The Pe can be further categorized into two components: frontocentral and centroparietal.

The frontocentral Pe, which is associated with the P3a, emerges immediately following the ERN (error-related negativity). On the other hand, the late Pe occurs in the centroparietal region and has a latency of 200-400 ms after the error. This late Pe component appears to be linked to the P3b [17]. Figure l.5 shows the multiple traces of the ErrP signal and their grand average.

1.5.3 P300 Signal

Another important signal used in BCI is the oddball signal which is commonly known as P300. Such brain signal is generated as a response to odd, rare, or infrequent stimuli [18]. When a subject recognizes any rare or odd stimulus, a positive going peak after approximately 300ms of onset of the stimulus is generated over the parietal, central, and frontal regions of the brain and mainly distributed over the "z" lines of electrodes i.e., P_z, C_z, and F_z.

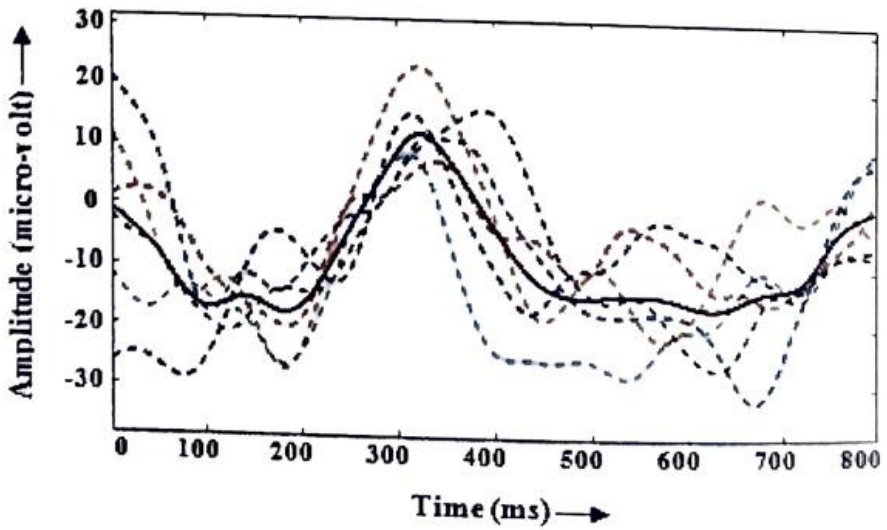


Figure 1.6: Figure showing P300 brain patterns in the dotted lines. The grand average of (the trials is marked with a solid line).

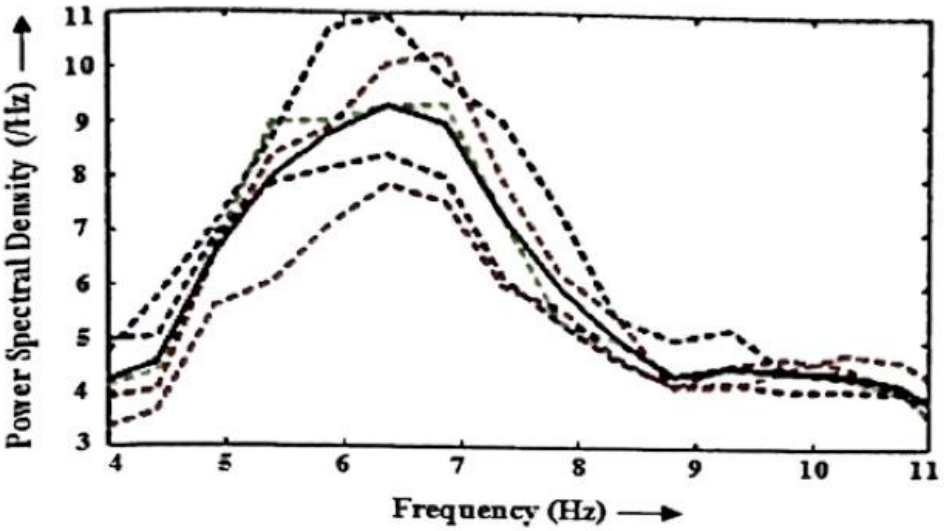


Figure 1.7: Figure showing SSVEP brain patterns in the dotted lines. The grand average of the trials is marked with a solid line.

However, the signal amplitude is highest in the P_z electrode and gradually attenuates with the distance over the scalp. The latency of the P300 signal usually varies between 250-750ms. The P300 signal, which usually responds to an oddball stimulus, here has been utilised to check the possible overshoot of the end-effector of a robot arm around a given target position. A typical P300 waveform is presented in Figure 1.6.

1.5.4 Steady-State Visual Evoked Potential

The third important class of signal is Steady-state visual evoked potential. Such a signal is generated as a response of the brain to repetitive visual stimuli. It is observed that a subject when perceives repetitive visual stimuli or gazes at flickering sources (such as flickering LED), a particular brain pattern modulated by the fundamental source frequency is generated in the primary visual cortex of the brain, which is popularly known as SSVEP. SSVEP along with the source frequency also contains the harmonics of the source frequency, however, their amplitude is relatively low. The frequency of the visual source stimulus ranges between 3.5Hz - 75Hz. The SSVEP signal has been extensively used in BCI for its high recognition rate and high information transfer rate. Another major advantage of using SSVEP is the minimum subject preparation time compared to the other modalities such as MI, ErrP, etc. SSVEP signal (in response to 6.5Hz flickering frequency) of multiple subjects is presented in

Figure 1.7. It is evident from the figure that the signal has the highest amplitude near 6.5Hz frequency which is the frequency of the source stimulus.

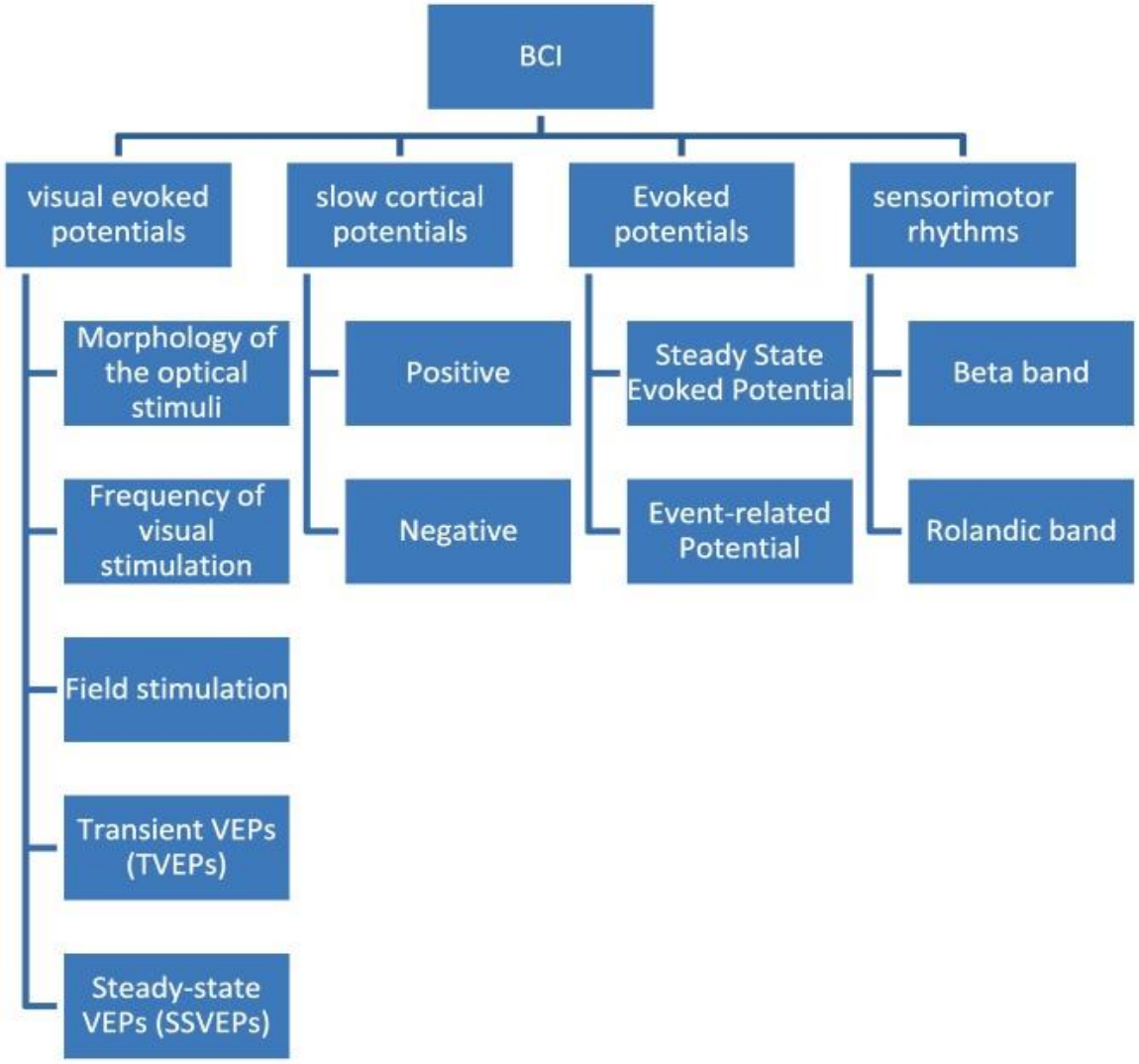


Figure 1.8: Types of brain signals used in BCI.

1.6 Closed-Loop Position Control Using MI signals

The most advanced BCI systems use “closed-loop” strategies in which the implanted devices have in-built read–response mechanisms and embedded algorithms that automatically adjust simulation-related factors to match the patient's needs. These devices sense the composition of the patient and stimulate signals only when required, thereby reducing the side-effects during treatment. This can help conserve power and thus minimize battery replacement surgeries. These systems profoundly impact the clinical pathways of patients with complex

nervous system diseases. This strategy has been used for mobility assistance—for example, for wheelchair control or rehabilitation purposes, such as for controlling an electrical stimulator.

A closed-loop BCI system usually involves a control paradigm, measurement, processing, prediction, and feedback from the application as shown in Figure 1.9. These functions help understand or modulate the user's mental condition or intention. The system uses these data to execute some predefined functions to interact with the environment by seeing, hearing, or sensing the action. An external device provides communication and neurofeedback, which enables the user to determine how well they can control the device. Closed-loop BCI can signal to the brain (e.g., through feedback *via* electrical/magnetic stimulation, and optogenetic and sonogenetic techniques) to correct the action or obtain additional information about it.

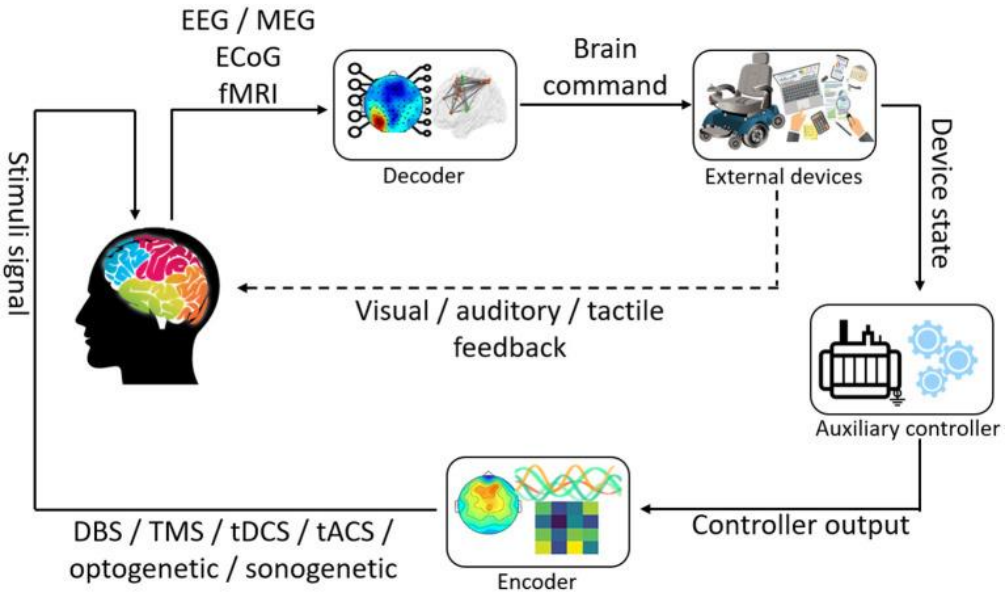


Figure 1.9: The closed-loop system based on brain stimulation with feedback

The control paradigm is the input provided by the BCI user to generate brain signals related to their intent. The user generates this input *via* mental tasks, including the kinematical/visual imagining of the physical movement of a body part, or by concentrating on a specific object to generate a P300 wave. Some BCI systems (e.g., affective BCI) do not require the users' intentions. Still, they function by identifying the emotional and mental statuses of the user,

and can be active, reactive, or passive. In any case, these generated signals must be measured *via* invasive or non-invasive techniques. Invasive techniques, including ECoG, microelectrode arrays, and single microelectrodes, can detect signals from the brain's surface and produce high-quality signals. However, these techniques require risky implantation surgeries.

Therefore, BCI research commonly uses non-invasive methods to detect signals (e.g., magnetoencephalography and functional-magnetic resonance imaging). EEG is the most popular and preferred technique in this regard (*Nicolas-Alonso and Gomez-Gil, 2012*) as it is economical and portable, and can even be measured by using wireless devices. The most popular closed-loop BCI is the one based on motor imagery, where the disabled can receive a piece of additional sensory information from the BCI device. This BCI-based control system of closed-loop brain stimulation can help sense the effect of a stimulus and adjust this stimulation in response to the observed effect. The closed-loop BCI can be used to create synaptic plasticity through spike-triggered stimulation.

In closed-loop position control applications, we often come across a feedback signal for automatic detection of zero positional error with respect to a desired step input of the angular position command. The ErrP used in the present context, often referred to as observational ErrP, is elicited from the medial frontal region with a negative deflection of approximately 250 ms after the subject observes a machine (or a person) to commit errors. Here, committing an error refers to crossing the desired angular position/set-point of the position-control experiment. ErrP, in general, is a reliable feedback signal. However, its magnitude is diminished in subjects with spinal cord injury and schizophrenic disorders [19][20]. ErrP amplitude and latency also suffers from inter-subject and inter-trial variability. Lastly, ErrP is best elicited with discrete events. Here, the robot motion is continuous which makes the ErrP signal less suited to being used as feedback marker. Because of the above limitations of ErrP, we prefer to use P300, which is released approximately 300 ms from the onset of positional zero-crossing errors, experienced by the subject.

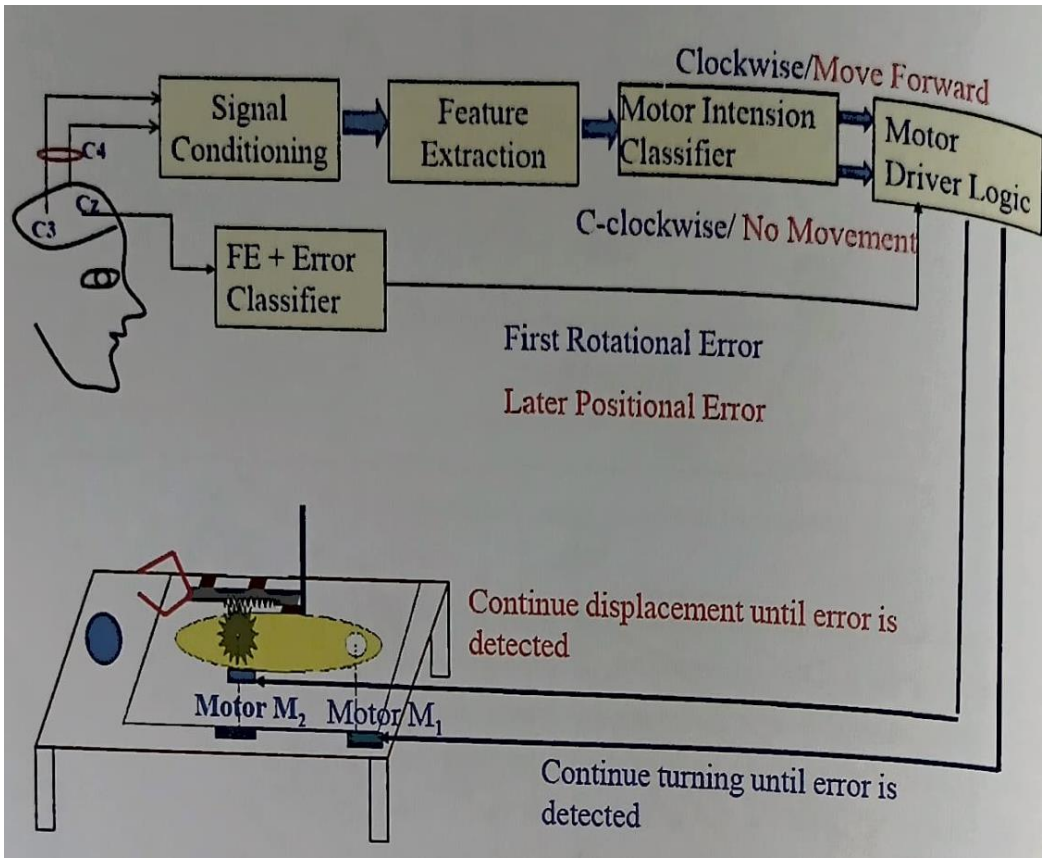


Figure 1.10: BCI-based complete position control scheme in 2D workspace.

The position of a robot's end-effecter in 3D space is shown in below Figure 1.10. The robot arm used here has 6-degrees of freedom (DOF) with the maximum reach of 580 mm in any arbitrary direction. The frame assignments for all the joints along with the directions of positive angular motions are shown in Figure 1.11.

The current work uses only the first three links, L1, L2, and L3, of the robot arm. Figure 1.12 illustrates the complete position control scheme. Three different brain signals, including SSVEP, ERD/ERS, and P300 are employed here to control the position of the robot arm in its workspace.

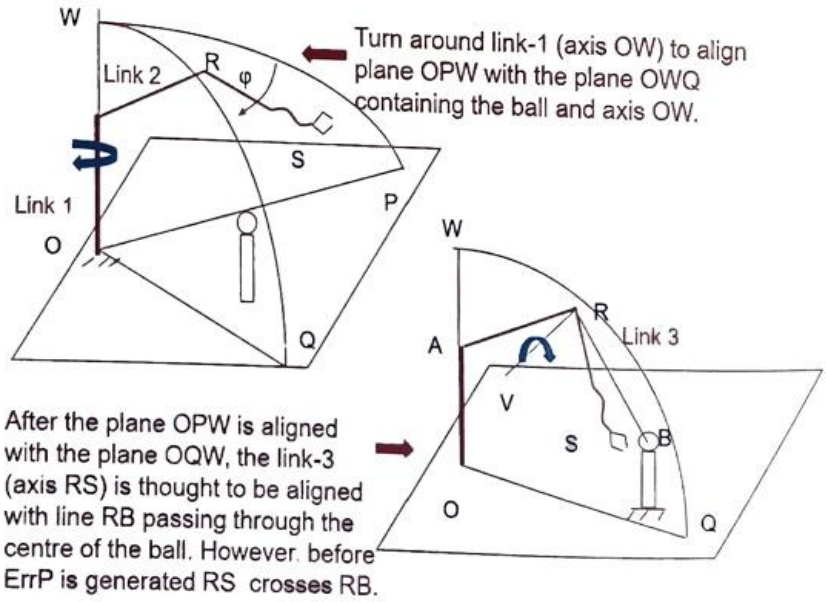
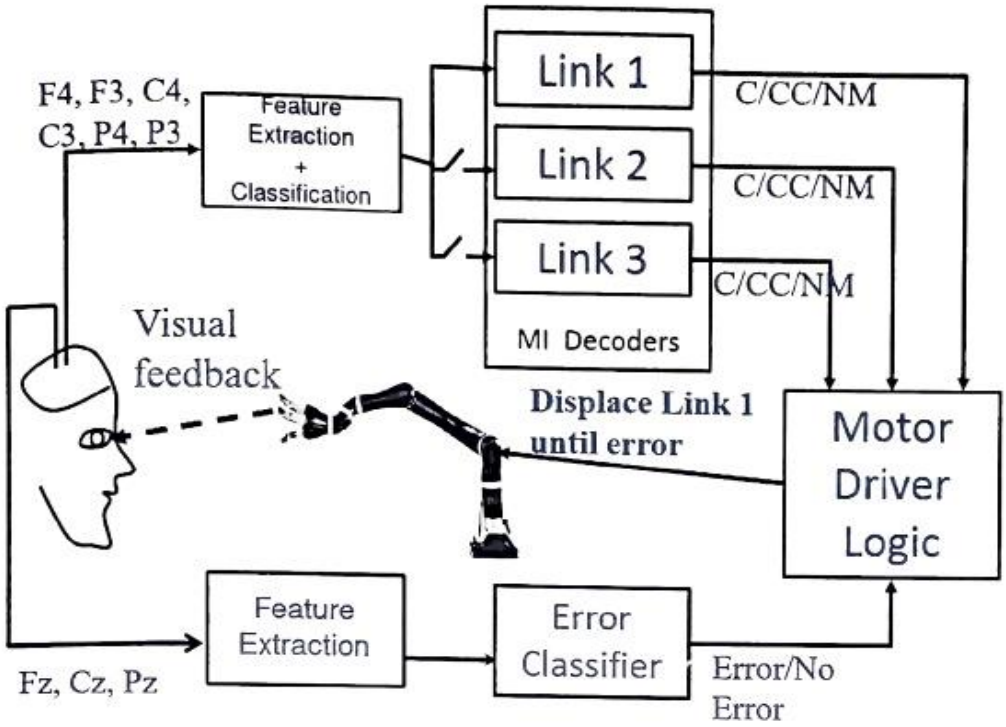


Figure 1.11: BCI-based position control of a robot arm in 3D workspace.

Figure 1.12: Complete closed-loop system of BCI-based position control of a robot arm in 3-D space.



The advent of inverse kinematics lies in the reduction of the cognitive load of the subject, as he/she simply plans to move the end-effecter towards the goal. Naturally, the BCI end-users, who usually are expected to be patients suffering from motor neuron diseases, would have a user-friendly rehabilitative aid that can be controlled with minimum effort.

1.7 Generic Approach of Designing a Closed-loop BCI Framework

Researchers realized that even though the current state of the external agent (e.g., position of the end-effector of a robot arm) is used as a feedback signal to the human operator to increase the accuracy and quality of the performance, still the result was not satisfactory. The main reason behind this was the stochastic nature of the human brain which causes the EEG signal to vary significantly over the sessions during the neural activity task and even within the same session. Such variability of EEG signals degrades the system's performance. Another reason is the researcher's inability to perfectly understand the biological underpinnings of any specific neural activity, hence decoding the brain signal with high accuracy is still a challenging task. Among the other reason, researchers have found that it is still not feasible for a human subject to perfectly control the brain rhythms to accomplish a complex task. Even if some of the subjects are able to control his/her brain activity in the desired manner but accomplishing a complex task using a limited number of BCI commands imposes a high cognitive load on them.

Hence, in order to achieve reliable and superior performance, the design of the Brain-Computer Interface (BCI)/ Brain-Machine Interface (BMI) system must contain an auxiliary controller which is introduced inside the control loop 10 mitigate the gap between desired performance and the actual performance. When placed in the forward path of the loop, the auxiliary controller takes the cognitive commands of the subject as the input and optimizes it by following a control strategy to puck a suitable control signal. The control signal actuates the external agent (e.g. motors of the robot joints) in such a way that the desired performance is achieved. Such auxiliary controllers enable the subject to perform complex tasks relatively easily without any mental fatigue. Such controllers are also responsible for ensuring the stability of the causing system and maintaining certain input-output constraints, when necessary, such tasks are not achievable without the auxiliary controller. The auxiliary controller also reduces the dependency of the system exclusively on the BCI decoding

performance hence increasing the system accuracy independent of BCI decoding performance.

It is apparent from the above discussion that the auxiliary controller has now become an in. dispensable part of designing the modern BCI/BMI system. Although the controller is generally placed in the forward loop, there are many examples where the auxiliary controller is placed in the feedback path. When placed in the feedback path, the controller receives the state information from the external agent to be controlled and optimizes it to actuate an encoder that creates the suitable stimulation signal based on the feedback (e.g. proprioceptive tactile feedback [21][22]) it receives from the auxiliary controller. The stimulation signal is used to stimulate a part of the human body (Cortical areas of the human brain [23][24], back of the human body [25]) to achieve better performance.

Now, the BCI system can be designed according to any of the generalized frameworks (GFMW) discussed below.

1. **Framework 1:** This framework is an open-loop system where the brain commands are directly applied to the external agent and the operating subject receives no feedback from the agent. This framework includes a neural interface that translates the cognitive commands to the control command of the robot through a series of steps like pre-processing, feature extraction, feature selection, and classification. The framework is represented in Figure 1.13

2. **Framework 2:** Such types of frameworks include a visual feedback path from the robot to the human subject. The human generates the control command based on the real-time visual feedback he/she receives from the robot or any external agent. As an example, for a position control application, the subject observes the present position of the end-effecter and mentally determines how much it should be moved to reach the target position. The framework is shown in Figure. 1.14.

3. **Framework 3:** This framework introduces an encoder in the feedback path to convert the current state information of the robot or an external agent into a vibrotactile or electrical stimulation to stimulate a body part like skin or brain. The electrical stimulation generated by the encoder provides the necessary feedback information to

the user to generate a suitable control signal for the agent. The scheme is shown in Figure. 1.15.

4. **Framework 4:** Such frameworks incorporate an auxiliary controller inside the control loop either in the forward path or ill feedback poll), The schematic diagram is presented in Figure. 1.16 consider the auxiliary controller forward path. As evident from the figure the auxiliary controller here receives the high-level brain command from the participating subject through the neural interface and modulates them to generate low level control commands to actuate the robot or any external agent present in the loop. The current thesis adopts this framework for designing the closed-loop system.

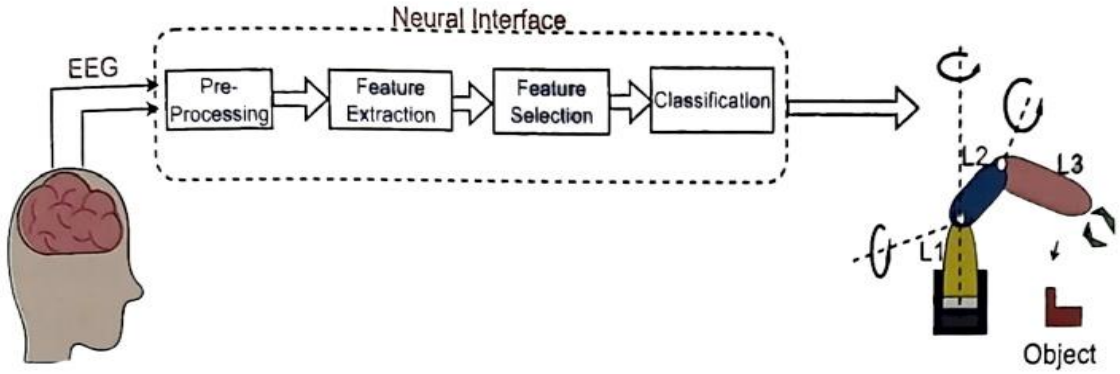


Figure 1.13: Schematic representation of Closed-loop BCI Framework 1

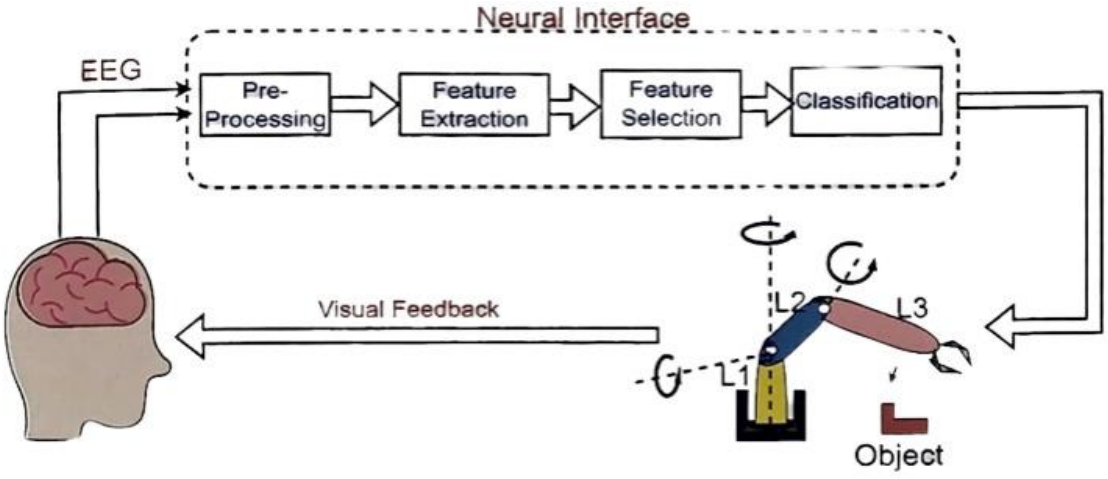


Figure 1.14: Schematic representation of Closed-loop BCI Framework 2

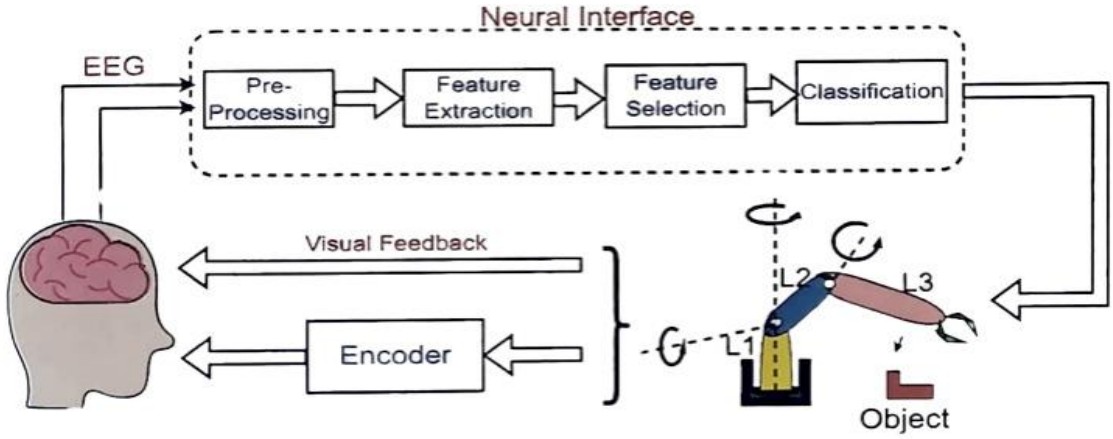


Figure 1.15: Schematic representation of Closed-loop BCI Framework 3

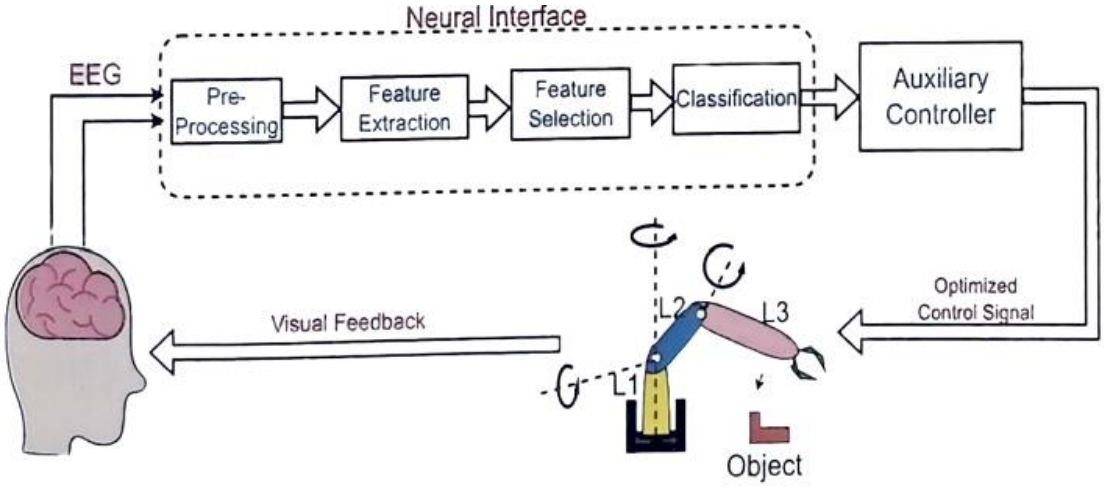


Figure 1.16: Schematic representation of Closed-loop BCI Framework 4

1.8 Modules of Closed-Loop Brain-Computer Interface System

The closed-loop BCI framework adopted in this thesis essentially contains two major components, a neural interface, and an auxiliary controller. These two components arc cascaded with the human brain to achieve robust and superior performance. Here a brief description of each of them is presented below.

1.8.1 Neural Interface

The neural interface is responsible for decoding high-level human intention into low-level control commands that can be applied to the external device or an auxiliary controller. As discussed earlier, the interface decodes the human intention through a sequence of processing steps i.e. Pre-processing or Artifact Removal, Feature Extraction, Feature Selection, and Classification. Each of the sub-components is described below.

A. Pre-processing

The raw EEG signal acquired from the brain contains noise and artifacts arising due to unwanted muscle movement, eye blinking, power line noise, and other environmental noises. The pre-processing step helps to eliminate the noise using some filtering techniques. Such steps are also important to extract the desired frequency sub-band (which contains the highest amount of information about a cognitive task) from the original EEG signal.

Fast-Fourier transform (FFT) is a widely used method to extract the relevant frequency sub-band from the EEG signal [26]. FFT provides an alternative representation of the time-domain signal in the frequency domain using Discrete Fourier Transform (DFT). It allows us to visualize the separate frequency contents present in the signal. A noisy signal is first converted to a frequency domain signal using DFT and then the inverse DFT(IDFT) is applied to get back the signal in the original domain. While reconstructing, the IDFT eliminates the co-efficient belonging to the undesired frequency components, hence the reconstructed time domain signal is free of noise. Sometimes another variant of FFT popularly known as the Short-time Fourier transform (STFT) is also used to handle the non-stationary nature of EEG signals whose frequency components vary with time [27].

Digital filters are also one of the widely used pre-processing methods in EEG signal processing. The digital filters are designed in such a way that when a signal passes through the filter it retains the desired frequency band of the signal and attenuates the other frequency components. The allowable frequency band is known as the passband and the attenuated frequency band is known as the stopband. The boundary frequency between the passband and

stopband is known as the cut-off frequency. Based on the nature of the passband and stopband the filter can be termed a High-pass, Low-pass, and Band-pass filter [28]

Both the Finite Impulse Response (FIR) and Infinite Impulse response filters are used in the BCI experiment. The FIR filters are non-recursive in nature and always provide a stable response however its computational efficiency is less than IIR filters which are recursive in nature and requires less amount of memory enabling them to be used in real-time BCI system. Different IIR filters like the Butterworth filter, Chebyshev filter, and Elliptic IIR filter are commonly used in BC1[29].

Blind source separation or BSS is also an effective technique to separate the desired source signal from a mixture of multiple signals 30]. Such a technique is used to eliminate muscle and ocular artifacts from the EEG signal. Another two commonly used techniques are Independent component analysis (ICA) and Principal Component Analysis (PCA). The ICA attempts to solve the BSS problem by representing the set of random variables (EEG observation) as a linear combination of statistically independent components [31]. On the contrary PCA attempts to find the directions (principal components) in the data that capture the maximum variance [32].

Apart from the spectral filtering techniques discussed above, spatial filtering techniques are also very popular in the BCI domain as they help to obtain more localized signals and to reduce the effect of far signal sources. One such spatial filtering technique is Common average referencing (CAR) where the average value of all the electrodes is subtracted from every electrode to reduce the effect of distant signal sources [33]. Laplacian filter on the other hand subtracts the weighted average of the surrounding electrodes from an individual electrode, and the weights are determined based on the distance between the electrodes [33].

B. Feature Extraction

Once the pre-processing phase is over, the brain patterns are subjected to further processing for extracting the hidden features which are not self-revealing in the raw EEG signal. The feature extraction method attempts to find the features that characterize the brain pattern and helps to distinguish between two different classes of brain patterns. There exists a number of feature extraction methods in the BCI literature, among them time domain feature extractors like Hjorth parameters [34], Adaptive Auto-regressive parameters [35], time-frequency domain feature extractors like Wavelet Transform [36], frequency domain feature extractors

like Canonical Correlation analysis [37], spatial domain feature extractors like Common-spatial pattern [38], Empirical mode decomposition [39] are mostly used in BCI experiments.

Here, we discuss four major feature extraction methods relevant to four major categories of brain signals (MI, P300, ErrP, and SSVEP).

Common Spatial Pattern:

The Common Spatial Pattern (CSP) [40] technique aims to generate spatial filters that maximize the variance of EEG signals for one class while minimizing it for the other class simultaneously, and vice versa. This approach facilitates the decoding of the user's intended actions in the subsequent phase of a Brain Computer Interface (BCI) system.

From a mathematical perspective, definition involves determining the coefficients of the spatial filter, denoted as 'w,' to the following objective function.

$$O(w) = \frac{w^T E_1^T E_1 w}{w^T E_2^T E_2 w} = \frac{w^T C_1 w}{w^T C_2 w} \qquad \textbf{(1.1)}$$

where; For a given class *i*, E*i* represents the trial matrix of N x Q dimension; N denotes the number of EEG electrodes and Q denotes the time samples corresponding to each electrode. C_i denotes the covariance matrix of class *i*. It is apparent from the above equation that maximizing the objective function is nothing but the maximization of the signal variance of class 1 and the minimization of the signal variation of class 2. On the other hand, minimizing the objective function leads to the minimization of class 1 variance and maximization of class 2 variance. Hence, the problem has been formulated as an optimization problem to obtain the optimal filter coefficients. The optimization problem is subjected to the following constraints $w^TC_2w=1$ while extremizing w^TC_1w Mathematically, the above expression can be represented in terms of the Lagrange multiplier as below;

$$\boldsymbol{L(\lambda,w)= w^TC_1w = \lambda\ (w^TC_2w - 1)} \qquad \textbf{(1.2)}$$

Here, the spatial filters are found to be the eigenvectors of $C_2^{-1}C_1$. However, we consider the eigenvectors associated with both the extreme (highest and lowest) eigenvalues. Once the

filter coefficients are obtained, the variance of the filtered signal is calculated, and the logarithm of the variance is taken as the CSP features.

Regularised Common Spatial Pattern: In recent years a common trend is to modify the objective function of the CSP by introducing custom terms to achieve a specific solution [38]. One such term is the "penalty term" that penalizes the filter which violates the constraints associated with the formulation of the objective function. The penalty term is generally introduced in the denominator of the objective function. The penalty term is generally introduced in the denominator of the objective function. After introducing the penalty term, the objective function takes the following form

$$O_{Reg} = \frac{w^T C_1 w}{w^T C_2 w + \beta S(w)} \quad \textbf{(1.3)}$$

here $S(w) = w^T M w$ is quadratic penalty term and ß is the parameter of regularization. Like the classical CSP method described above, the optimization of the modified objective function can also be represented in terms of the Lagrange multiplier as below;

$$L(\lambda, w) = w^T C_1 w - \lambda(w^T (C_2 + \beta M) w - 1) \quad \textbf{(1.4)}$$

The spatial filters are obtained as the eigenvectors of the matrix $(C_2 + \beta M)\ C_1^{-1}$. However, unlike the classical CSP methods, the minimization of the objective function is not desirable here as it leads to the maximization of the penalty term. Hence the objective function is re-formulated here as below;

$$O_{Reg} = \frac{w^T C_2 w}{w^T C_1 w + \beta S(w)} \quad \textbf{(1.5)}$$

C. Feature Selection

It is observed that the feature extraction method sometimes generates complex and high-dimensional features from the original raw EEG data. However, it is not necessary that all the features generated by the feature extractor will be relevant for identifying the targeted mental state. Hence, a subset of features having the highest importance with respect to the targeted

mental state must be judiciously selected from the original feature pool. Such a procedure is known as feature selection. The feature selection process has multiple benefits in the BCI application.

First, it helps to extract the most relevant features and discard the redundant features. Relevant features have high inter-class variance and low intra-class variance.

Second, the feature extraction method reduces the dimension of the feature which has a positive effect on the classifier's performance. As the number of features gets reduced the classifier needs to adjust only fewer number of parameters and also reduces the chance of overfitting especially when the number of training samples is small.

Third, fewer number of features speed up the classification process, which is highly required for real-time BCI applications.

There exist quite a few feature selection methods that are extensively used in BCI applications. Among them, Wrapper based methods like linear regressor [41], evolutionary algorithms [42], genetic algorithm [43], filter-based methods like Principal Component Analysis [44][45][32], maximal mutual information [46], embedded methods like SWLDA [47], metaheuristic algorithms like Particle Swarm Optimization [48], Ant colony optimization [49] are very popular. Apart from the above methods, mRMR [50], and Relief [51] are also used as the feature selection tool in EEG-based BCI. Feature selection methods from each of the three major categories are discussed in detail in this thesis.

Principal Component Analysis:

PCA aims to reduce the dimensionality of the original dataset while preserving the most important information captured by the principal component, which arc the directions in the data space that maximize the variance.

Let us consider $\mathbf{X} \in \mathbf{R}^{n \times p}$ to be the EEG feature set of a single trial arising from n EEG channels. and having p number of features. PCA first normalizes the data by subtracting the mean(m) of each feature (mean is computed by averaging the feature values across all channels: $m=m_1,m_2 \ldots m_p$) from each channel. The normalized data matrix is then utilized to compute the covariance matrix. For the normalized matrix $\hat{X}$, the covariance matrix Σ is calculated as $\mathbf{\Sigma} = \frac{\mathbf{1}}{\boldsymbol{n}} \widehat{\boldsymbol{X}}^{\boldsymbol{T}} \widehat{\widehat{\boldsymbol{X}}}$ Next, the covariance matrix passes through the eigen decomposition method which

reveals the eigenvalues(λ_1,λ_2 ,.....λ_p) and eigenvectors(V_1,V_2, ...V_p) of the matrix. Next the eigenvectors are sorted in descending order according to their corresponding eigenvalue.This ensures that the principal components are ranked by the amount of variance they explain Now. we select the d principal components by taking the first d eigenvectors to create a projection matrix S. The original normalized EEG data matrix R is now projected onto the S to obtain the matrix $\mathbf{P} \in \mathbf{R}^{n \times d}$ with reduced dimension, where each row corresponds to a transformed data point and each column represents a principal component score.

D. Classification

Classification is the last component of the neural interface. A properly designed classifier helps to distinguish between different mental states corresponding to the different mental intentions of the subject. Once the feature vector consisting of the discriminative features of an EEG trial is obtained, the classifier categorizes the feature vector and assigns a pre-defined class label to it. The categorized signal coming from the output of a classifier is used as an input to the auxiliary controller. In the case of traditional BCI control where the auxiliary controller is absent, the output of the classifier is directly used to actuate the external device such as motors of robot joints.

The classifiers learn through the instances to categorize the different cognitive states; hence the classifiers are trained with the available data generated during the training phase where the subjects are instructed to perform a given mental task whose class labels are known as apriori. The EEG signal acquired from the scalp of the subject while performing the tasks is processed to obtain the feature vector of that specific class label, which is utilized to train the classifier. Once the training process is over, the trained classifiers are employed in the real-time system for testing their performance. The BCI system employs various classifiers for different applications,

For the robot control application, some of the widely used traditional classifiers are given below.

Discriminant analysis is a classification technique that falls under the category of generative modelling methods. In this approach, the goal is to estimate the density of EEG feature vector *x* within each class C_i based on the given class label. By incorporating the prior probability (unconditioned probability) of classes, we can calculate the posterior probability of c; using Bayes formula.

Linear-discriminant Analysis (LDA) classifier is the simplest form of discriminative classifier widely used for classifying motor imagery, P300, ErrP, and other brain signals [52][53]. The main assumption of the LDA is the equal covariance matrix of all classes, hence it presumes that the classes are linearly separable. It attempts to find the optimal direction in which the classes are best separable [54]. The advantage of the LDA is its low complexity and ability to handle multicollinearity.

For a given feature vector x and class labels C_i where *i*= 1,2,3...n the discriminant function of the LDA is given below;

$$\hat{D}(x) = -\frac{1}{2}(x-\mu_{c_i})^T\Sigma^{-1}(x-\mu_{c_i})^T + log(\pi_{c_i}) \quad \textbf{(1.6)}$$

where Σ is the covariance matrix, μ_k, and π_k is the mean and prior probability of class c_i. The LDA finds the class label ci (for a given test vector) that maximizes the discriminant function. It should be noted that while formulating the discriminant function the LDA drops the quadratic terms and considers only linear terms.

Another important class of classifier is Quadratic Discriminant Analysis (QDA) which is an extension of previously described LDA[55]. Unlike the LDA, the QDA assumes a different covariance matrix for each class. It attempts to maximize a discriminant function that is quadratic in nature. The discriminant function is very similar to that of LDA but also includes the quadratic terms that were previously discarded in the LDA formulation. The discriminant function is given below;

$$\hat{D}(x) = -\frac{1}{2}(x-\mu_{c_i})^T\Sigma_{c_i}^{-1}(x-\mu_{c_i})^T + log(\pi_{c_i}) \quad \textbf{(1.7)}$$

the notation of the equation remains the same as LDA but with an exception, the covariance matrix Σc_i is now class dependent. Like the LDA, QDA also tries to find the class label c_i for which the discriminant function gets maximized. In some recent literature, QDA is found to be used as a classifier to classify different cognitive states [56][57].

In LDA and QDA class density is assumed to be Gaussian in nature, but based on Baye's rule, there is another important classifier called Naive Bayes classifier which assumes the input features governing the class densities are independent, hence the class density can be obtained

by simply multiplying the marginal densities of each input features [58]. Such an assumption of conditional independence helps to simplify the calculation and increases the classification speed. The Naive Bayes classifier is well suited for real-time EEG classification applications, hence has been widely used in BCI domain [59][60].

Sometimes it is found that due to the complex nature of EEG data, it becomes almost impossible to distinguish between two different classes of data using "Hard" margins, i.e. it is impossible to construct a decision boundary for which all the feature points belong to a class label will be on the one side of the boundary and feature points belong to another class label will be on another side of the boundary. Such situations are tackled by introducing the "soft" margin which allows a small number of feature points to lie on the wrong side of the boundary but with an aim to increase the generalization capability of the classifier. Support Vector Machine (SVM) is one of the very popular classifiers which attempts to maximize this soft margin/hyperplane by minimizing the classification errors [61][62].

Let's say we have EEG feature vectors x_i, where i ranges from I to N, representing the training set X. Our objective is to create an ideal hyperplane g(x) = $w^T x + w_0$x that accurately Classifies the training sectors into two linearly separable classes, $w_1$and w_2. In the equation, *w* represents the direction of the hyperplane, and w_0 represents its position. To achieve this Support Vector Machines (SVM) aim to find the hyperplane direction that maximizes the mar, gin between both classes, ensuring a clear separation. The distance of a particular point from hyperplane g(x) can be expressed as z =$\frac{|g(x)|}{\|w\|}$. Now, w and w_0 can be scaled so that the value g(x) is +1 in the case of w_1, and -l in the case of w_2. Hence, the task reduces the problem of computing parameters w and w_0 to minimize the objective function

$$J(\omega, \omega_0) = \frac{1}{2}||\omega||^2 \qquad \textbf{(1.8)}$$

subject to the constraint $y_i(w^T x_i + w_0) \geq 1$ *for* $i = 1,2,3 \ldots N$

The above optimization problem is solved using the method of Karush-Kuhn-Tucker(KKT) conditions. The vector parameter ω of the optimal solution comes out to be a linear combination of the number of feature vectors corresponding to non-zero Lagrange

multipliers. These vectors are known as Support Vectors. In case the feature points are not linearly separable, a nonlinear mapping function popularly known as the kernel function is used to map the feature points in a higher dimensional space. Once the above mapping is done, the SVM attempts to find an optimal hyperplane that linearly separates the feature points in that higher dimension. Literature shows the widespread usage of this classifier for classifying various brain patterns [63][64][65].

Another important classifier for brain signal classification is k-NN [66]. k-NN is a classifier that maps the feature vector to class labels by storing k-feature points that are nearest to the test feature point under consideration and then it calculates the Euclidian distance of the test feature point from all other feature points. The most probable classes get the nomination from previously selected k-nearest neighbours and the class which gets the most nomination is selected as the class of that particular test feature point. k is a very important parameter of the k-NN classifier as the local density of data is controlled by it and of course, it is much smaller than the training sample size [62].

Apart from the statistical classifiers, Artificial Neural Network is also used as classifier in the BCI task. The ANN is completely data-driven, hence doesn't depend on the probability distribution of the data [67]. The ANN attempts to learn the mapping between feature vectors and class labels by adapting the connection weights between the artificial neurons. It uses EEG feature vectors with known class labels along with a learning rule to update the connection weight [68][69].

However, due to the low signal-to-noise ratio and non-stationarity of the EEG signals, the classification performance is not optimal. Hence, a recent trend is seen where the parameters of the classifier model are updated continuously to tackle the above drawbacks and increase the classification accuracy [70]. A very popular approach called transfer learning is also used to deal with the problem of less data, it enables the classifier trained in one BCI domain and session to be used in another BCI domain [71][72][73]. There exist many other techniques to increase classification accuracy like merging the feature extraction, feature selection, and classification process is one of them [70].

Parameter adaptation is done using both supervised and unsupervised learning [74], i.e. with or without having prior knowledge about the class of the data. although most of the adaptive classifiers are designed using supervised learning [75][76][77]. In motor imagery-based BCI, adaptive LDA and QDA were used to classify the MI signals [78][79][80][81][82][83]. An adaptive probabilistic neural network was also used to classify different classes of MI patterns, such models assume a distribution model of feature sets of each class and update it with the new incoming feature vector [84]. Likewise, an altered non-linear Bayesian classifier employed unsupervised or semi-supervised learning methods, where a subset of the incoming trials was labelled. This adaptation incorporated extended Kalman filtering to monitor the fluctuations in the parameters of the class distribution alongside auto-regressive (AR) features [85].

Another important class of classifiers is Convolutional Neural Networks, which is popularly known as CNN. A convolutional neural network is a type of neural network that follows a forward propagation approach, where information moves unidirectionally from the input through the hidden layers to the output. It is characterized by the presence of at least one convolutional layer [86][87]. The convolutional layer employs a convolutional operator that transforms the input signal into an output signal through (Eq.1.9). For a given trial of EEG data x_i with N number of samples, the convolutional filter g_l having size L, transforms the input x_i into output y_i

$$y(n) = \sum_{i=0}^{L-1} g_i x_{n-i} \forall n = 0..1,2,...N-1 \quad \textbf{(1.9)}$$

Although the above equation is given for 1-D signal input, but the idea can be safely extended for multidimensional input. Hence, CNN can be used for multichannel EEG inputs also.

In a general framework of CNN, non-linearities and pooling layers are introduced after the convolutional layer. Such layers combine the relevant local data coming from the convolutional layer output into a solitary value, usually by utilizing an average or maximum operation. Typically, in standard ConvNet architectures, multiple layers consisting of convolution, and nonlinearity (and pooling) are sequentially stacked, followed by additional

layers, commonly fully connected, which function as a classification layer [88]. It is worth noting that certain architectures employ solely convolutional layers for classification. The model parameters in these architectures consist of the weights assigned to all the convolution filters, as well as the weights associated with the fully connected layers.

Parameters of the network are trained through supervised learning with the aim to minimize the cost function of the following generic form

$$\hat{w} = \underset{w}{argmin} \frac{1}{m} \sum_{i} J(y_i, D_w(x_i)) + R(w) \quad \textbf{(1.10)}$$

The training data above is represented as $[x_i, y_i]$ for i ranging from 1 to the total number of samples. The prediction function D_w, associated with the ConvNet, is used to predict the labels for the input data x_i. The loss function J is used to measure the discrepancy between the true class of EEG trials x_i and the predicted class. Additionally, *R* represents a regularization function that helps in controlling the parameters of the ConvNct. Stochastic gradient descent and its variants are widely used for optimizing deep ConvNcts due to the specific form of global loss, Which the average loss over individual samples. Moreover, the feedforward architecture of D_w enables the computation of gradients at any layer using the chain rule. This efficient Computation is accomplished through the back-propagation algorithm [89].

In the BCI domain, CNN is being extensively used to identify and distinguish between different mental commands (brain patterns) due to their superior ability to learn the most discriminating features present in that specific brain pattern [90]. Although there exist quite a few papers that use CNN to detect various brain patterns like Motor Imagery, SSVEP, P300, etc., here we will discuss some of the landmark papers for each category of brain signal.

The initial exploration of CNN for P300-BCI (Brain-Computer Interface) was conducted by *Cecotti et al*. in their pioneering paper [91]. Their CNN architecture consisted of two convolutional layers, where one layer was designed to learn spatial filters and the other layer to learn temporal filters. These layers were followed by a fully connected layer. In addition to this, the researchers also investigated the use of ensembles comprising multiple CNNs with similar architectures. In another instance, *Manor R et al*. [92] used CNN with one spatial convolutional layer along with two other temporal convolutional layers to detect the presence of P300 generated in the context of Rapid Serial Visual Presentation. The network also employed two dense fully connected layers at the end for the classification purpose.

The CNN is also extensively used in deciphering motor imagery signals in BCI. Tabar Y R et al. [93] used CNN in conjunction with Deep Belief network (DBN) to classify motor imagery signals. *Schirrmeister et al* [94] investigated different CNN architectures including shallow CNN, deep CNN, hybrid shallow+deep CNN, and residual NN. The shallow CNN consisted of one temporal convolution, one spatial convolution, squaring, mean pooling, and a softmax layer. The deep CNN involved a temporal convolution, a spatial convolution, followed by three layers of standard convolution, and a softmax layer. The hybrid shallow+deep CNN combined the architectures of shallow and deep CNNs by concatenating them. The residual NN consisted of a temporal convolution, a spatial convolution, 34 residual layers, and a softmax layer. Both the deep and shallow CNN architectures outperformed FBCSP significantly in their performance, however, the hybrid and residual CNN failed to do that. Another paper [95] used CNN to classify multiple brain patterns like Motor Imagery (MI), P300, ErrP, etc. They used a compact structure of CNN with few layers and parameters.

1.8.2 Auxiliary Controller

Performance requirements of different BCI applications cannot be met only with human efforts because of the subject's inability to perform complex tasks (such as complex trajectory generation for the robots, avoiding obstacles during the robot movement, proper grasping of objects using robot gripper, etc) using limited number of BCI commands. It also imposes a high cognitive load on the participating subjects. Hence an additional controller is needed to

take care of the low-level tasks. Such controllers are termed auxiliary controllers. The auxiliary controller receives the human command from the neural interface and modulates it to actuate a robot arm or an external device to achieve any specific task. The main role of the auxiliary controller is to provide high-precision control, which usually is difficult to achieve by human agents.

Different control strategies based on the requirements of the BCI application are adopted for designing the auxiliary controller. Here, we will briefly discuss three major strategies used predominantly in the Brain-controlled robot application.

A. PID Controller

Proportional-Integral-Derivative (PID) controller is a traditional and one of the simple control strategies which have got widespread application in various domains like robotics, process industry, the aerospace industry, etc. Such controllers are also implemented in closed-loop BCI for their easy realization technique [96][97] The control signal *u(t)* can be represented by Eq. (1.11)

$$u(t) = K_p e(t) + K_i \int_0^t e(t)\,dt + K_d \frac{de(t)}{dt} \qquad \textbf{(1.11)}$$

where *e(t)* is the error signal that arises due to the mismatch between the actual and desired value. K_p,K_i, and K_d are the proportional constant, derivative constant, and integral constant respectively. It is evident from (1.11) that the control signal *u(t)* is a function of the error signal, rate of the error, and integral of the error. The objective is to optimize the values of K_p,K_i, and K_d to obtain the desired control signal which can actuate the external agent to get the desired performance. The proportional gain helps to obtain a fast response time, and the integral constant helps to get a zero steady-state error while the derivative constant yields a reduced overshoot by predicting the rate of change of error in advance.

Many studies have used PID controllers in the closed-loop BCI for various applications like robot control, regulating the vibrotactile feedback, generating proprioceptive feedback from the robot, etc[96][97][98][99].

B. Shared Controller

The utilization of a shared controller in a Brain-Computer Interface (BCI)-based robot manipulation task offers inherent advantages. It serves to enhance the accuracy of task completion by the robot while simultaneously reducing cognitive fatigue experienced by the human operator through a reduction of subject involvement in repetitive tasks. The primary objective of the shared controller is to optimize the capabilities of both the human and robot agents within the system by breaking down the task into smaller sub-tasks and assigning them to the most suitable agent (either human or robot) based on their specific strengths. High-level decision-making subtasks are entrusted to the human agent, while lower-level tasks like local navigation and object grasping are autonomously performed by the robot agent using its onboard sensors like RGB(D) camera, ultrasonic sensors, etc. This approach ensures that human intervention is only required when uncertainties arise in the decision-making process.

Typically. shared control methods employed in BCI applications can be classified into two main types: sequential shared control and all-time shared control [100]. In the case of sequential shared control, the task is shared between the autonomous controller and the human subject in a sequential manner. Initially, the human subject provides high-level commands, such as the desired destination to reach and the autonomous controller then executes the task while ensuring specific conditions are met. In the other type of control method human operator and the shared controller continuously shares the task and the decision is generated at each instant by combining the decisions of the human and the shared controller.

C. Model Predictive Controller

Model Predictive Control (MPC) is a control strategy that utilizes a predictive model of the system's behaviour to optimize control actions over a future time horizon [101]. First, a mathematical model of the system's dynamics is developed from the experimental data to describe the dynamic behaviour of the system. Based on the present state and control input of the system, the model predicts the behaviour of the system over a specified time. An objective function with certain input-output constraints is optimized to obtain the optimal control input. Once the control input is applied to the system, the state or the system gets updated, which becomes the present the prediction model.

Such Model-based predictive controllers are currently being used to design the auxiliary controller in closed-loop BCI for their superior performance in terms of precision and accuracy [102][103][104][105].

1.9 State-of-the-art BCI-based Control Schemes

The BCI has become an emerging field in the last ten years, hence there exists a large number of literatures in this domain. However, here we provide a review of recent BCI works which focus on the design of closed-loop BCI systems from the control-theoretic perspective and are relevant to the main theme of the present thesis.

In 2016 *Meng et al.* [106] developed a novel approach to cursor control (and also position control of an end-effecter) using two sequential steps. The first step utilizes the left/right MI for cursor control in the x-direction on a horizontal plane. In the second phase, the authors employed both hand-movement together to control the movement of the cursor (end-effecter) in the y-direction of the horizontal plane. Next, they arranged to hover over the target object using Mu-power. The position of the cursor/end-effecter is displayed as a feedback signal to the user for necessary corrective actions in subsequent steps.

Meng et al. [107] in their other work, proposed an interesting approach to controlling the position of a cursor on a computer screen. They employed overt spatial attention (OSA) to control the movement of a cursor on the left/right side of the screen depending on the subject's alertness towards the left/right ends of the screen. After the cursor hits the left/right bar of the screen, it would have a change of colour to signify success. Once the cursor control in the horizontal direction is over, the user utilizes OSA to control the movement of the cursor in the up-down direction. A third strategy to control the motion of the cursor in a virtual plane perpendicular to the screen is to employ a left/right motor imagery signal to move the cursor outward/inward on the plane. An alternative strategy is to control the left/right and up/down movement of the cursor by motor imagery and motion in the perpendicular plane by OSA control.

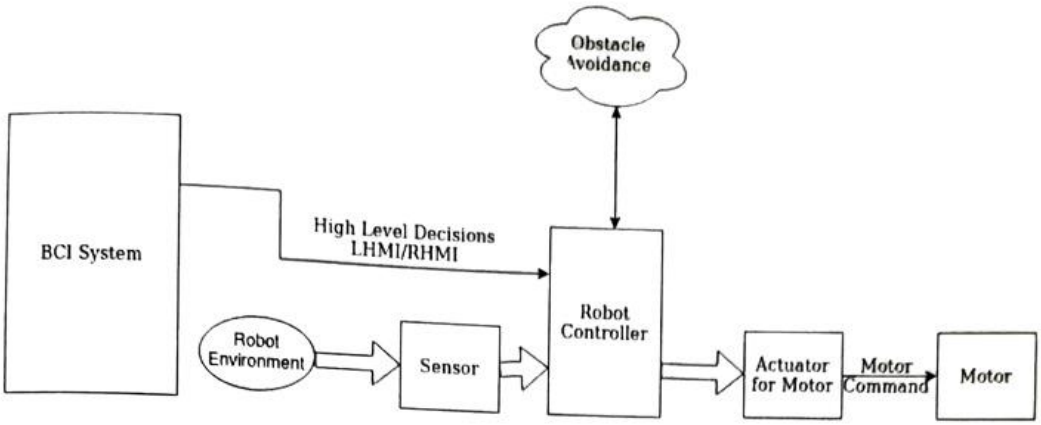


Figure 1.17: Schematic diagram of BCI-based control strategy proposed by Tariq et al

Liu et al. [108] proposed a novel scheme where left-arm motor imagery is utilized to lift the robotic limbs and right-hand motor imagery to move down the limbs. Additionally, they utilized inverse kinematics to determine the angular positions of the joints of the 6 degrees of freedom manipulator. Lastly, they employed a novel neural-net-based position controller, that optimizes a given control objective to reduce to optimize the angular velocity and angular acceleration of each joint. The scheme is presented in Figure 1.18

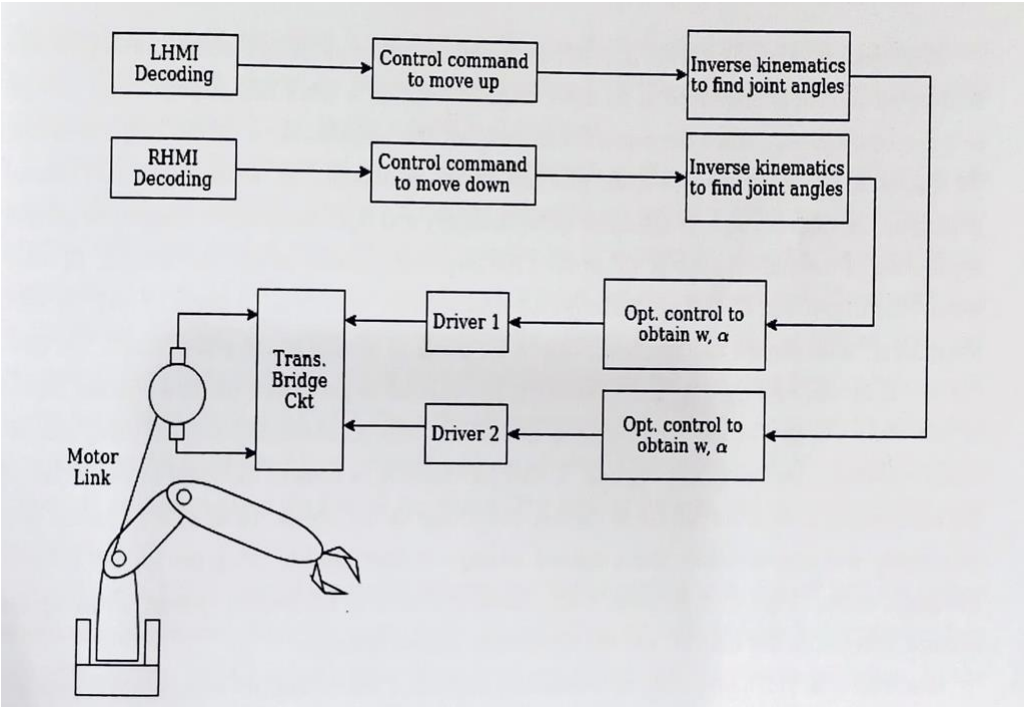


Figure 1.18: Schematic diagram of BCI-based control strategy proposed by Liu et al.

Tang et al. [109] proposed an interesting technique to control the movement of an end-effecter in a plane parallel to the plane of a camera mounted on the moving robotic arm. They introduced an on-off type control strategy by utilizing the following principle.

- l. The left/Right movement of the end-effecter on the coronal plane (parallel to the plane of the camera) is done by left/right-hand motor imagery.
- 2. The motion of the cnd-cffcctor is stopped when the camera detects the object of intent on the coronal plane.

Another work by *Zhang et al.* [7] proposes the following strategy to mentally control a robot arm using a custom-designed neural interface.

l. The subject selects the objects using SSVEP.

2. The subject uses motor imagery to control the robot arm.

3. There are 6 types if movements involved in grasping control: left, right, up, down, open and close.

4. By image analysis, the robot determines the displacement in left, right, up, down, opening and closure of end-effecter.

5. Additionally, the robot plans the same movement patterns of the end-effecter.

6. Now, the probability of the end-effecter to grasp object due to up, down, left, right etc. movement are compared from the visual inspection data both by the Kinect sensor and the subject. A data fusion algorithm is run to obtain the optimized constraints.

The work undertaken by *Xu et al.* [110] deals with switched mode dual control strategy where BCI-based control is employed at an early stage to position a robot end-effecter close enough to a targeted object. After the end-effecter reaches the neighbourhood of the target position, the manual to automatic camera-based position control is switched on. In the BCI-based control paradigm, the subject employs left-hand motor imagery and right-hand motor imagery to control the motion of the end-effector at 45^0 around the targeted position of the end-effecter. In other words, the LHMI and RHMI are transformed into velocity vectors at an angle of $+45^0$ or -45^0 respectively with respect to a reference line in the plane of motion of the end-effecter. The end-effecter is moved in a zig-zag path toward the pre-defined target. Once the end-effecter comes within close vicinity of the target object, the switch over to automatic control using

vision-based movement planning is instigated. Under this scheme, a camera mounted at the corner of the robot-work table is turned on to capture the image of the object, localize it by image preprocessing and segmentation, and a control strategy is developed to bring the gripper towards the target object. Figure 1.19 provides a schematic overview of the overall system involving the camera, robot arm, the subject, and the distributed control strategy.

Sorbello et al. [111] proposed an interesting scheme of shared control to control the position of the end-effecter. First, the subject selects the on-screen navigational commands, (such as move horizontal, vertical, left, right, gripper open/close, and the like by using P300 signals. A camera mounted on the top of the robot is used to determine the direction of navigation of the end-effector intelligently. In case the direction indicated by the camera matches with the one selected by the subject using P300, the action is selected, but not executed. Before execution of the command, a second step of confirmation is obtained by the bio-feedback. The "biofeedback module" inputs 3 parameters: Attention, Focus, and Intent, and evaluates a metric as the weighted sum of the above 3 parameters. In case the weighted sum crosses a pre-defined threshold, the action chosen by the subject is executed. If the weighted sum goes below the threshold, the action selected by the subject is abandoned.

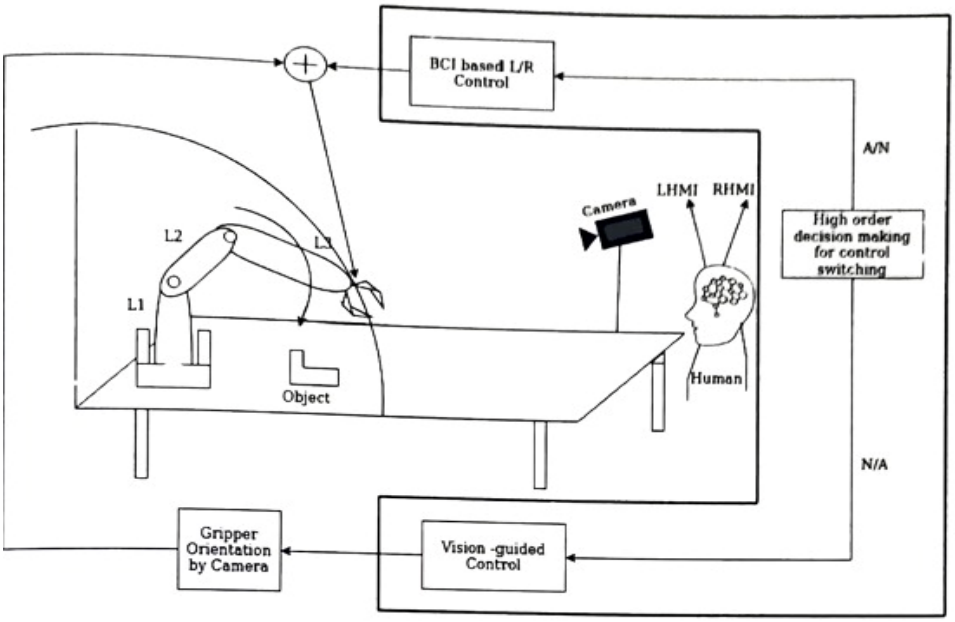


Figure 1.19: Schematic diagram of BCI-based control strategy proposed by Xu et al.

Wang et al. [112] presented an interesting approach to object selection through a camera using SSVEP. The scheme employs a camera mounted on top of a robot arm to explore the objects within the field of view, which are transferred to a computer monitor for selecting the target object using SSVEP. Here for each object, a bounding box is developed. These bounding boxes flicker at different frequencies to represent the identity of the individual objects. A subject intending of selecting a specific object focuses on the item and the flickering frequency is picked up by the subject through SSVEP. Once the object is selected, the navigation of the robot arm is automated by a camera-based position control system, The distance of the object from the camera is calibrated using the size of the object. The smaller the size, the closer the object with the robot arm.

Lillio et al. [113] proposed a novel strategy for shared control to develop a BCI-controlled assistive manipulator. Here the entire task of controlling the manipulator is partitioned into two components: i) BCI-based human interaction and ii) Intelligent autonomous action. In the BCI-based human interface, the subject selects three items in sequence: i) Object selection, ii) Robotic Action selection, iii) Action execution. Selections are done using P300. The BCI modality of the subject is now complete, and the control policy now is transferred to robot automation. In the automated phases, a Kinect-based camera is used for object recognition and mouth recognition. This information is passed to the waypoint generator which generates a reference trajectory to be followed by the robot. A task priority-based inverse kinematics algorithm is employed which takes care of the obstacles present in the environment and communicates with a low-level robot joint velocity controller. The joint velocity controls the torque of each joint of the robot and manipulates it towards the desired direction.

Batzianoulis ct al. [113] proposed an interesting approach for shared control by utilizing the ErrP signal and Inverse reinforcement learning (IRL) paradigm. Herc the subject has its own choice of trajectory planning of a robot, for instance, obstacle avoidance and trajectory Planning toward the fixed target. Each time the robot reaches an obstacle before reaching the destination the subject releases an ErrP signal. The decoded ErrP signal is used to move away the robot from the obstacle without violating the planned trajectory of the robot. An IRL algorithm is employed to change the trajectory following the user's preferred trajectory of motion.

Duan et al. [114] in a recent paper presented a novel scheme for shared control with a hybrid BCI system. They employed a camera-based capturing of robots' movement. The camera back-plane and the human retinal backplane are parallel. So, the information extracted by

the camera is the same as could be obtained by the subject, if he attempted to see the robot by his naked eyes. The computer screen displaying camera view about the robot's trajectory of motion includes provisions for generating navigational commands for the robot using SSVEP. Navigational commands include turn right/turn left/grasping etc. After the SSVEP-driven commands are issued to the robotic device, the robot gets aware of the task it has to do with. Next, motor imagination is carried out to turn the motor clockwise/counter-clockwise. The switching from SSVEP to MI is performed by thresholding of a parameter.

Yuan et al. [114] developed a novel approach for BCI-based navigational planning of a mobile robot. A camera mounted on top of a mobile robot is used to capture scenes including obstacles present in the environment. The camera output is visible to a subject through a computer screen. The camera front plane and the computer screen are placed in parallel, so the subject has the same impact due to the onscreen video, rather than watching the robot motion directly. A SSVEP based selection of robotic actions is included in the front panel of the computer. The control decisions are taken by the subject are communicated to the robot wirelessly, to perform the required task. The control decision includes avoid obstacles and move towards the targeted goal.

Zeng et al. [115] provide a novel approach to BCI and camera-based object positioning and gripping. The camera back-plane is kept in parallel with the plane containing several objects around the robot arm. Naturally, the image acquired, when displayed on the computer screen, all objects seen by the camera take specific positions/coordinates on the screen. A second camera is mounted on the screen to develop the gaze-detection system. The gaze detection system determines the direction of the gaze of the user to select one of several objects in the local neighbourhood of the robot. Later the subject controls the speed of the robot by repeated ERD/ERS and the direction of the movement of the robot using gaze control. When the gripper reaches above the object, the gripper vertically gets down to the object and grips it, and takes its precise position.

Tidoni et al. [116] proposed a faster and easier way to navigate a walking bipedal humanoid robot by combining SSVEP brain signals and audio-visual feedback from the robot. The task was to l. Navigate a humanoid robot towards a target object, 2. Pick the object 3. Place the object in the desired location. Participating subjects used their SSVEP signal to navigate the robot in the desired direction (left, right, forward, backward and stop movement) and also to select the desired object to be picked and desired location where the object to be placed. A camera is placed on the robot's head which captures the live feed of the robot's local

environment and transmits the feed to a remote computer. The feed of the camera is visible to the user through a computer. Now the subject mentally issues navigational commands to the robot by observing the robot's movement on the computer screen. While navigating the robot through mental commands, the subject receives the footstep sound of the robot synchronous to the actual robot movement. It was observed that subject could navigate the robot with the increasing speed and accuracy while they receive audio and visual feedback from the robot through footstep sound and camera respectively. The authors also placed mirror near the robot, through which the robot itself became visible to the subject. Such placement of the mirror enhanced the accuracy of operation.

Fransicso et al. [117] introduced a novel approach for EEG-BCI based on-off control of home appliances. In the said scheme, the subject selects control commands on a computer screen to communicate his/her desire to activate external devices (such as a light, fan, AC, TV and the like). The automatic selection of control commands is performed using P300 brain signal. Once a control command is selected, it is transformed into a speech signal by a text-to-speech translator. A Google Assistant is activated, once the speech is generated with a codeword used to activate Google Assistant. The rest of the communication is actuated by Google Assistant. For example, if the message needs to be communicated to a subject by phone, a phone call to the recipient may be initiated. In case the speech needs to be communicated to the speaker, the voice message is sent to the subscriber by phone. In case a TV or an AC needs to switched ON/OFF, an IR device is activated to be used as a remote controller through a Wi-Fi device to switch ON/OFF the TV/AC or similar devices.

Mao et al. [118] proposed a novel strategy for brain-robot interaction by fusing human and machine intelligence. They attempted to develop an intelligent system to navigate a mobile humanoid robot in a fixed workspace through BCI-based control commands. The workspace is captured by a camera mounted on the head of the robot. The captured frames about the local neighbourhood of the robot is mapped onto a computer screen. The motivation here is to make the robot move along a user-intended path. This is done by generating two brain signals P300 and SSVEP in sequence. To make the problem simplified, let us assume the robot is desired to move to a fixed object position. This is realized by liberating P300 through flashing the desired object on the screen. However, in case, a trajectory of the robot is required, the first object the robot needs to reach is commanded by generating P300 (by flashing the selected object on screen) and the motion of the robot therefrom is controlled by generating SSVEP by gazing at a flickering source. Such movement of robot from one location to the

other is needed in many applications like transportation, assembling in factory automation, and fire extinguishing at several places. The schematic diagram of the control strategy is given in Figure 1.20

Mengfan et al. [119] extended their previous work by judiciously selecting the 2-step motion commands of a robot using N200 and P300 signals. The first step involves the selection of forward motion, while the latter involves one of the three possible motions like continuous, discrete or stepwise. In both cases, they utilize N200 followed by P300 signals for command generation. The classification accuracy is here increased by 2 parallel classifiers: SVM and FDA and the classifier decision is communicated to the robot when the response of the classifiers is matched.

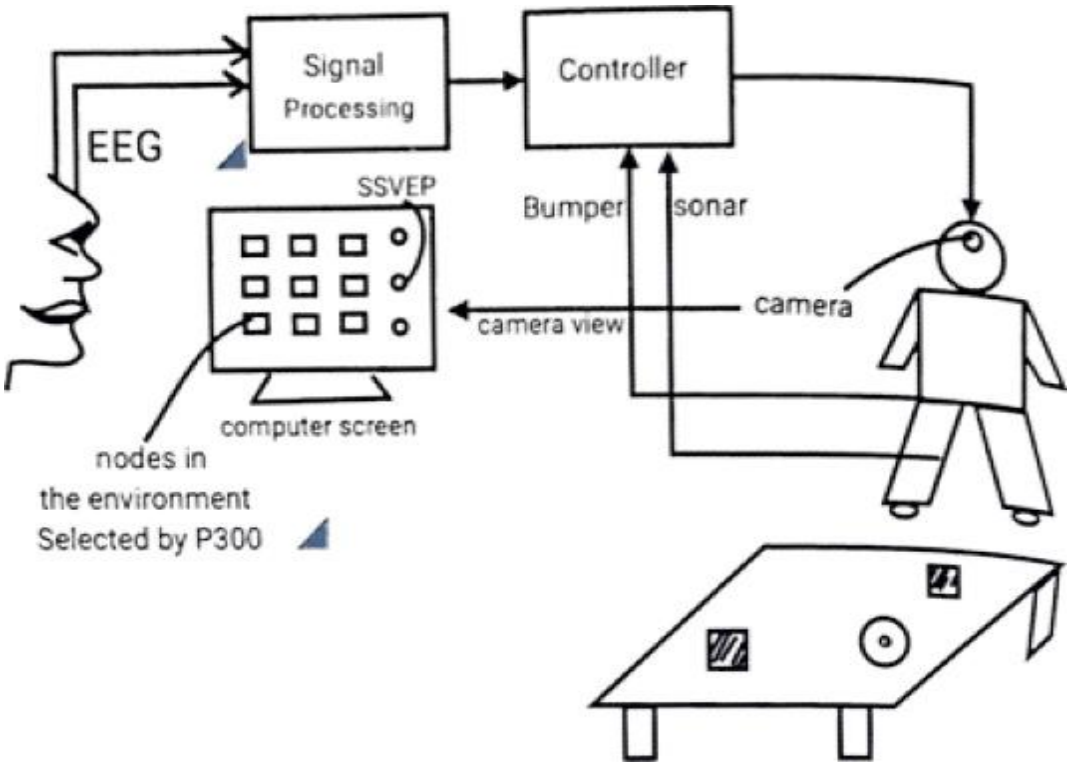


Figure 1.20: Schematic diagram of the BCI strategy proposed by Mao et al.

The robotic neural prosthesis is an effective way to restore the function of disabled or amputated limbs but poses a restriction on the subject to receive somatosensory feedback. Such drawback is overcome by reanimating the original limb of the subject instead of using a robotic prosthesis. A novel strategy following the above protocol is proposed by *Liu et al.* [120], where they used a custom-designed low power, miniaturized, tactile force sensor, and

an electro goniometer to encode tactile and proprioceptive feedback signals respectively from the re-animated limb. The subject wears the sensors which encode the feedback signal from the limb and transfers it to a bidirectional invasive brain-machine interface (BMI) which in turn generates a frequency/pulse-modulated stimulation to actuate a specific brain region. The BMI interface was designed using SOC technology, which integrates a neural activity recorder, electrical stimulator, analog-to-digital converter, ultra-wideband transceivers, and a digital signal processor for suitable stimulus signal generation.

As an improvised method of post-stroke rehabilitation, *Romero-Laiseca et al.* [121] proposed a novel brain-machine interface where the participating subjects perform pedaling imagery to trigger a motorized exercise bike which is highly effective for gait and lower-limb rehabilitation. The system is beneficial for post-stroke patients who cannot voluntarily actuate a movement but now become able to do it using the proposed brain-machine interface. They focused on minimizing the computational cost of the system using a few strategies which includes the use of i) Fast Fourier Transform(FFT) followed by inverse FFV for the pre-processing of EEG signal, ii) Riemannian geometry based feature extraction, iii) pairwise feature proximity for feature selection and using low-cost LDA classifier for pedaling motor imagery classification, The highest accuracy achieved by the two post-stroke patients was as high as 41.67 % and 91.7% although the average accuracy achieved by them were bit low. Significant improvement in the actuating time shows the efficacy of the system for its longer use.

Another efficient way of decoding the neural signals for the generation of suitable control signals in a closed-loop BCI system is proposed by *Dangie et al.* [122]. The method is particularly suitable for decoding the non-stationary brain signal in an online BCI task. Instead of using a traditional Kalman filter-based decoder which uses batch estimation for updating its parameters, here the researchers have proposed an adaptive version of the Kalman filter which continuously updates its parameter through a stochastic gradient descent algorithm. The proposed adaptive Kalman filter (AKF) updates the estimation of the state matrix and observation matrix at each time step. The efficiency of the algorithm is validated using the centre-out cursor movement task in a 2D virtual plane and the brain function is mimicked using a simulated model of cortical neurons. The algorithm results in a faster

learning process and increased success rate. The algorithm proves to be more robust to the sudden disturbances than it's non-adaptive version.

Kyung-Huan Shim et al. [123] proposes a novel technique of brain-machine interface-based robot reaching and grasping tasks using a custom-designed neural interface and a 3D vision camera. The neural interface translates the human intention captured by the EEG signal into robot commands using a novel convolutional neural network. The proposed CNN uses a smaller receptive field of 3x3 dimension to extract the minimal difference between the imagined movements of different parts of the same limb. The lower receptive field has the advantage of increasing the spatial resolution of EEG feature vectors. The proposed CNN also rules out the usage of any max-pooling layer that considers only the active features and neglects other important features, which may cause the robot to follow any unwanted command. The experiment consists of reaching and grasping an object with the mentally guided robot arm and pouring a beverage from the grasped object. All the tasks are carried out by five mentally imagined commands (Right/Left MI, twisting wrist imagery etc.). The imagined commands decoded by the neural interface actuate the robot-end-effecter to reach the correct region where the target object is located and then a 3D Kinect camera determines the exact location of the target object using a YOLO object detection algorithm and guides the robot end-effecter to grasp the target object. Results obtained in this study reveal that the proposed CNN yields an online accuracy of 90% and also performs better than other CNN-based decoding algorithms that use the maxpool in their architecture.

A similar approach of using a Model Predictive auxiliary controller in a Brain-machine interface setup can be seen in a recent research paper by *Fuizon He et al.* [115]. They used a model predictive controller for the safe operation of a brain commanded mobile robot. The proposed controller modulates the control signal issued by the human operating subject to provide a safe and collision-free trajectory for the mobile robot. It also overcomes the shortcomings of the direct BCI control (without any auxiliary controller) that may lead to poor performance due to i. longer response time, ii. no guaranteed safety and iii. the higher number of control commands required to navigate the robot. The MPC uses a virtual model of a mobile robot to estimate the system behaviour and generates a sequence of optimal control signals by satisfying the safety constraints at each time instant. The scheme was tested in a

virtual environment where the subject uses SSVEP brain signal to issue different navigational commands which get optimized by the proposed model predictive controller. The accuracy of the robot navigation task reached 100% without any incident of collision with the obstacles and the task completion time was also reduced significantly.

The use of a model predictive controller in a BMI-based prosthesis control task (describe above) requires the mathematical model of the system, which is often very complex in nature due to the inclusion of a complex human brain model and other bio-physiological models in the loop. *Pan et al*. [124] provided an interesting solution to it by designing a model-free controller which is entirely data-driven and does not require an explicit system model. However, the proposed controller was used in the feedback path of a closed-loop brain-machine interface to generate a suitable control command to actuate a device that can stimulate a specific brain region so that the subject can mentally guide the robot to achieve the desired response (such as a specific trajectory). They considered a simulated model of the cortical circuit for single-joint movement and used a model-free controller to generate artificial sensory feedback to actuate the group of perceived position vector (PPV) neurons of the cortical circuit to achieve their target firing rate which is required to control the robotic prosthesis. The controller performance was compared with a model predictive controller and the result shows that although the MPC controller shows slightly better performance but the proposed model-free controller has a faster response.

Shared autonomy in a BCI-based robot manipulation task has the intrinsic advantage of increasing the task accomplishment accuracy of the robot and also minimizing the cognitive fatigue of the human operator by reducing the human involvement in repetitive tasks. A generalized hierarchical structure for achieving suitable shared autonomy in a BCI system was proposed by *Akinola et al.* [125]. The proposed hierarchical system is universal in nature and hence can be adopted in any BCI-based robotic system. It aims to leverage the fullest power of each agent (human and robot) present in the system by subdividing the task into smaller sub-tasks and assigning those sub-tasks to the best agent (human/robot) for that specific sub-task. The sub-tasks involving high-level decisions are carried out by the human agent while the low-level tasks such as navigation in the local environment, and object

grasping are carried out by the robot agent autonomously using its onboard sensors. It ensures that human involvement is only required when uncertainty about a decision arises. The performance of the system was evaluated in a home-like environment where a mobile robot has to perform certain tasks like food delivery, table cleaning, etc. The robot receives the higher-level navigational commands from the human subject through an SSVEP-based neural interface and navigates to the target location using SLAM. A vision-based camera is then actuated to identify the desired object in the target location and a suitable grasping strategy is applied to grasp the desired object, The experiment achieved a task completion accuracy of 96.2%.

The shared-control-based strategy adopts various modalities to convey the user intent to the auxiliary controller. Among them, SSVEP is widely used for its high information transfer rate and high detection accuracy. Flickering sources on the screen are used to evoke the SSVEP in the subject's brain. In the vision-based strategy, SSVEP is often utilized by the subject to provide the necessary navigational command to the robot by observing its surrounding environment through a camera whose live video is presented on a screen. In all the cases the camera feed and the SSVEP sources are represented separately. However, a more interesting approach was proposed by *Yang et al*. [126] where they embedded the flickering sources directly on the objects visible in the live camera feed. A stereo-vision camera located in a fixed frame is utilized to capture the surrounding environment of a Baxter robot and identifies the nearby objects through colour segmentation. Subjects having the intent to select a particular object focus on the flickering source virtually embedded in it. A decoder interface was designed to decode the response of the brain, which enables the system to identify the target object. Once the object is identified, its location (after suitable coordinate transformation is conveyed to a vision-based controller which guides the robot to reach the target object. The controller is also responsible for avoiding collision with obstacles by coordinating the self and task motion of the robot They also proposed a novel adaptive algorithm to identify objects in different lighting conditions. Apan from the above contribution they introduced the least mean square method in the co-ordinate calibration task between robot and the camera. The experiment was validated using an object-picking task where two subjects participated and achieved an accuracy of 100% and 80% respectively.

Generally, shared control methods used in BCI applications are broadly categorized into two types i.e. sequential shared control and all-time shared control. In the first case, human the

autonomous controller and the human subject share the task in sequential order. The human subject delivers high-level commands such as the destination to reach and the autonomous controller performs the above task with maintaining certain conditions. The main drawback of such systems is the user's inability to intervene in the task while the autonomous controller is executing the task, i.e. once the task is assigned to the auxiliary/autonomous controller the user can no longer issue any further command until the controller becomes free. Such phenomena reduce the sense of authority of the user. *Deng et al.* [100] proposed a novel shared control scheme for the continuous sharing of tasks between humans and the auxiliary controller in a virtual wheelchair control application. A Bayesian shared controller was proposed to intelligently bine brain-actuated control and autonomous control introduced by the auxiliary controller to generate an optimal steering command for the wheelchair.

Concluding, Chapter 1 aims to provide a detailed review the Brain-Computer Interface (BCI) technology along with its different controller modules.

CHAPTER 2

PROPOSED WORK

ABSTRACT: Chapter 2 provides an approach to design and develop a brain-actuated 2-loop position control with an inner loop to control speed and an outer loop to control position of an artificial robotic limb for neuro-motor rehabilitation. Three distinct models of brain-actuated speed-setting with possible control policies and stability analysis are presented. The analysis reveals that *Takagi–Sugeno* type fuzzy control yields the best results. Additionally, cognitive load is also reduced significantly as the user needs to generate error-related potential once only to identify the position of the targeted object he needs to translate. Traditional BCI-based position control schemes utilize acquired motor imagery signals of the subject for motor actuation and error-related potential signals to detect positional overshoots. The positional overshoot results in steady-state positional error. Current BCI research attempts to reduce steady-state errors at the cost of high cognitive load of the subjects. The motivation here is to reduce the steady-state positional error without enhancing cognitive load of the subjects.

2.1 Introduction

Traditional brain-computer interface (BCI)-based position control schemes meant for neuro-motor prosthetic applications highly rely on two specific brain signals, called motor imagery (MI) and error-related potential (ErrP) [126][127]. While MI is used to initiate the movement of an electromechanical motor associated with a robot arm, the ErrP is used to stop its motion. So, MI-ErrP together acts as a simple on–off position control [128]. As on–off position control suffers from positional overshoot, causing non-zero steady-state error, current BCI research revolves around designing alternative modalities of position control schemes. However, the primary hindrance in realizing alternative modality lies in the inability of determining the amplitude of positional error from any well-known brain signals. For instance, ErrP can be utilized to detect the occurrence of positional error only, but neither the magnitude nor the sign of positional error can be detected from the occurrence of ErrP [129]. The paper makes an attempt to design different modalities of speed-setting based on the measured value of the positional error signal to examine the most appropriate scheme. The

choice of the appropriateness of the scheme is determined by two factors: stability margin of the control system and the cognitive load of the subject. In fact, there exist varieties of velocity modulation scheme in traditional 2-loop position control schemes [130]. However, due to experimental constraints, these schemes are not directly applicable in the present work. The paper proposes three alternative schemes of velocity modulation in BCI-induced position control. Although the schemes have their own diversity, there still remains commonality in utilizing the occurrence of the ErrP signal to identify the location of the target. The variation in the brain actuated velocity-adaptation scheme arises due to the choice of the nonlinearity in the positional error to speed mapping. The first scheme utilizes a proportional gain setting of K (< 1) to the signed error to develop the speed-adaptation law. The second scheme sets the current speed half of its last value and also asserts sign reversal, each time the robotic arm crosses the target position. In other words, at each zero-crossing of positional error signal, the speed is set half of its last value with a sign reversal. This scheme ensures that ultimately speed is decaying toward zero before the link comes to a halt position. The third scheme employs the well-known Takagi–Sugeno approach for fuzzy reasoning for automatic speed-setting of the robotic arm [131]. The Takagi–Sugeno scheme considers error and its time-derivative for speed-setting of the robotic arm.

An analysis of stability of the three velocity-adaptation strategies is undertaken here using root locus technique. An insightful look into the root loci reveals that the Takagi–Sugeno scheme of speed-setting yields the best performance with reference to stability margin. Cognitive load in all the proposed schemes being uniformly low, the Takagi–Sugeno scheme is given importance for its better stability.

Chapter 2 is classified into seven sections. In Section 2.1, an overview of the 2-loop position control scheme for the neuro-prosthetic limb is given. Section 2.2 provides three alternative strategies for speed-setting. Stability analysis of the proposed schemes using root locus technique is examined in Section 2.3. Experimental details are presented in Section 2.4. Performance analysis is given in Section 2.5. The list of concluding remarks is summarized in Section 2.6.

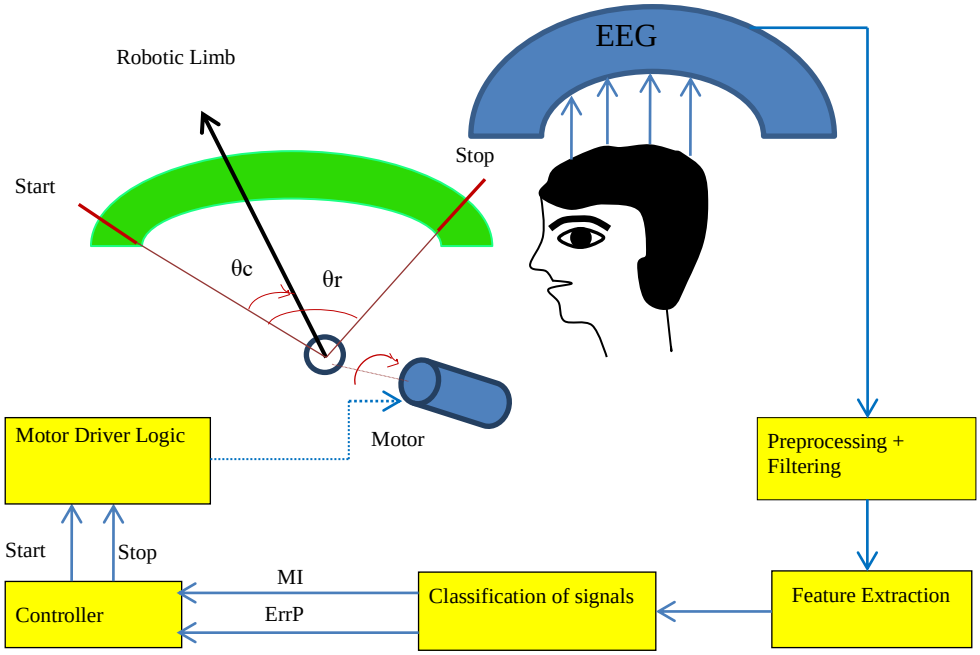


Figure 2.1: Motor on-off control by MI and ErrP signals

2.2 System Overview

Traditional BCI-schemes for position control of neuro-prosthetic limbs utilize on– off control strategy, where MI signal is used to initiate motor-movement and the ErrP signal to switch off the motor [126][127][128]. Such types of on–off position control schemes yield positional overshoot, resulting in nonzero steady-state positional error.

Large positional overshoot is undesirable for the present application, concerning people with neuro-motor diseases. The present research thus is targeted to reduce the positional overshoot. There are several approaches in traditional control theory [130] to reduce positional overshoots. The one chosen for the current application is velocity modulation of the end-effecter of the robotic limb driving the artificial neuro prosthetic upper limb. A commonsense reasoning reveals that for small overshoot, a small (negative) speed-setting of the end-effecter is needed, so that the robotic limb reaches the target with reduced or no overshoot. The negativity in speed-setting refers to speed reversal each time the robotic link crosses the target position. The sign reversal and reduction in speed guarantees stabilization of the position control system, which is examined in detail in the next section. Three different strategies for velocity modulation are proposed here based on the philosophy narrated above.

The first, probably the simplest, strategy deals with proportional gain setting of the velocity modulator with signed positional error as the input. The proportional gain factor is kept below one, so that the stability of the velocity adapter toward zero positional error is ascertained. The second scheme of velocity modulation is concerned with both speed reversal at each zero-crossings of positional error and also reduction of speed by a fixed factor, here chosen 2, with respect to the last speed of the robotic link before the zero-crossing. The choice of the speed-reduction factor by 2 is somewhat arbitrary, but the effect of such choice is interesting for mathematical simplicity in designing the transfer function of the velocity modulator.

Both the above schemes have fixed gain setting of the velocity adapter. The third strategy makes an attempt for variable gain of the speed modulator realized with rule-based system. Again, there are several approaches of rule-based gain setting of the velocity modulator. The well-known Takagi–Sugeno fuzzy reasoning technique is used here to select the variable DC gain based on the measurement of error in all except the first error cycle [132][133]. The first error cycle is used to identify the position of the target based on the occurrence of the ErrP signal when the robotic limb has a fixed pre-defined trajectory of motion toward the target. The user can observe the target and automatically select its position indirectly by the first occurrence of the ErrP signal, when the robotic link crosses the visually examined target position.

Figure 2.2 provides a schematic overview of the complete proposal for the 2-loop position control. The scheme is meant for one-dimensional position control of a robotic arm over a semi-circular are with a pre-defined start and variable stop position defined online by the end-user. The variability in the stop position is needed to assist an end-user with neuro-motor disability to select an object of his/her interest to be picked up by the robot arm. Like traditional BCI-based position control, here too, MI and ErrP signals, respectively, are utilized to switch on and off the motor associated with the robotic link. The motor is switched on when the end-user wants to start moving the robotic link. On the other hand, ErrP is released by the end-user when he/she finds the robotic link to cross the target position. The occurrence of the ErrP thus determines the location of the target position, where the end-user wants the robotic link to stop. However, because of inertia, the motor employed in the robot arm is sluggish and thus turns by extra angle even after generation of stop command. So, the stop position cannot correctly describe the location of the target mentally fixed by the subject. Here lies the importance of the present work. The solution is presented next.

The problem of correctly determining the location of the user-intended target position here is performed by utilizing the onset of the ErrP signal. This is accomplished by allowing a capacitor to charge up to a maximum voltage corresponding to the angular position of the target at the onset of ErrP-release. The capacitor, which here is charged up through a rotary reference potentiometer driven by the motor, is disconnected from the moving armature of the potentiometer by a switch at the onset of the ErrP. Thus, the charged up voltage across the capacitance represents the reference angular position of the robotic link. A buffer with high input impedance is connected across the capacitance to avoid voltage-drooping. Thus, the target position can be correctly determined automatically by the end-user using the ErrP signal. The reference position once known, the control policy does not require end-user's attention further during the rest of the control task, thereby reducing the cognitive load of the experimental subject.

The rest of the control task is similar to traditional regulatory-type control. In the present realization, a 2-loop position control scheme is adopted with the outer loop used for setting the speed of the robotic arm based on the positional error, and the inner loop to control the speed using tacho-generator feedback [134]. Such 2-loop control policy enhances response-speed without losing stability of the control system. The fundamental aspect of the proposed 2-loop control policy that differs from its traditional counterpart lies in the design of the brain-actuated speed controller (BASC) block. This block also is new to the domain of BCI research. The BASC fixes the reference speed of the inner control loop by assessing the positional error. Three different models of BASC are proposed, details of which are given in Section 2.4.

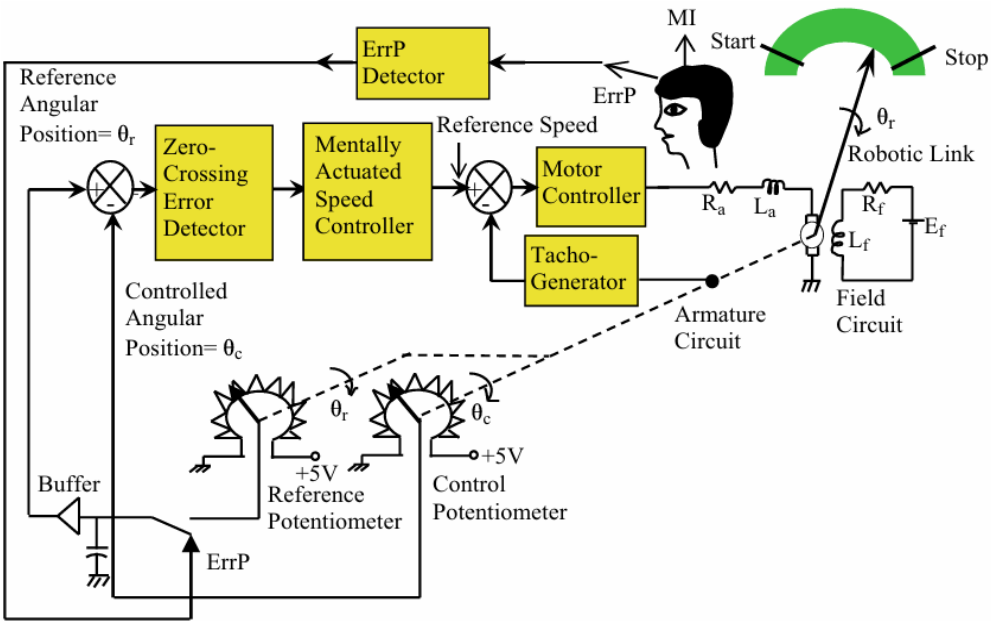


Figure 2.2: Schematic diagram of the 2-loop position control system

2.3 MI/ErrP Classification

EEG signals are often found to be contaminated with muscle artifact and electrical noise picked up from the external environment. Common Average Referencing (CAR) [135] is employed here to filter the external noise that appears uniformly across all channels. Additional filtering is undertaken by employing Band-Pass Filters (BPFs) of suitable pass-bands to select signals of specific frequencies for selected cognitive tasks, planned for signal acquisition from given channels [136] [137]. The filtered signals are processed for extraction of certain features, which are fed to classifiers for classification of the targeted cognitive tasks, here MI and occurrence of error.

MI and ErrP Pre-Processing:

The MI signals that appear in Mu (8-12 Hz) and Beta (16-24 Hz) bands are passed through an elliptical BPF filter of order 6 and pass-band: 8-24Hz. The choice of elliptical filters is inspired by its sharp roll-off characteristics around the boundaries of the pass-band. The ErrP signals are passed through a elliptical BPF of order 4 and pass-band: 0.1-10 Hz.

MI/ErrP Feature Extraction:

Common Spatial Pattern (CSP) features have remarkable performance in MI classification [138][139]. The past success of CSP prompted us to realize extraction of MI features using CSP. Here CSP-Filter-Bank approach is employed following *Fabien et al.* [140] to extract MI features. Adaptive Auto-Regressive (AAR) parameters have also shown excellent performance in ErrP classification [141]. This motivated us to select AAR parameters for ErrP classification. Here 7^{th} order AAR parameters are utilized for feeding to ErrP classifier for its classification.

MI/ErrP Decoding/Classification:

Linear Support Vector Machine (L-SVM) classifier is selected to classify both the MI and ErrP signals. The choice of L-SVM is induced by its exceptional performance in MI and ErrP classification in the literature.

2.4 Modelling of the Proposed Brain-Actuated Speed Controller

In this chapter, three distinct models of BASC are proposed. The BASC is required to switch over the control task from brain-inspired activation mode to automatic mode using the reference potentiometer to the capacitor connection switch, activated by the ErrP signal [142]. After the BASC is activated, the zero-crossing in positional error is detected by additional electronic hardware, such as a comparator circuit (referred to as zero-crossing error detector in Figure 2.2. The three controller models proposed are presented below.

2.4.1 Brain-Actuated Proportional-Type Speed Modulation

In proportional-type speed control, the angular speed θ_c is set proportional to signed positional error $(\theta_r - \theta_c)$, where θ_r and θ_c, respectively, denote reference angular position and feedback position of the motor shaft/armature of the control potentiometer.

$$\dot{\theta c} = K\,(\theta_r - \theta_c) \qquad (2.1)$$

where *K* essentially needs to be less than 1 for stability. The stability for the above choice of K is ensured for convergence of $\dot{\theta c}$ approaching zero, when error $(\theta_r - \theta_c)$ approaches zero. It is

apparent from (2.1) that in Laplace (s) domain, the transfer function of the proportional-type speed controller is given by

$$s\theta_c(s)/(\theta_r(s) - \theta_c(s)) = K \qquad (2.2)$$

Expression (2.2) takes care of automatic sign reversal of the speed for sign reversal of positional error. It is important to note that proportional-type speed controller does not require any zero-crossing detector, introduced in Figure 2.2, as (2.1) holds at zero-crossing and nonzero values of error as well.

2.4.2 Zero-Crossing Sensitive Brain-Actuated Speed Modulation

The zero-crossing sensitive speed modulator sets the current speed of the robotic link at each zero-crossing of error as half of the last speed before zero-crossing. The speed reversal also takes place at each zero-crossing. Formally, the current speed $\dot{\theta}c$ is half of its last speed ($\dot{\theta}c - 1$).

$$\dot{\theta}c = -(1/2)\,(\dot{\theta}c - 1) \qquad (2.3)$$

The formal approach to modelling (2.3) is presented graphically in Figure 2.3. In this figure, it is assumed that each error cycle period, T is reduced by δ.

$$c(t) = [u(t) - u(t - T)] - [u(t - T) - u(t - (2T - \delta))] + [u(t - (2T - \delta)) - u(t - (3T - \delta))] - \cdots + [u(t - (nT - (n - 1)\delta)] \qquad (2.4)$$

Simplifying (2.4) we obtain (2.5),

$$c(t) = u(t) - 2u(t - T) + 2u(t - (2T - \delta)) - \cdots + u(t - (nT - (n - 1)\delta)) \qquad (2.5)$$

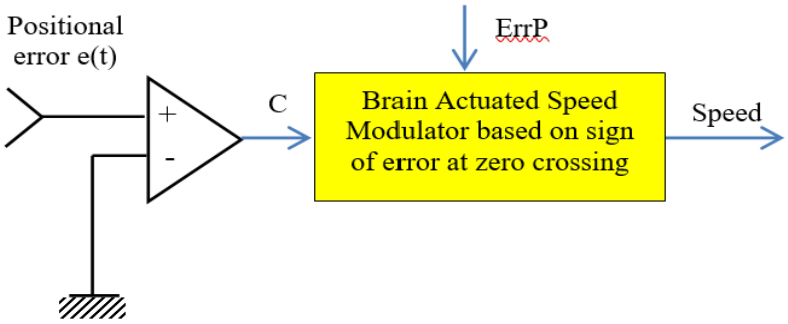


Figure 2.3: Brain Actuated Speed Modulator Model

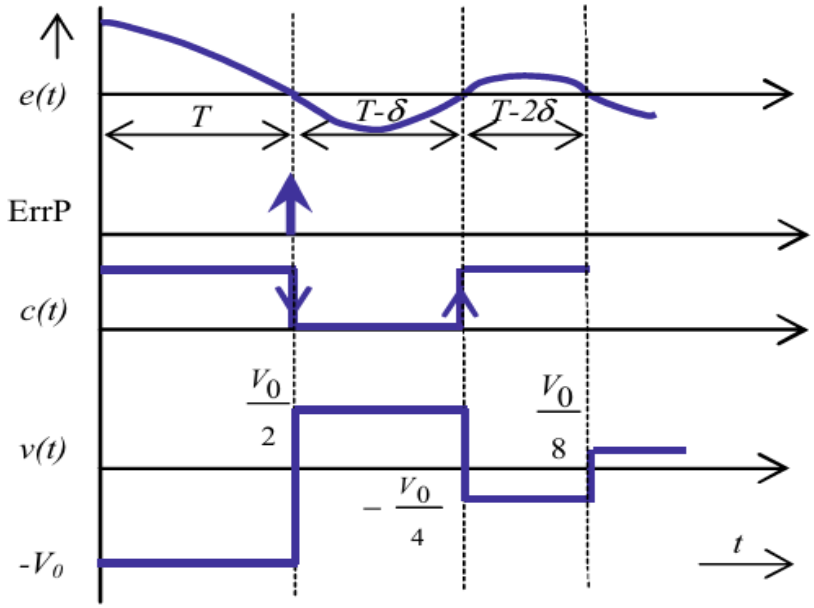


Figure 2.4: Timing diagram of zero-crossing sensitive speed modulator

Velocity setting of the zero-crossing sensitive speed modulation can be expressed as:

$$v(t) = (v_0/2)\,[u(t) - u(t - T)] - (v_0/4)[u(t - T) - u(t - 2T + \delta)] + \cdots + (v_0/2n)[u(t - (n-1)T + (n-2)\delta - u(t - nT + (n-1)\delta)] \quad (2.6)$$

where v_0 denotes the initial speed of the robotic link.

Taking Laplace transform of (2.5) and (2.6) we, respectively, obtain (2.7) and (2.8).

$$C(s) = (1/s)\,(1 - 2e^{-sT} + 2e^{-s(2T-\delta)} - 2e^{-s(3T-2\delta)} + \cdots + e^{-s(nT-(n-1)\delta)}) \quad (2.7)$$

$$V(s) = \left(\frac{v_0}{s}\right)\left(\frac{1}{2} - \frac{3}{4}e^{-sT} + \frac{3}{8}e^{-2sT+\delta s} - \cdots + \frac{1}{2^n}e^{-(n-1)sT+(n-2)\delta s}\right) \quad (2.8)$$

Simplifying (2.7) and (2.8) by approximating $e^{-sT} = 1 - sT$, and substituting T = 1s,

$$C(s) = \frac{1}{s}\left[\frac{s+2}{s+1}\right] \quad (2.9)$$

and

$$V(s) = \frac{v_o}{2}\left[\frac{1}{4s+3}\right] \quad (2.10)$$

2.4.3 Takagi–Sugeno Fuzzy Model for Speed Adaptation

The Takagi–Sugeno (T-S)-type fuzzy controller is selected to handle the diversity of amplitude and sign of error and its time-derivative to determine the speed of the robotic link at each zero-

crossing of error. Sample rules used for T-S-type control involving fuzzy quantifiers: SMALL POSITIVE, SMALL NEGATIVE, NEAR ZERO and the like to errors and error derivatives are given below to compute the speed as a linear combiner of the said parameters.

Rule 1: If error (e) is Small Positive and error derivative ($\dot{e}$) is Small Negative then speed is ($0.1 \times (e) - 10 \times (\dot{e})$).

Rule 2: If error (e) is Large Positive and error derivative ($\dot{e}$) is Small Negative then speed is ($0.5 \times (e) - 100 \times (\dot{e})$).

Rule 3: If error (e) is Small Positive and error derivative ($\dot{e}$) is Large Negative then speed is ($0.1 \times (e) - 10 \times (\dot{e})$).

Rule 4: If error (e) is Large Positive and error derivative ($\dot{e}$) is Small Positive then speed is ($0.5 \times (e) - 100 \times (\dot{e})$).

Rule 5: If error (e) is Small Positive and error derivative ($\dot{e}$) is Small Positive then speed is ($0.1 \times (e) - 10 \times (\dot{e})$).

Rule 6: If error (e) is Small Positive and error derivative ($\dot{e}$) is Large Positive then speed is ($0.1 \times (e) - 10 \times (\dot{e})$).

Rule 7: If error (e) is Large Positive and error derivative ($\dot{e}$) is Large Negative then speed is ($0.5 \times (e) - 100 \times (\dot{e})$).

Rule 8: If error (e) is Large Positive and error derivative ($\dot{e}$) is Large Negative then speed is ($0.5 \times (e) - 100 \times (\dot{e})$).

Rule 9: If error (e) is Small Negative and error derivative ($\dot{e}$) is Small Negative then speed is ($0.1 \times (e) - 10 \times (\dot{e})$).

Rule 10: If error (e) is Small Negative and error derivative ($\dot{e}$) is Small Positive then speed is ($0.1 \times (e) - 10 \times (\dot{e})$).

Rule 11: If error (e) is Large Negative and error derivative ($\dot{e}$) is Small Negative then speed is ($0.5 \times (e) - 100 \times (\dot{e})$).

Rule 12: If error (e) is Near Zero and error derivative ($\dot{e}$) is Small Negative then speed is ($0.04 \times (e) - 0.01 \times (\dot{e})$).

The coefficients of the error and error time-derivatives in the above rules are selected intuitively. It is apparent from the structure of the fuzzy rules that in Takagi– Sugeno-type fuzzy adaptation, that the speed of the robotic controller is determined by the positional error and its derivative [131]. Formally, let the current speed of the controller be $\dot{\theta}c(t)$ and the positional error is given by $(\theta_r - \theta_c)$. Then the Takagi– Sugeno response of the controller is given by (2.11).

$$\dot{\theta}_c(t) = K_1\, \dot{\theta}c(t-1) + L_1(\theta_r(t) - \theta_c(t)), \qquad (2.11)$$

where *K1* and *L1* are gain constants of user's choice.

On taking Laplace transform of (2.11), it is found that the ratio of speed and positional error is given by

$$s\theta c(s)/(\theta r(s) - \theta c(s)) = L_1 s/\{1 - (K_1 e^{-sT}) + (L_1/s)\}\, L_1 s/(K_1 T s^2 + (1 - K_1)sT + L_1)$$

$$\text{with } e^{-sT} = 1 - sT \qquad \textbf{(2.12)}$$

It is apparent that the above transfer function is stable for all K1 < 1.

2.5 Analysis of Stability Margin of the Proposed Controllers

The BCI-based position control system may get stuck into limit cycles for possible range of parameters of the velocity-adaptation unit. Limit cycles are small amplitude oscillations around the equilibrium point of a control system. They are undesirable as stable limit cycles bring the system at the verge of instability. An analysis of stability of the proposed BCI-based control system thus is needed. Several approaches are available in the literature [143]. Root locus is one such popular technique to analyse stability of the control system. Given the open-loop transfer function *G(s)H(s)*, where *G(s)* is the forward path gain and *H(s)* is the feedback factor, one can determine the location of the roots of the characteristic equation: $1 + G(s)H(s) = 0$ for varying DC gain $K = 0$ toward infinity. It may be added that the DC gain *K* lies in the forward path of the system, and large vale of *K* pushes the system toward instability. Determining maximum DC gain to keep the system stable thus is an important issue in control system design. Root locus technique provides a simple means to evaluate the theoretical maximum DC gain above which the system becomes unstable.

In this paper, the stability analysis of the closed-loop system is performed by root locus technique. Consequently, for each of the three proposals for speed modulation, the root locus diagram is plotted, and stability analysis is performed in terms of maximum allowable DC gain of the system. The maximum DC gain here is defined as the gain of the system at the crossover points of the root locus plot with the $j\omega$ axis. It is known that the system remains stable as long as the roots of the characteristic equation lie within the left half of $\sigma + j\omega$ plane.

The following parameters are used to construct the root loci. In Figure 2.2, the motor open-loop transfer function is found as $G_{motor}(s) = 16.13/(s^2 + 61s + 303)$. The tacho-generator has a gain of $K_t = -1$. The transfer function of the proportional type speed modulator is K. Transfer function of the zero-crossing sensitive speed modulation based on positional error at each zero-crossing obtained from (2.9) and (2.10) is $C(s)/V(s) = (v_0/2)\,[s(s + 1)/(s^2 + 6s + 8)]$, where v_0 is the initial speed of the robotic link. The transfer function of the Takagi–Sugeno fuzzy controller can be expressed as $L_1/[1 + (L_1/s) - K_1 e^{-sT}]$. K_1 and L_1 are the multiplication factors to error and error derivate, respectively, with $K_1 < 1$ and an unbounded L_1. The choice of the restrictive bound on K_1 and boundlessness of L_1 are determined by stability considerations of the Takagi–Sugeno fuzzy velocity-adaptation rules.

Figure 2.5(a) provides the block diagram of the complete loop of the position control system, where speed adaptation is performed by proportional gain setting. The corresponding root locus diagram is given in Figure 2.5(b).

Figure 2.6(a) provides the block diagram of the complete loop of the position control system, where speed adaptation is performed by reversing and reducing the speed on each zero-crossing of the positional error. The corresponding root locus diagram of zero-crossing sensitive speed modulation system is given in Figure 2.6(b).

Figure 2.7(a) provides the block diagram of the complete loop of the position control system, where speed adaptation is performed by Takagi–Sugeno fuzzy rules [144].
The corresponding root locus diagram for two different choices of K1and L1 is given in Figure 2.7(b), (c)

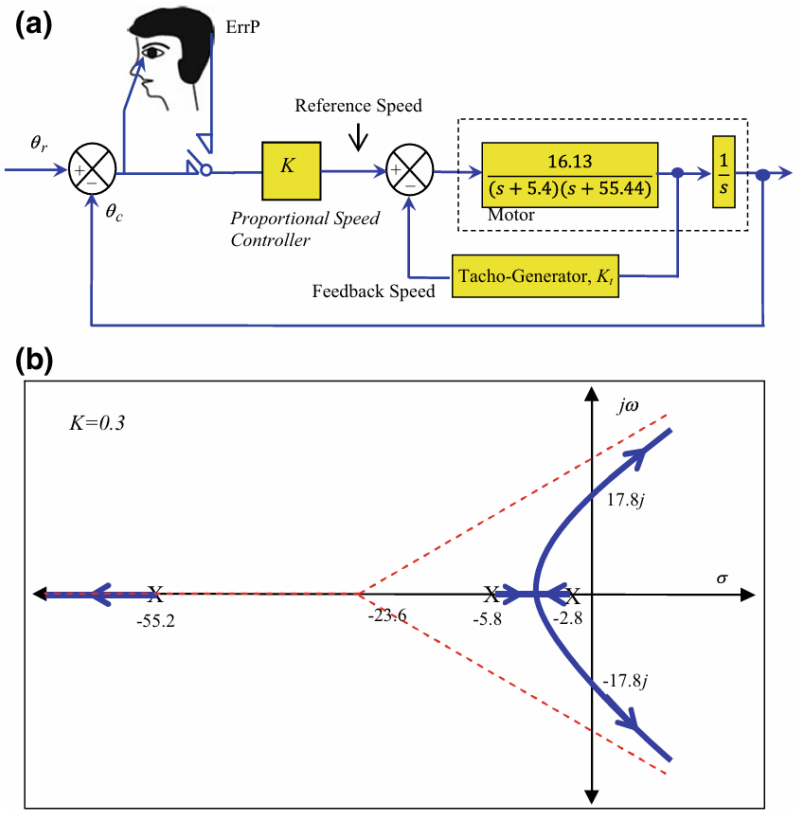


Figure 2.5: a) Block diagram of the proportional-type modulation system, **b)** Root locus for proportional type speed modulation with K = 0.3

2.6 Experiments and Results

An experimental setup is developed in artificial intelligence lab, Department of Electronics and Tele-Communication Engineering, Jadavpur University to undertake the experiment for BCI-based position control for a 2-link robot arm developed in the laboratory and 6-link Jaco humanoid robot arm, manufactured by Kinova. The 2-link robot arm includes two motors, one for turning one link, and the other for displacing the second link. In the present experiment, only the first link used for turning the robot is utilized (Figure 2.8(a)). The motivation here is to move the end-effecter at the desired position (right pad, clockwise) from the start position (left pad) in Figure 2.8(b)). The control parameters, including steady-state error, peak overshoot and settling time are evaluated and reported later in a table.

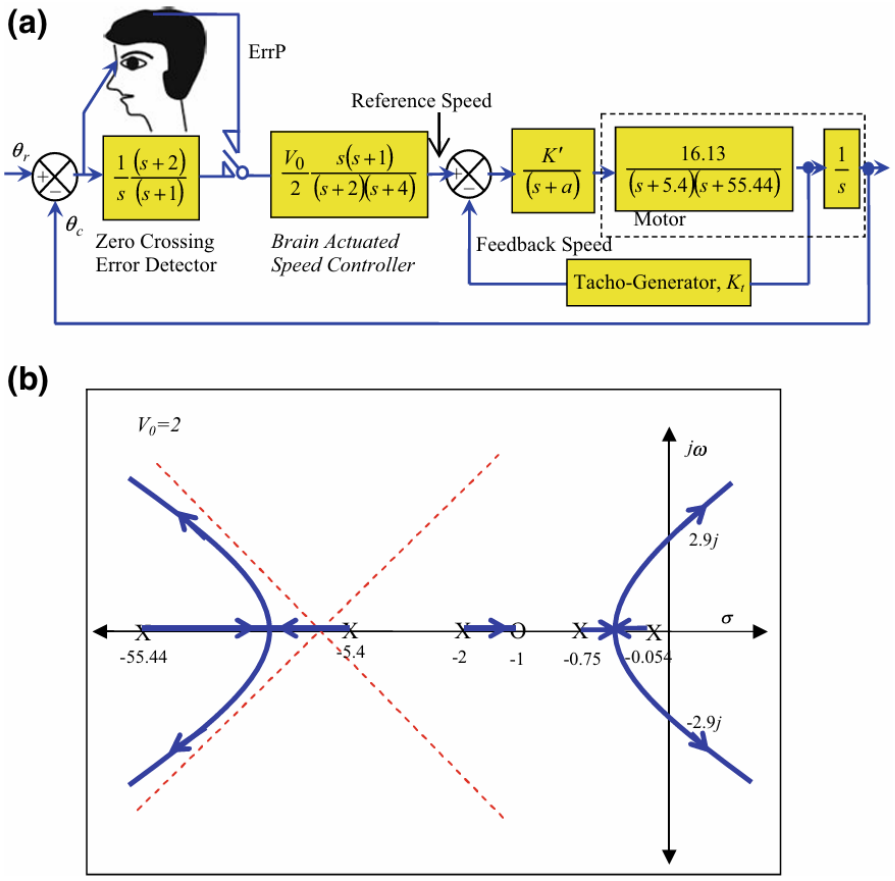


Figure 2.6: (a) Block diagram of the zero-crossing sensitive speed modulation system, **(b)** Root locus for zero-crossing sensitive speed modulation system with $V_0 = 2$

A 6-link Jaco humanoid robot arm also is employed to serve the necessary position control task using three links. Here, an experimental subject needs to move an object from a given start position to a pre-defined terminal position in the robot's workspace (Figure 2.9). The links are here triggered in a random order as per user-requirement. To select individual link Steady-State Visual Evoked Potential (SSVEP) is utilized. This is accomplished by the following means.

2.6.1 Preamble

Light emitting diodes (LEDs) flickering at distinct frequencies are connected with the links of given robot arm. When the user wants to select a particular link, he/she needs to look at the

selected link. Naturally, the flickering frequency of the LED is picked up by the brain, and the BCI-system comes to learn the right link the user wants to select for the present task [145].

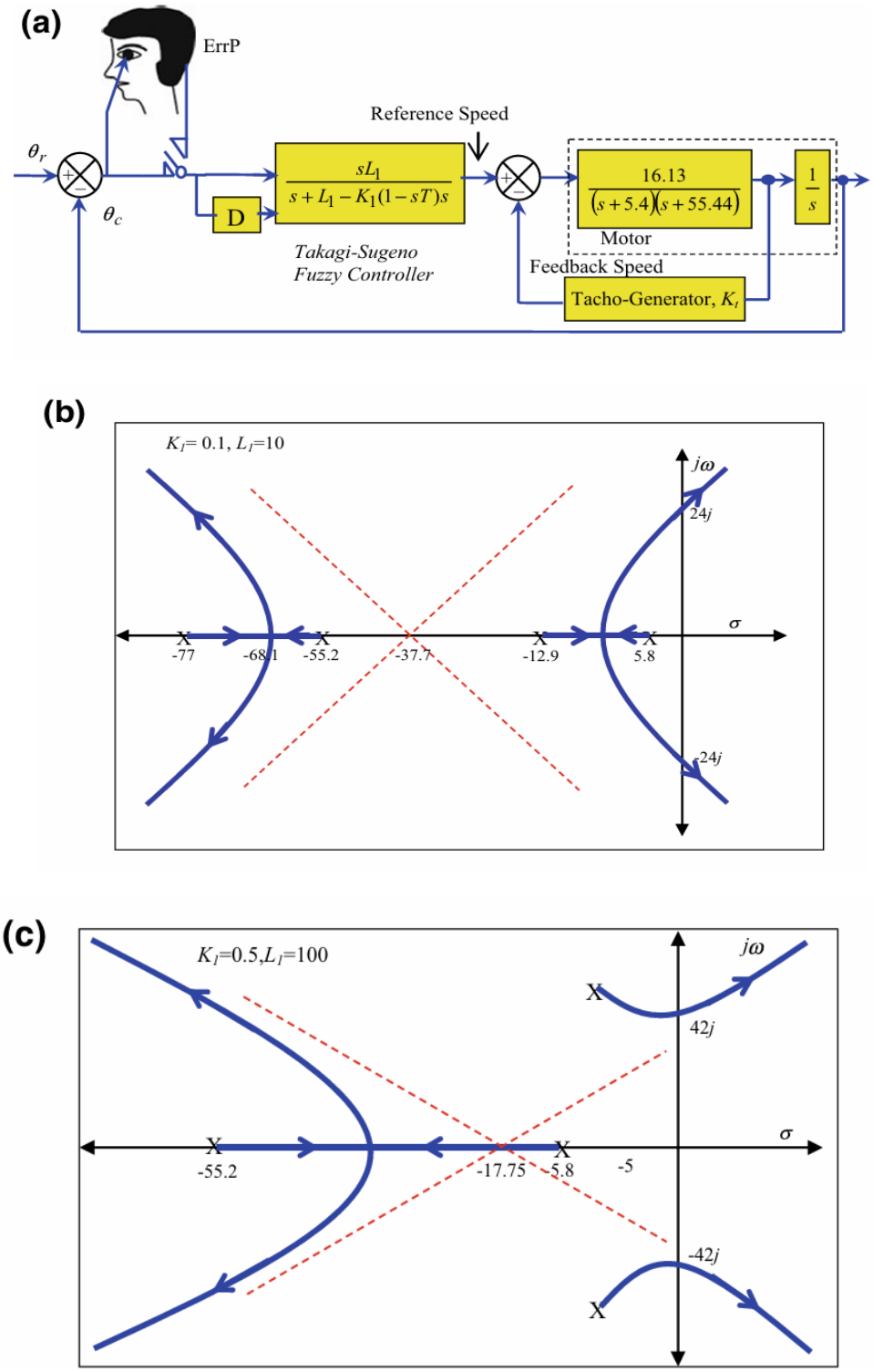


Figure 2.7: a) Block diagram of Takagi–Sugeno fuzzy speed modulation system, **b)** Root locus for Takagi– Sugeno speed modulation with K_1 = 0.1, L_1 = 10, **c)** Root locus for Takagi–Sugeno speed modulation with K_1 = 0.5, L_1 = 10

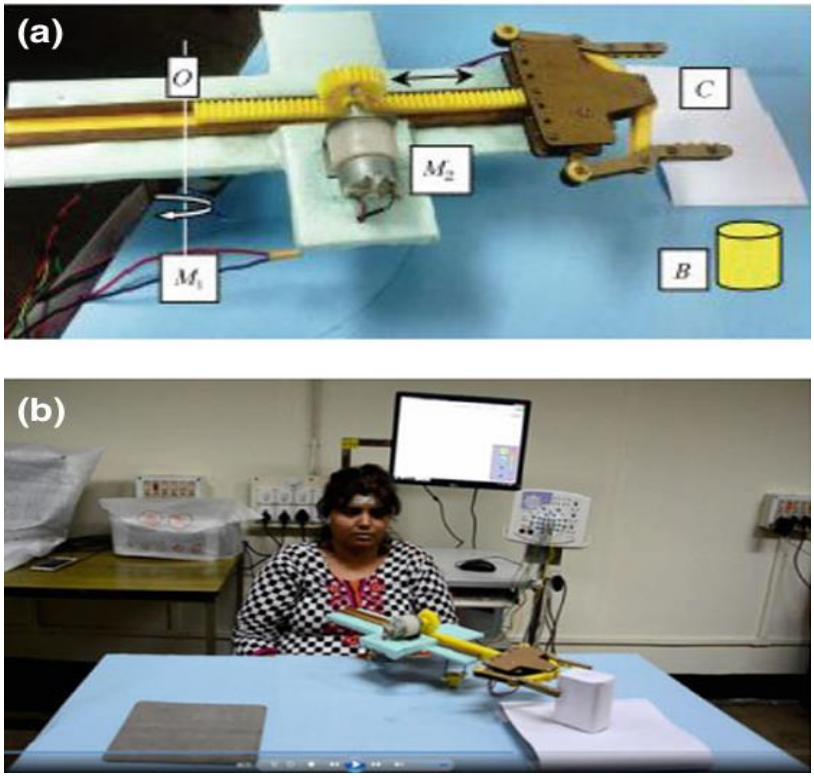


Figure 2.8: (a) Lab-developed model of a 2-link robot arm, **(b)** Single-link position control using motor M_1



Figure 2.9: Photograph of the experimental setup for 3-link Position Control

After the link selection by the SSVEP is undertaken, the user performs motor imagination signal to make a link aware that the user wants the link to start moving in the intended direction. The intended direction is here selected by right/left hand motor imagination. For

clockwise motion of the link, the right-hand MI is needed. For the counter clockwise movement of the link, the left-hand MI is needed. After a link is selected for motion and MI is performed to make the link moving, the subject has to continuously monitor whether the link crosses the target position. Once the link attempts to cross the target position, the ErrP is released by the brain. The target position in the present context is a point in 1-dimension, a straight line in 2-dimension and a plane in 3-dimensional position control [126]. On detection of the ErrP, the robot is commanded to stop the motion of the link. However, because of the inertia of motor, the link by that time has advanced by an offset angle. To avoid this overshoot one approach is to turn the link in reverse direction with lower speed. The turning of the link in reverse direction is repeated till convergence of the algorithm.

Table 1: List of features extracted from the EEG signals

EEG signals	Features	No. of features
MI	Common spatial pattern (CSP) features (obtained by filter-bank approach)	126
ErrP	Adaptive auto regressive (AAR) parameter	21
SSVEP	Power spectral density (PSD)	198
	Auto regressive (AR) features	200

The control policy adapted then identifies the position of the target by the occurrence of the ErrP and switches it to automatic human-free mode by traditional error-based position control subsequently. Three different speed modulation techniques and hence control policies are proposed. The analysis of the modalities is discussed in the last section.

2.6.2 Signal Processing

This paper emphasizes artifact removal, filtering and feature extraction from three distinct types of EEG-waveforms: (I) SSVEP, (II) MI and (III) ErrP [146]. Artifacts due to eye-blinking and muscle artifacts are removed by independent component analysis (ICA) [147]. Narrow band spatial filters with appropriate mid-frequency and bandwidth are used to filter

the above signals. After filtering and artifact removal, specific signal features are extracted from the said signals [148], [149]. The list of the features extracted is given in Table 1.

2.6.3 Classification

Once the features extraction is over, the feature of the signal is fed to a classifier. The task of the classifier is to classify each signal into true positive or false negative. Such classification needs prior generation of training instances for each class and training the classifier with the instances of the said two classes [150]. After classifier training is over, it can be done for classification of unknown input instances. Any traditional supervised learning classifier can be used to serve the present problem. We here used linear discriminant analysis (LDA) classifier for the present 2-class classification problem for the three brain signals [151], [152]. Classification accuracies obtained during training and test phases are given in Table 2.

Table 2: Classification accuracy in the training and the test phase.

Brain signal	% Classification accuracy in	
	Training phase	Test phase
SSVEP	99.2	96.2
MI	98.6	96.1
ErrP	98.4	96.3

2.6.4 Performance Analysis

The performance of the proposed BCI-based control system is examined here with respect to the state-of-the-art research in the said domain. Table 3 provides the results of comparative study in performance of the proposed and existing technique with reference to four different metrics: percentage steady-state error, percentage peak overshoot, settling time and cognitive load. The first three parameters reflect the control theoretic merits of individual schemes. The last metric, called cognitive load, is a coinage from the BCI literature. Here, it represents the attention the subject needs to pay for execution of the control task. In the existing BCI-based control literature [128], the subject has to continuously monitor zero-crossings in positional error, which incurs extra cognitive load to the subject. This has been avoided here by

restricting ErrP detection once only to determine the target position of the robotic arm. Subsequent zero-crossings are detected here automatically by additional hardware, thereby reducing the cognitive load of the subject significantly.

It is apparent from Table 3 that the proposed Takagi–Sugeno-based fuzzy controller outperforms existing BCI-based controllers and the proposed other two controllers in all respects. The remaining two proposed controllers outperform existing ones with respect to all four metrics.

2.6.5 Conclusions

Chapter 2 provides a scheme for BCI-based 2-loop controller design with an outer loop for position control and speed-setting, and an inner loop for speed control of a robot arm. Three different models for brain-actuated speed-setting are proposed and the stability analysis of the models is performed using the well-known root locus technique. The results of stability analysis envisage that the proposed Takagi–Sugeno model outperforms the existing and other competitive models. In addition, control theoretic performance analysis undertaken over the models confirms the exceptional performance of the Takagi–Sugeno model over the existing and other two proposed models. Experiments have been undertaken over both healthy subjects and patients with neuro-motor disability to study the performance of the proposed system. It is noted that because of low cognitive load, patients with neuro-motor disability could also execute the control task easily without difficulty.

Table 3: Comparative controller performance analysis

Technique used	Performance metrics			
	Steady-state error (e_{ss})%	Peak overshoot (M_p)%	Settling time (t_s) sec	Cognitive load
Only MI	7.73	5.4	35	High
MI + ErrP	2.10	4.9	31	High
MI speed-setting + ErrP +	0.20	4.2	24	Medium
Scheme I (proportional-type speed modulation)	0.18	3.8	22	Low
Scheme II (zero-crossing sensitive speed modulation)	0.04	1.1	12	Low
Scheme III (Takagi–Sugeno fuzzy control)	0.02	1.05	10	Low

CHAPTER 3

SIMULATION AND RESULTS

The experiment includes 2 phases, called training and test phases. During the training phase, the subject is trained to release MI (motor imagery), when he is asked to perform RHMI using a PPT presentation. He is also trained to produce ErrP(error-related potential) during the occurrence of zero-positional error for the first time. During the test phase, the subject performs MI and ErrP based on her previous experience in a natural mode. During the training phase we identified the best features-classifier combination for the best results of classification accuracy. Here, for MI classification, we use Common Spatial Pattern (CSP) features, and for ErrP classification we utilized Adaptive Auto-regressive (AAR) parameters. The classifier in the present context is a Linear Discriminant Analysis (LDA) classifier. We could use Support Vector Machine (SVM) classifier, but the LDA performance was comparable with Linear SVM classifier. So, we have chosen LDA.

3.4 Design of the Brain-Actuated Speed Modulator

The brain-actuated speed modulator/controller asserts the linear speed of the motor to half of its last value after each zero-crossing of the positional error signal and also reverses the direction of motion of the robotic link. The first cycle of zero-crossing in positional error is notified by the occurrence of ErrP, while the subsequent zero-crossing in positional error is determined by additional hardware involving a comparator as shown in Figure. When the positional error crosses sign from positive to negative, the comparator output changes from one to zero, and vice-versa. Thus, for each one-to-zero change of the comparator output, the sign of speed is positive, and for each change in comparator output from zero to one, the sign of speed is negative. In both the cases, current speed is set to half the value it had before last zero-crossing in error. The velocity and speed profiles are shown in Figure 3.1.

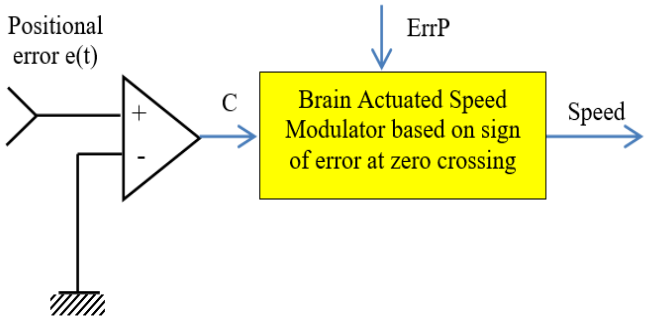


Figure 3.1: Brain actuated speed modulator model

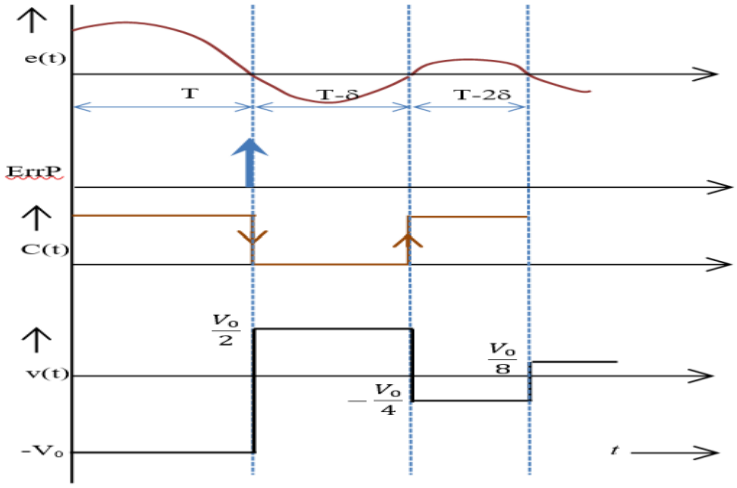


Figure 3.2: An example of the speed modulation with respect to positional error

In Figure 3.2, we presumed that the positional error in its positive or negative half cycles is reduced by δ. Presuming that the first half-cycle has a duration of T sec, the subsequent half cycles will have duration T- δ, T-2δ, …, and the like. The comparator output given in Figure 3.2 can be mathematically expressed as in Equation 3.1.

$$c(t) = [u(t) - u(t-T)] - \left[u(t-T) - u\left(t-(2T-\delta)\right)\right] + \left[u\left(t-(2T-\delta)\right) - u\left(t-(3T-2\delta)\right)\right] + \left[u\left(t-(2T-\delta)\right) - u\left(t-(3T-2\delta)\right)\right] - [u(t-(3T-2\delta)) - u(t-(4T-3\delta))] + \ldots + [u(t-(nT-(n-1)\delta)]$$

$$= \boldsymbol{u(t) - 2u(t-T) + 2u\left(t-(2T-\delta)\right) - 2u\left(t-(3T-2\delta)\right) + \cdots \ldots} \\ \boldsymbol{+u\left(t-(nT-(n-1)\delta)\right)} \qquad (3.1)$$

It is also apparent from Figure 3.2 that the speed-profile v(t) generated by the brain-actuated

controller is given by Equation 3.2, where V_0 is the initial speed.

$$v(t) = \frac{V_0}{2^1}[u(t) - u(t-T)] - \frac{V_0}{2^2}[u(t-T) - u(t-2T+\delta)] + \frac{V_0}{2^3}[u(t-2T+\delta) - u(t-3T+2\delta)] - \frac{V_0}{2^4}[u(t-3T+2\delta) - u(t-4T+3\delta)] + \cdots + \frac{V_0}{2^n}[u(t-(n-1)T+(n-2)\delta) - u(t-nT+(n-1)\delta)]$$

$$= \boldsymbol{\frac{V_0}{2}u(t) - \frac{3V_0}{4}u(t-T) + \frac{3V_0}{8}u(t-2T+\delta) - \frac{3V_0}{16}u(t-3T+2\delta) + \frac{3V_0}{32}u(t-4T+3\delta) - \ldots + \frac{V_0}{2^n}u(t-(n-1)T + (n-2)\delta)} \quad \boldsymbol{(3.2)}$$

Taking Laplace Transform of Equation 3.1, we obtain (3.3).

$$C(s) = \frac{1}{s} - \frac{2}{s}e^{-sT} + \frac{2}{s}e^{-s(2T-\delta)} - \frac{2}{s}e^{-s(3T-2\delta)} + \ldots \ldots + \frac{1}{s}e^{-s(nT-(n-1)\delta)}$$

$$= \boldsymbol{\left(\frac{1}{s} + \frac{2}{s}e^{-2sT}e^{\delta s} + \frac{2}{s}e^{-4sT}e^{3\delta s} + \ldots\right) - 2\left(\frac{1}{s}e^{-sT} + \frac{1}{s}e^{-3sT}e^{2\delta s} + \frac{1}{s}e^{-5sT}e^{4\delta s} + \ldots\right)} \quad \boldsymbol{(3.3)}$$

Using the rules of summation of an infinite geometric series (with common ratio: |r|<1) from Equation 3.3, we re-write (3.3) as (3.4).

$$C(s) = \left[\frac{1}{s} + \frac{2}{s}\left(\frac{e^{-2sT}e^{\delta s}}{1 - e^{-2sT}e^{2\delta s}}\right)\right] - \frac{2}{s}\left[\frac{e^{-sT}}{1 - e^{-2sT}e^{2\delta s}}\right]$$

$$= \frac{1}{s} + \frac{2}{s}\left(\frac{e^{-2sT}e^{\delta s} - e^{-sT}}{1 - e^{-2sT}e^{2\delta s}}\right)$$

$$= \frac{1}{s} + \frac{2}{s}\frac{(e^{-sT})(e^{-sT}e^{\delta s} - 1)}{(e^{-sT})(e^{sT} - e^{-sT}e^{2\delta s})}$$

$$= \boldsymbol{\frac{1}{s} + \frac{2}{s}\frac{e^{-s(T-\delta)} - 1}{e^{sT}(1 - e^{-2(sT-\delta s)})}} \quad \boldsymbol{(3.4)}$$

Approximating e^{sT} by $1 + sT$ in (3.4), we obtain (3.5).

$$C(s) = \frac{1 - s(T-\delta) - 1}{e^{sT}(1 - (1 + 2(sT - \delta s))}$$

$$= \frac{1}{s} + \frac{2}{s}\frac{(-s(T-\delta))}{(1+sT)(-2)(sT-\delta s)}$$

$$= \boldsymbol{\frac{1}{s}\left[\frac{2+sT}{1+sT}\right]} \qquad \textbf{(3.5)}$$

Taking Laplace Transform of (3.2) we obtain (3.6).

$$\boldsymbol{V(s) = \frac{V_0}{2s} - \frac{3V_0}{4}\frac{e^{-sT}}{s} + \frac{3V_0}{8}\frac{e^{-2sT+\delta s}}{s} - \frac{3V_0}{16}\frac{e^{-3sT+2\delta s}}{s}}$$

$$\boldsymbol{+ \frac{3V_0}{32}\frac{e^{-4sT+3\delta s}}{s} - \ldots + \frac{V_0}{2^n}\frac{e^{-(n-1)sT+(n-2)\delta s}}{s}} \qquad \textbf{(3.6)}$$

Using the rule of infinite geometric series summation with common ratio <1 in (3.6), we obtain (3.7).

$$V(s) = \frac{V_0}{2s} + \frac{3V_0}{8s}\left[\frac{e^{-2sT}e^{\delta s}}{1 - \frac{1}{4}e^{-2sT}e^{2\delta s}}\right] - \frac{3V_0}{4s}e^{-sT}\left[\frac{1}{1 - \frac{1}{4}e^{-2sT}e^{2\delta s}}\right]$$

$$= \frac{V_0}{2s} + \frac{3V_0}{4s}\left(\frac{\frac{1}{2}e^{-2sT}e^{\delta s} - e^{-sT}}{1 - \frac{1}{4}e^{-2sT}e^{2\delta s}}\right)$$

$$= \boldsymbol{\frac{V_0}{2s} + \frac{3V_0}{4s}\frac{\frac{1}{2}e^{-s(T-\delta)} - 1}{e^{sT} - \frac{1}{4}e^{-(T-2\delta)s}}} \qquad \textbf{(3.7)}$$

Approximating e^{sT} by $1 + sT$ in (3.7) we obtain (3.8):

$$V(s) = \frac{V_0}{2s} + \frac{3V_0}{4s}\frac{\frac{1}{2}(1 - sT + \delta s) - 1}{(1 + sT) - \frac{1}{4}(1 - (T - 2\delta)s)}$$

$$= \frac{V_0}{2s} + \frac{3V_0}{8s}\frac{-s(T-\delta) - 1}{\left[\frac{3}{4} + \frac{5}{4}sT - \frac{1}{2}\delta s\right]}$$

$$= \frac{V_0}{2s} - \frac{V_0}{2s}\left[\frac{1 + 2s(T-\delta)}{1 + \frac{s}{3}(5T - 2\delta)}\right]$$

$$= \frac{\boldsymbol{V_0}}{\boldsymbol{2s}} \frac{\boldsymbol{s(4\delta - T)}}{\boldsymbol{(5T - 2\delta)s + 3}} \quad \textbf{(3.8)}$$

Theoretically,δmay take any real value in (0, T). For the sake of simplicity in analysis, let us assume $\delta = \frac{T}{2}$. Substituting $\delta = \frac{T}{2}$ in (3.8), we obtain (3.9).

$$V(s) = \frac{V_0}{2s} \frac{Ts}{4Ts + 3}$$

$$= \frac{\boldsymbol{V_0}}{\boldsymbol{2}} \frac{\boldsymbol{T}}{\boldsymbol{(3 + 4Ts)}} \quad \textbf{(3.9)}$$

Expression (3.5) and (3.9) involve only one model parameter T, which is any positive real number. Choosing T=1 in (3.5) and (3.9), we obtain (3.10) and (3.11) respectively.

$$\boldsymbol{C(s) = \frac{1}{s} \frac{(2+s)}{(1+s)}} \quad \textbf{(3.10)}$$

$$\boldsymbol{V(S) = \frac{V_0}{2} \frac{1}{(4s+3)}} \quad \textbf{(3.11)}$$

The transfer function of the brain-actuated controller based on the input-output shown in Figure 3.3 is obtained as

$$\boldsymbol{G_c(s) = \frac{V(s)}{C(s)} = \frac{\frac{V_0}{2} \frac{1}{(4s+3)}}{\frac{1}{s} \frac{(2+s)}{(1+s)}}}$$

$$= \frac{\boldsymbol{V_0}}{\boldsymbol{2}} \frac{\boldsymbol{s(1+s)}}{\boldsymbol{(s+2)(4s+3)}} \quad \textbf{(3.12)}$$

With proper choice K, T_S, $T_S^{/}$ and K_t in for practical motor and tacho-generator and also setting controller gain $K^{/}$ =1 in the inner loop for simplicity, we have the closed-loop gain for the inner loop as $G_{inner}(s)$.

$$\boldsymbol{G_{inner}(s) = \frac{16.13}{(s+0.054)(s+5.4)(s+55.44)}} \quad \textbf{(3.13)}$$

The loop gain of the overall system now is obtained as $G(s) = G_c(s).\ G_{inner}(s)$.

$$\boldsymbol{G(s) = V_0 \frac{2.016(s+1)}{(s+0.054)(s+0.75)(s+2)(s+5.4)(s+55.44)}} \quad \textbf{(3.14)}$$

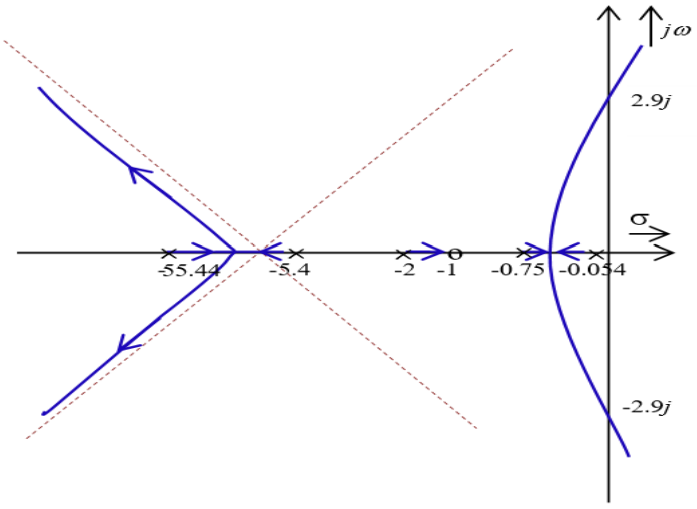


Figure 3.3: Root Locus plot of the proposed model

3.2 Matlab Simulink

Step (1):- Open Simulink Library

Step (2):- In search panel enter Transfer Function and select Transfer Function with initial inputs option.

Step (3):- Enter the Coefficients of the transfer function according to the degree of equation.

Here, the transfer function of a system is $\frac{s^2+s}{4s^2+11s+6}$

Then the numerator coefficients will be [1 1 0] and denominator coefficients will be [4 11 6] for the above transfer function.

Step (4):- Choose Transfer function as defined in Step (3) for motor and integrator.

Step (5):- From search panel select 'Sum' which would represent summer for the system.

Step (6):- From search panel select 'Gain' and put Gain=1 and place it in the feedback path.

Step (7):- From search panel go to 'Source' and select 'Step' and place it as an input to the system.

Step (8):- From search panel go to 'Sink' and select 'Scope' to analyse the output response.

Step (9):- Connect all the blocks as shown in the Simulink.

Step (10):- Click on run.

Step (11):- Double click on the scope to see the response.

3.3 Simulink Model

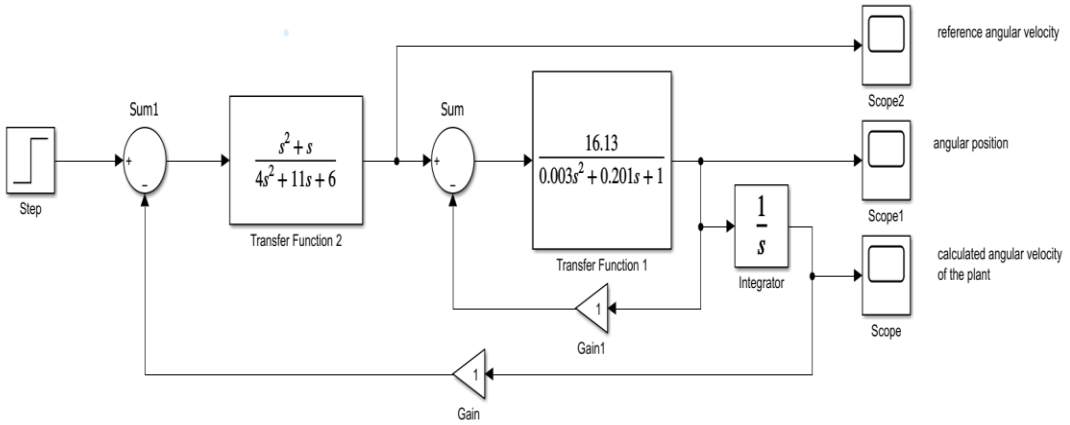


Figure 3.4: Simulink Model

Step Parameters

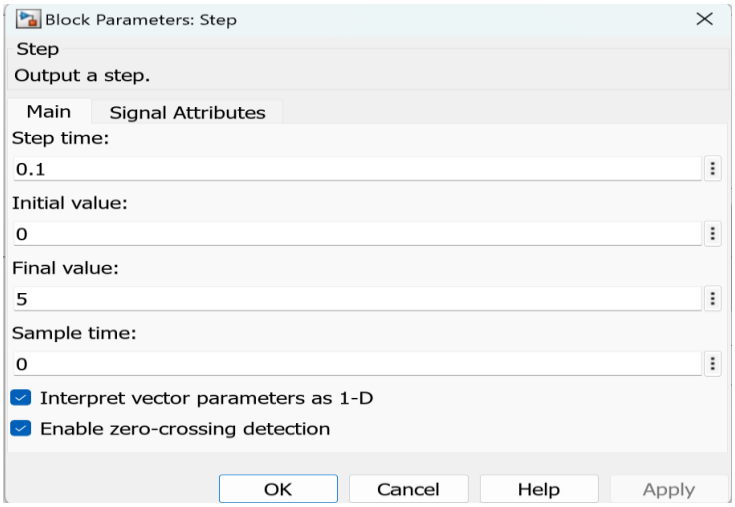


Figure 3.5: Step Parameters

3.4 Output Plots

A. Scope2:

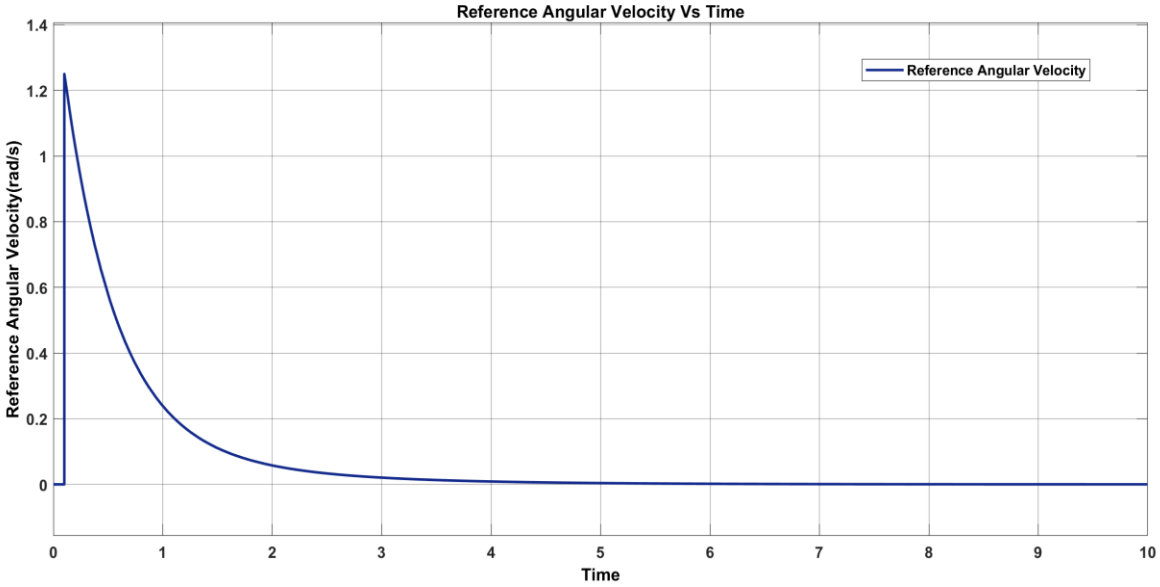


Figure 3.6: Reference Angular Velocity Vs Time

B. Scope1:

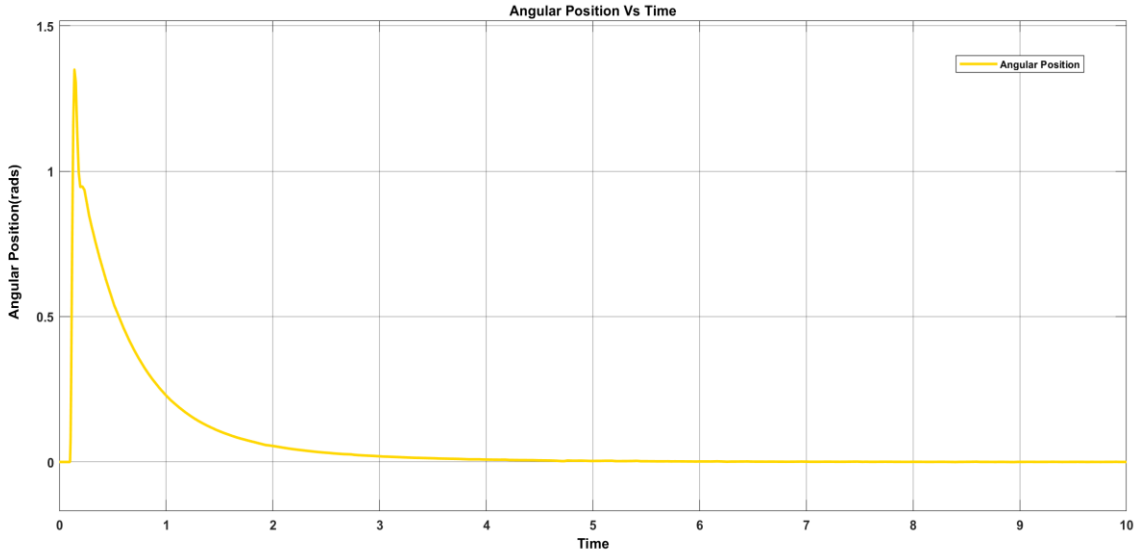


Figure 3.7: Angular Position Vs Time

C. Scope:

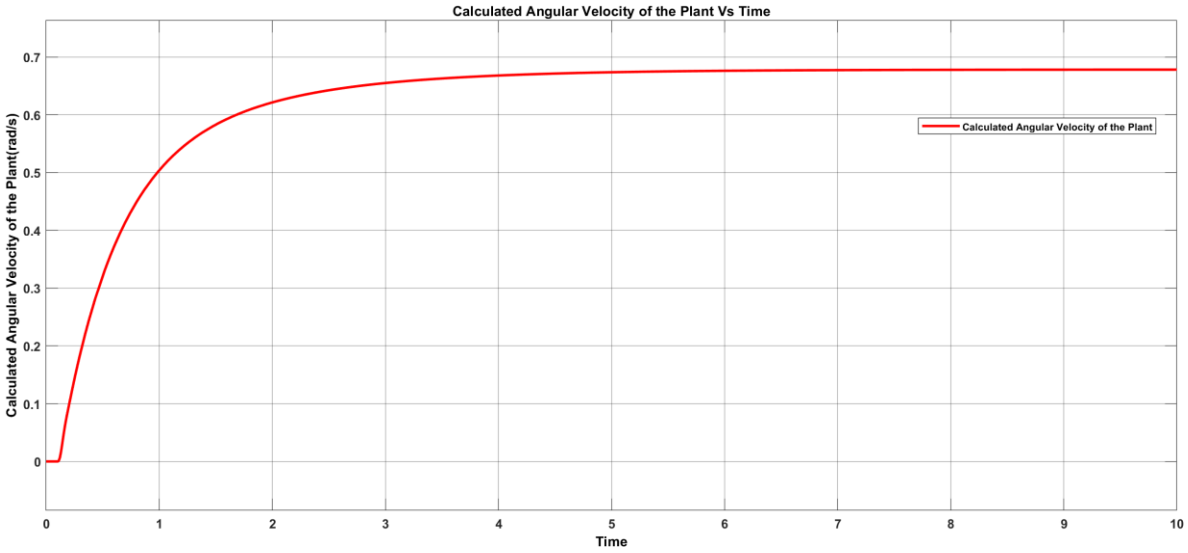


Figure 3.8: Calculated Angular Velocity Vs Time

CHAPTER 4

CONCLUSION & FUTURE SCOPE

The main motivation of the present work is developing a new technique for 2-loop BCI-based position control system has been proposed, where the inner loop takes care of speed control and the outer loop takes care of position control. The subject utilizes motor imagery brain signal to drive the robotic limb-motor at a fixed speed until he finds the limb crossing the desired target position. The subject releases an ErrP brain signal, when the robotic limb crosses the target position first time. The brain-computer interface system recognizes the target position by identifying the location on the trajectory of the robot arm, at the instance when ErrP is released by the subject. The position of the robot arm at the said instance corresponds to zero-crossing in positional error. Depending on reaction-time of the subject in releasing ErrP, the positional offset-error usually has a non-zero (variable) magnitude, which needs corrections by the subsequent mode of automatic control. The important contribution of the work is brain-actuated controller design and stability analysis of the overall system using root locus technique. It is apparent from the root locus plot that the system is stable with large stability margin (DC gain =4.03) for a proper upper bound on initial velocity= 2 units. The merit of the proposed scheme lies in reduced cognitive load of the subject as he is set free after releasing the ErrP at the first zero-crossing of positional error.

4.1 Future Directions and Innovations

Brain-Computer Interface (BCI) technology is a rapidly evolving field with significant potential across various domains. The future scope of BCI research can be broadly categorized into several key areas:-

1. **Improvement in Signal Acquisition and Processing:-**

- **Non-invasive Techniques:-** Enhancing the resolution and reliability of non-invasive methods like EEG, MEG, and fNIRS.
- **Invasive Techniques:-** Developing safer and more effective invasive methods like ECoG and intracortical recording.
- **Signal Processing Algorithms:-** Advancing machine learning and AI techniques for more accurate and efficient signal decoding.

2. **Neuroprosthetics and Rehabilitation:-**

- **Prosthetic Control:-** Improving the control of prosthetic limbs through more intuitive and responsive interfaces.
- **Motor Rehabilitation:-** Developing BCIs for aiding recovery in stroke and spinal cord injury patients.
- **Sensory Feedback:-** Integrating sensory feedback mechanisms to provide users with a more natural experience.

3. **Hybrid BCIs:-**

- Combining different signal acquisition methods (e.g., EEG and fNIRS) to enhance the accuracy and reliability of BCIs.
- Integration with other technologies such as eye-tracking and EMG to create more versatile and robust systems.

4. **AI and Machine Learning:-**

- Leveraging advanced algorithms to improve signal processing, pattern recognition, and adaptive control in BCIs.
- Enhancing user experience by making BCIs more intuitive and reducing training time.

5. **Wearable and Portable BCIs:-**

- Development of compact, user-friendly BCI devices that can be easily worn and used in everyday environments.
- Potential applications in consumer electronics, gaming, and smart home controls.

6. **Neurofeedback and Cognitive Enhancement:-**

- Using BCIs for neurofeedback to improve cognitive functions, manage stress, and enhance mental performance.
- Potential applications in education, mental health, and professional training.

7. **Improved Neural Interfaces:-**

- **Invasive Interfaces:-** Innovating more biocompatible and durable invasive interfaces that can provide stable, long-term recordings of neural activity.
- **Non-invasive Interfaces:-** Advancing non-invasive methods to approach the performance of invasive systems while maintaining user comfort and safety.

8. Ethical and Privacy Considerations:-

- Addressing ethical issues related to user consent, data privacy, and long-term effects of BCI usage.
- Developing guidelines and regulations to ensure safe and responsible use of BCI technologies.

The future scope of BCI research is vast and multidisciplinary, with significant potential to revolutionize various aspects of human life. Advancements in this field will likely result in more sophisticated, reliable, and accessible BCI technologies, offering profound benefits in healthcare, communication, entertainment, and beyond. Addressing the challenges and ethical considerations associated with BCIs will be crucial for the responsible and equitable development of this transformative technology.

BCI-based position control of neuroprosthetic artificial arms is set to witness significant advancements that will make these devices more accurate, intuitive, and accessible. The integration of advanced signal processing, adaptive algorithms, sensory feedback, and wearable technology will play crucial roles in enhancing the functionality and user experience of neuroprosthetic arms. As research progresses, interdisciplinary collaboration and careful consideration of ethical and regulatory issues will be vital in bringing these innovations to those who need them.

REFERENCES

[1] Eric R Kandel, James H Schwartz, Thomas M Jessell, Steven Siegelbaum, A James Hudspeth, Sarah Mack, et al. *Principles of neural science*, volume 4. McGraw-hill New York, 2000.

[2] Endel Tulving and Fergus 1M Craik. *The Oxford handbook of memory*. Oxford University Press, 2000.

[3] Michael A Arbib. *The handbook of brain theory and neural networks*. MIT press, 2003.

[4] Bernhard Obermaier, Gemot R Muller, and Gert Pfurtscheller. " virtual keyboard" controlled by spontaneous eeg activity. *IEEE Transactions on Neural Systems and Rehabilitation Engineering*, 11(4):422-426,2003.

[5] Reinhold Scherer, GR Muller, Christa Neuper, Bernhard Graimann, and Gert Pfurtscheller. An asynchronously controlled eeg-based virtual keyboard: improvement of the spelling rate. *IEEE Transactions on Biomedical Engineering*, 51(6):979—984, 2004.

[6] Jinyi Long, Yuanqing Li, Hongtao Wang, Tianyou Yu, Jiahui Pan, and Feng Li. A hybrid brain computer interface to control the direction and speed of a simulated or real wheelchair. *IEEE Transactions on Neural Systems and Rehabilitation Engineering*,20(5):720-729, 2012.

[7] Wenchang Zhang, Fuchun Sun, Chunfang Liu, Weihua Su, Chuanqi Tan, and Shaobo Liu. A hybrid eeg-based bci for robot grasp controlling. In 2017 *IEEE International Conference on Systems, Man, and Cybernetics (SMC*), pages 3278—3283. IEEE, 2017.

[8] David Marshall, Damien Coyle, Shane Wilson, and Michael Callaghan. Games, gameplay, and bci: the state of the art. *IEEE Transactions on Computational Intelligence and Al in Games*, 5(2):82-99, 2013.

[9] Zhihua Wang, Yang Yu, Ming Xu, Yadong Liu, Erwei Yin, and Zongtan Zhou. Towards a hybrid bci gaming paradigm based on motor imagery and ssvep. *International Journal of Human—Computer Interaction*, 35(3): 197—205, 2019.

[10] Gert Pfurtscheller, Christa Neuper, Christoph Guger, WAHW, Alois Schlogl, BAOB
Obermaier, and MAPM Pregenzer. Current trends in graz brain computer interface (bci) research. *IEEE transactions on rehabilitation engineering*, 8(2):216-219,2000.

[11] Piotr Stawicki. Felix Gcnlbler. and Ivan Volosyak. Driving a semiautonomous mobile robotic car controlled by an ssvcp-bascd bci. *Computational intelligence and neuroscience*,2016,2016

[12] Wendi song, Xiangzhou Wang, shuhua zhcng, and Yingzi Lin. Mobile robot by bci based on motor imagery., In *2014 Sixth International Conference on Intelligent Human Machine Systems and Cybernetics IEEE, Sixth*, volume 2, pages 383-387, IEEE,2014.

[13] Christoph Kapcllcr, Christoph Hintcrmüllcr, Mohammad Abu-Alqumsan, Robert Prückl, Angelika Peer, and Christoph Guger. A bci using vep for continuous control of a mobile robot. In 2013 *35th Annual International Conference of the IEEE Engineering in Medicine and Biology society (EMBC)*, pages 5254-5257. IEEE, 2013.

[14] Cong Wang, Bin Xia, Jie Li, Wenlu Yang, Alejandro Cardona Velez, Hong Yang, al. Motor imagery bci-based robot arm system. In 2011 *Seventh International Conference on Natural Computation*, volume 1, pages 181—184. IEEE, 2011.

[15] William J Gehring, Yanni Liu, Joseph M Orr, and Joshua Carp. The error-related negativity (ern/ne). *Oxford handbook of event-related potential components*, pages 231—291, 2012.

[16] Akshay Kumar, Lin Gao, Elena Pirogova, and Qiang Fang. A review of error-related potential-based brain-computer interfaces for motor impaired people. *IEEE Access*, 7: 142451-142466, 2019.

[17] Markus Ullsperger, Adrian G Fischer, Roland Nigbur, and Tanja Endrass. Neural mechanisms and temporal dynamics of performance monitoring. *Trends in cognitive sciences*, 18(5):259-267, 2014.

[18] E Donchin. Is the p300 component a measure of context updating? behavioural and brain science. *Science*, 11:357—374, 1988.

[19] C. Alain, H. E. McNeely, Y. He, B. K. Christensen, and R. West, "*Neurophysiological evidence of error-monitoring deficits in patients with schizophrenia*," Cereb. Cortex, vol. 12, no. 8, pp. 840–846, Aug. 2002.

[20] J. G. Kerns, J. D. Cohen, A. W. McDonald III, M. K. Johnson, V. A. Stenger, H. Aizenstein, and C. S. Carter, "*Decreased conflict-and error related activity in the anterior cingulate cortex in subjects with schizophrenia*," Am. J. Psychiatry, vol. 162, no. 10, pp. 1833–1839, Oct. 2005.

[21] Jing Wei Tan and Yimesker Yihun. Application of forearm fmg signals in closed loop modality-matched sensory feedback stimulation. *Journal of Bionic Engineering* 908, 2020.

[22] Kotaro Nishikawa, Masayuki Shakutsui, Kcntaro Hirata, and Masahiro Takaiwa. Development of pneumatic bellows myoelectric hand with tactile feedback. *IEEEJ Transactions on Electronics, Information and Systems*, 137(1):127-135,2017.

[23] Sharlene N Flesher, Jennifer L Coflinger, Stephen T Foides, Jeffrey M Weiss, John E Downey, Elizabeth C Tyler-Kabara, Sliman J Bensmaia, Andrew B Schwartz, Michael L Boninger, and Robert A Gaunt. Intracortical microstimulation of human somatosensory cortex. *Science translational medicine*, ^{8}(361):361ra141-361ra141, 2016.

[24] Edoardo D'Anna, Giacomo Valle, Alberto Mazzoni, lvo Strauss, Francesco Iberite, Jeremy Patton, Francesco M Petrini, Stanisa Raspopovic, Giuseppe Granata, Riccardo Di Iorio, et al. A closed-loop hand prosthesis with simultaneous intraneural tactile and position feedback. *Science Robotics*, 4(27):eaau8892, 2019.

[25] Anwesha Khasnobish, Monalisa Pal, Dwaipayan Sardar, DN Tibarewala, and Amit Konar. Vibrotactile feedback for conveying object shape information as perceived by artificial sensing of robotic arm. *Cognitive neurodynamics*, 10:327-338, 2016.

[26] Henri J Nussbaumer and Henri J Nussbaumer. *The fast Fourier transform*. Springer, 1981.

[27] Shaima Miqdad Mohamed Najeeb, Haider Th Salim Al Rikabi, and Shaima Mohammed Ali. Finding the discriminative frequencies of motor electroencephalography signal using genetic algorithm. *TELKOMN1KA (Telecommunication Computing Electronics and Control)*, 19(1):285-292, 2021

[28] Richard Wesley Hamming. *Digital filters*. Courier Corporation, 1998.

[29] Louis Litwin. Fir and iir digital filters. *IEEE potentials*, 19(4):28-31, 2000.

[30] Christos Stergiadis, Vasiliki-Despoina Kostaridou, and Manousos A Klados. Which bss method separates better the eeg signals? a comparison of five different algorithms. *Biomedical Signal Processing and Control*, 72:103292, 2022

[31] Filipa Campos Viola, Stefan Debener, Jeremy Thorne, and Till R Schneider. Using ica for the analysis of multi-channel eeg data. *Simultaneous EEG andfMRI: Recording, Analysis, andApplication: Recording, Analysis, andApplication*, pages 121—133, 2010.

[32] Xinyang Yu, Pharino Chum, and Kwee-Bo Sim. Analysis the effect of pca for feature reduction in non-stationary eeg based motor imagery of bci system. Optik, 125(3): 1498— 1502, 2014.

[33] Dennis J McFarland, Lynn M McCane, Stephen V David, and Jonathan R Wolpaw. Spatial filter selection for eeg-based communication. Electroencephalography and clinical Neurophysiology, 103(3):386—394, 1997.

[34] Carmen VidaulTC, A Schlogl, Rafael Cabcza, Reinhold Scherer, and Gert Pfurtscheller. A fully on-line adaptive bci. *IEEE Transactions on biomedical engineering*, 53(6),1214,1219, 2006.

[35] Imali Thanuja Hettiarachchi, Thanh Thi Nguyen, and Saeid Nahavandi. Motor imagery data classification for bci application using wavelet packet feature extraction. *In Neural Information Processing: 21st International Conference, ICONIP 2014*, Kuching, Malaysia, November 3-6, 2014. Proceedings, Part Ill 21, pages 519—526. Springer, 2014.

[36] Zhonglin Lin, Changshui Zhang, Wei Wu, and Xiaorong Gao. Frequency recognition based on canonical correlation analysis for ssvep-based bcis. *IEEE transactions on biomedical engineering*, 53(12):2610—2614, 2006.

[37] Fabien Lotte and Cuntai Guan. Regularizing common spatial patterns to improve bci designs: unified theory and new algorithms. *IEEE Transactions on biomedical Engineering*, 2010.

[38] Varun Bajaj and Ram Bilas Pachori. Classification of seizure and nonseizure eeg signals using empirical mode decomposition. *IEEE Transactions on Information Technology in Biomedicine*, 2011.

[39] Fabien Lotte. A tutorial on eeg signal-processing techniques for mental-state recognition in brain—computer interfaces. *Guide to brain-computer music interfacing*, pages 133-161, 2014.

[40] Abdel-Ouahab Boudraa and Jean-Christophe Cexus. Emd-based signal filtering. *IEEE transactions on instrumentation and measurement*, 2007.

[41] Bruce Thompson. Canonical correlation analysis. 2000.

[42] Nanying Liang and Laurent Bougrain. Decoding finger flexion from band-specified eeg signals in humans. *Frontiers in neuroscience*, 6.91, 2012.

[43] Julio Ortega, Javier Asensio-Cubero, John Q Gan, and Andrés Ortiz. Classification motor imagery tasks for bci with multiresolution analysis and multiobjective feature selection. *BioMedical Engineering OnLine,* 15.149-164, 2016

[44] Rifai Chai, Yvonne Iran, Ganesh R Naik, Tuan N Nguyen, Sai Ho Li ng, Ashley Crai g, and Hung T Nguyen. Classification of ecg based-mental fatigue using principal component analysis and bayesian neural network. In *2016 38th Annual International Conference of the IEEE Engineering in Medicine and Biology Society (EMBC)* pages 4654-4657. IEEE, 2016.

[45] Dong Kang and Luo Zhizeng. A method of denoising multi-channel *eeg* signals fast based on pca and debss algorithm. In *2012 International Conference on Computer Science and Electronics Engineering,* volume 3, pages 322-326. IEEE, 2012.

[46] Kai Keng Ang, Zheng Yang Chin, Chuanchu Wang, Cuntai Guan, and Haihong Zhang. Filter bank common spatial pattern algorithm on bci competition iv datasets 2a and 2b. *Frontiers in neuroscience,* 6:39, 2012.

[47] Mikito Ogino and Yasue Mitsukura. Portable drowsiness detection through use of a prefrontal single-channel electroencephalogram. *Sensors,* 18(12):4477, 2018.

[48] Adham Atyabi, Martin H Luerssen, and David MW Powers. Pso-based dimension reduction of eeg recordings: implications for subject transfer in bci. *Neurocomputing,* 119:319-331, 2013.

[49] Alberto Ortega, Juan Jose Escobar, Julio Ortega, Jestis Gonzalez, Alfredo Alcayde, Jorge Munilla, and Miguel Damas. Performance study of ant colony optimization for feature selection *in eeg* classification. *In International Conference on Bioengineering and Biomedical Signal and Image Processing,* pages 323-336. Springer, 2021.

[50] Christian Mal, Camille Jeunet, and Fabien Lotte. Eeg-based workload estimation across affective contexts. *Frontiers in neuroscience,* 8:114, 2014.

[51] Kenji Kira and Larry A Rendell. A practical approach to feature selection. In *Machine learning proceedings 1992,* pages 249-256. Elsevier, 1992.

[52] Saugat Bhattacharyya, Anwesha Khasnobish, Sornsirsa Chatterjee, Amit Konar, and DN Tibarewala. Performance analysis of Ida, qda and knn algorithms in left-right limb movement classification from eeg data. *In 2010 International conference on systems in medicine and biology,* pages 126-131. IEEE, 2010.

[53] Abdulhamit Subasi and M Ismail Gursoy. Eeg signal classification using pca, ica, Ida and support vector machines. *Expert systems with applications,* 37(12):8659-8666,2010.

[54] Suresh Balakrishnama and Aravind Ganapathiraju. *Linear discriminant analysis-a brief tutorial. Institute for Signal and information Processing,* 18(1998): 1—8, 1998.

[55] Alaa Tharwat. Linear vs. quadratic discriminant analysis classifier: a tutorial. *International Pattern Recognition*, 3(2): 145-180, 2016.

[56] Obed Carrera-Leon. Juan Manuel Raniircz, Vicen(c Alarcon-Aquino, Mary Baker, David D'Cmz-Baron, and Pilar Gonocz-GiI. A motor imagery workshop on wavelet analysis and spatial patterns fcature extraction. *In 2012 workshop on engineering applications*. pages 1-6. IEEE, 2012.

[57] Chivalai Temiyasathit et al. Increase performance of four-class classification for motor. imagery based brain-computer interface. In *2014 International Conference on Computer, Information and Telecommunication Systems (CITS)*, pages 1—5. IEEE, 2014

[58] Irina Rish et al. An empirical study of the naive bayes classifier. In IJCAI 2001 *workshop on empirical methods in artificial intelligence*, volume 3, pages 41—46, 2001.

[59] Hua Wang, Yanchun Zhang, et al. Detection of motor imagery eeg signals employing naive bayes based learning process. *Measurement*, 86: 148—158, 2016.

[60] Arnab Rakshit, Anwesha Khasnobish, and DN Tibarewala. A naive bayesian approach to lower limb classification from eeg signals. In 2016 2nd International Conference on Control, Instrumentation, Energy & Communication (CIEC), pages 140—144. IEEE, 2016.

[61] MNAH Sha'Abani, N Fuad, Norezmi Jamal, and MF Ismail. knn and svm classification for eeg: a review. In In ECCE2019: *Proceedings of the 5th International Conference on Electrical, Control & Computer Engineering, Kuantan, Pahang, Malaysia, 29th July 2019*, pages 555—565. Springer, 2020.

[62] Christopher M Bishop and Nasser M Nasrabadi. *Pattern recognition and machine learning*, volume 4. Springer, 2006.

[63] Mervyn VM Yeo, Xiaoping Li, Kaiquan Shen, and Einar PV Wilder-Smith. Can svm be used for automatic eeg detection of drowsiness during car driving? *Safety Science*, :115–1242009.

[64] Mohammad-Parsa Hosseini, Amin Hosseini, and Kiarash Ahi. A review on machine learning for eeg signal processing in bioengineering. *IEEE reviews in biomedical engineering*, 14:204—218, 2020.

[65] LR F cavrini, L Sbernini, F Riillo, L Bianchi, S Seri, and G saggio. support vector machines to detect physiological patterns for eeg and emg-based human—computer interaction: a review. *Journal of neural engineering*, 14(1):011001, 2017.

[66] Ashkan Yazdani, Touradj Ebrahimi, and Ulrich Hoffmann. Classification of eeg using dempster Shafer theory and a k-nearest neighbor classifier. In 2009 *4th Internationals IEEE/EMBS Conference on Neural Engineering*, pages 327-330. IEEE, 2009

[62] M Serdar Bascil, Ahmet Y Tesneli, and Feyzullah Temurtas. Spectral feature extraction of eeg signals and pattern recognition during mental tasks of 2-d cursor movements for bci using svm and ann. *Australasian physical & engineering sciences in medicine*, 39:665.

[63] Advait Balaji, Aparajita Haldar, Keshav Patil, T Sai Ruthvik, CA Valliappan, Mayur Jartarkar, and Veeky Baths. Eeg-based classification of bilingual unspoken speech using ann. In 2017 *39th Annual International Conference of the IEEE Engineering in Medicine and Biology society (EMBC)*, pages 1022-1025. IEEE, 2017.

[64] Fabien Lotte, Laurent Bougrain, Andrzej Cichocki, Maureen Clerc, Marco Congedo, Alain Rakotomamonjy, and Florian Yger. A review of classification algorithms for eeg-based brain—computer interfaces: a 10 year update. *Journal of neural engineering*, 2018.

[65] SJ Pan and Q Yang. A survey on transfer learning. *IEEE transaction on knowledge discovery and data engineering*, 22 (10), 2010.

[66] Si Si, Dacheng Tao, and Bo Geng. Bregman divergence-based regularization for transfer subspace learning. IEEE Transactions on Knowledge and Data Engineering, 22(7):929— 942, 2009.

[67] Mingsheng Long, Jianmin Wang, Guiguang Ding, Jiaguang Sun, and Philip S Yu. Transfer feature learning with joint distribution adaptation. In Proceedings of the *IEEE international conference on computer vision*, pages 2200—2207, 2013.

[68] Guangquan Liu, Dingguo Zhang, Jianjun Meng, Gan Huang, and Xiangyang Zhu. Unsupervised adaptation of electroencephalogram signal processing based on fuzzy c-means algorithm. *International Journal of Adaptive Control and Signal Processing*, 26(6):482— 495, 2012.

[69] Alois Schlögl, Carmen Vidaurre, and Klaus-Robert Müller. Adaptive methods in bci research-an introductory tutorial. *In Brain-Computer Interfaces: Revolutionizing Human Computer Interaction*, pages 331—355. Springer, 2010.

[70] Ji Won Yoon, Stephen J Roberts, Matt Dyson, and John Q Gan. Adaptive classification for brain computer interface systems using sequential monte carlo sampling. *Neural Networks*, 22(9): 1286-1294, 2009.

[71] Julie Blumberg, Jorn Rickert, Stephan Waldert, Andreas Schulze-Bonhage, Ad Aertsen, and Carsten Mehring. Adaptive classification for brain computer interfaces. In 2007 29th

Annual International Conference of the IEEE Engineering in Medicine and Biology Society, pages 2536-2539. IEEE

[72] Alberto Liera, Vicenq CJ6mez, and Hilbert J Kappen. Adaptive multiclass classification for brain computer interfaces. *Neural computation*, 2014.

[73] Fabien Lotte. Signal processing approaches to minimize or suppress calibration time in oscillatory activity-based brain-computer interfaces. *Proceedings of the IEEE*, 2015.

[74] Carmen Vidaurre, A Schlogl, Rafael Cabeza, Reinhold Scherer, and Gert Pfurtscheller. Study of on-line adaptive discriminant analysis for eeg-based brain computer interfaces. *IEEE transactions on biomedical engineering*, 54(3):550—556, 2007.

[75] Mehrnaz Kh Hazrati and Abbas Erfanian. An online eeg-based brain—computer interface for controlling hand grasp using an adaptive probabilistic neural network. *Medical engineering & physics*, 2010.

[76] DR Lowne, Stephen J Roberts, and Roman Garnett. Sequential non-stationary dynamic classification with sparse feedback. *Pattern Recognition*, 43(3):897—905, 2010.

[77] Fatih Özyurt, Türker Tuncer, Engin Avci, Mustafa Koc, and lhsan Serhatlioélu. A novel liver image classification method using perceptual hash-based convolutional neural network. *Arabian Journal for Science and Engineering*, 44:3173—3182, 2019.

[78] Yann LeCun, Bernhard Boser, John S Denker, Donnie Henderson, Richard E Howard, Wayne Hubbard, and Lawrence D Jackel. Backpropagation applied to handwritten zip code recognition. *Neural computation*, 1(4):541—551, 1989.

[79] Xavier Glorot, Antoine Bordes, and Yoshua Bengio. Deep sparse rectifier neural networks. *In Proceedings of the fourteenth international conference on artificial intelligence and statistics*, pages 3 15-323. JMLR Workshop and Conference Proceedings, 2011

[80] David E Rumelhart, Geoffrey E Hinton, and Ronald J Williams. *Learning by back-propagating errors. nature*, 323(6088):533—536, 1986.

[81] Muhammad Tariq sadiq, Muhammad Zulkifal Aziz, Ahmad Almogren, Adnan Yc Siuly Siuly, and Ateeq Ur Rehman. Exploiting pretrained cnn models for the develop:' of an eeg-based robust bci framework. *Computers in Biology and Medicine*, 143: I

[82] Ran Manor and Amir B Geva. Convolutional neural network for multi-category rapid serial visual presentation bci. *Frontiers in computational neuroscience*, 9: 146, 2015.

[83] No-Sang Kwak, Klaus-Robert Müller, and Scong-Whan Lee. A convolutionaJ neural network for steady state visual evoked potential classification under ambulatory environment. *PloS one*, 72578, 2017.

[84] Yousef Rezaei Tabar and Ugur Halici. A novel deep learning approach for classification of eeg motor imagery signals. Journal of neural engineering, 6003, 2016.

[85] Robin Tibor Schirrmeister, Jost Tobias Springenberg, Lukas Dominique Josef Fiederer, Martin Glasstetter, Katharina Eggensperger, Michael Tangermann, Frank Hutter, Wolfram Burgard, and Tonio Ball. Deep learning with convolutional neural networks for eeg decoding and visualization. *Human brain mapping*, 2017.

[86] Vernon J Lawhern, Amelia J Solon, Nicholas R Waytowich, Stephen M Gordon, Chou P Hung, and Brent J Lance. Eegnet: a compact convolutional neural network for eeg-based brain—computer interfaces. *Journal of neural engineering*, 15(5):056013, 2018.

[87] Xilin Liu, Milin Zhang, Andrew G Richardson, Timothy H Lucas, and Jan Van der Spiegel. Design of a closed-loop, bidirectional brain machine interface system with energy efficient neural feature extraction and pid control. IEEE transactions on biomedical circuits and systems, 1 1(4):729—742, 2016.

[88] Carmen Vidaurre, Christian Klauer, Thomas Schauer, Ander Ramos-Murguialday, and Klaus-Robert Müller. Eeg-based bci for the linear control of an upper-limb neuroprosthesis. Medical engineering & physics, 38(11): 1195—1204, 2016.

[89] Kristin M Quick, Jeffrey M Weiss, Francesco Clemente, Robert A Gaunt, and Jennifer L Collinger. Intracortical micro stimulation feedback improves grasp force accuracy in a human using a brain-computer interface. In 2020 42nd Annual International Conference of the IEEE Engineering in Medicine & Biology society (EMBC), pages 3355-3358. IEEE, 2020.

[90] Ramin Pashaie, Ryan Baumgartner, Thomas J Richner, Sarah K Brodnick, Mehdi Azimipour, Kevin W Eliceiri, and Justin C Williams. Closed-loop optogenetic brain interface. IEEE Transactions on Biomedical Engineering, 2015.

[91] Zhichuan Tang, Lingtao Zhang, Xin Chen, Jichen Ying, Xinyang Wang, and Hang Wang. Wearable supernumerary robotic limb system using a hybrid control approach based on motor imagery and object detection. IEEE Transactions on Neural Systems and Rehabilitation Engineering, 30: 1298—1 3()9, 2022.

[92] Yang xu, Cheng Ding, Xiaokang Shu, Kai Gui, Yulia Bezsudnova, Xinjun Sheng, and Dingguo Zhang. Shared control of a robotic arm using non-invasive brain-computer interface and computer vision guidance. Robotics and Autonomous Systems, 129, 2019.

[93] Feng man, Dongxue Lin, wenyu Li, and Zhao Zhang. Design of a multimodal eeg-based hybrid bci system with visual servo module. IEEE Transactions on Autonomous Mental Development, 2015.

[94] Ross Girshick, Jeff Donahue, Trevor Darrell, and Jitendra Malik. Rich feature hierarchies for accurate object detection and semantic segmentation. In Proceedings of the IEEE conference on computer vision and pattern recognition, pages 580—587, 2014.

[95] Ross Girshick. Fast r-cnn. In Proceedings of the IEEE International Conference on Computer Vision, 2015.

[96] Shaoqing Ren, Kaiming He, Ross Girshick, and Jian Sun. Faster r-cnn: Towards realtime object detection with region proposal networks. In Advances in neural information processing systems, 2015.

[97] Kaiming He, Xiangyu Zhang, Shaoqing Ren, and Jian Sun. Deep residual learning for image recognition. In Proceedings of the IEEE conference on computer vision and pattern recognition, 2016.

[98] Karen Simonyan and Andrew Zisserman. Very deep convolutional networks for largescale image recognition. arXiv preprint arXiv:1409.1556, 2014.

[99] Fujian He, Luzheng Bi, Yun Lu, Hongqi Li, and Ling Wang. Model predictive control for a brain-controlled mobile robot. In 2017 IEEE International Conference on Systems• Man, and Cybernetics (SMC), pages 3184-3188. IEEE, 2017.

[100] Hongguang Pan, Wenyu Mi, Xinyu Lei, and Jun Deng. A closed-loop brain-machine interface framework design for motor rehabilitation, Biomedical Signal Processing and Control, 58: 101877, 2020.

[101] Jianjun Meng, Shuying Zhang, Angeliki Bekyo, Jaron Olsoe, Bryan Baxter, and Bin He. Noninvasive electroencephalogram based control of a robotic arm for reach and grasp tasks. Scientific Reports, 6(1):38565, 2016.

[102] Jianjun Meng, Taylor Streitz, Nicholas Gulachek, Daniel Suma, and Bin He. Threedimensional brain—computer interface control through simultaneous overt spatial attentional and motor imagery tasks. IEEE Transactions on Biomedical Engineering, 2018.

[103] Madiha Tariq, Pavel M Trivailo, and Milan Simic. Eeg-based bci control schemes for lower-limb assistive-robots. Frontiers in human neuroscience, 12:312, 2018.

[104] Yiliang Liu, Wenbin Su, Zhijun Li, Guangming Shi, Xiaoli Chu, Yu Kang, and Weiwei Shang. Motor-imagery-based teleoperation of a dual-arm robot performing manipulation tasks. IEEE Transactions on Cognitive and Developmental Systems, 11(3):414—424, 2018.

[105] Rosario Sorbello, Salvatore Tramonte, Marcello Emanuele Giardina, Vincenzo La Bella, Rossella Spataro, Brendan Allison, Christoph Guger, and Antonio Chella. A human— humanoid interaction through the use of bci for locked-in als patients using neurobiological feedback fusion. IEEE Transactions on Neural Systems and Rehabilitation Engineering.

[106] Paolo Di Lillo, Filippo Arrichiello, Daniele Di Vito, and Gianluca Antonelli. Bcicontrolled assistive manipulator: developed architecture and experimental results. IEEE Transactions on Cognitive and Developmental Systems, 2020.

[107] lason Batzianoulis, Fumiaki Iwane, Shupeng Wei, Carolina Gaspar Pinto Ramos Correia, Ricardo Chavarriaga, José del R Millån, and Aude Billard. Customizing skills for assislive robotic manipulators, an inverse reinforcement learning approach with error-related potentials. Communications biology, 4(1):1—14, 2021.

[108] Bhattacharyya, S., Konar, A., Tibarewala, D. N. (2017, October). Motor imagery and error related potential induced position control of a robotic arm. IEEE/CAA Journal of Automatica Sinica, 4(4).

[109] Pan, H., Song, H., Zhang, Q., & Mi, W. (2022). Review of closed-loop brain-machine interface systems from a control perspective. IEEE Transactions on Human-Machine Systems, 52(5).

[110] Rakshit, A., Konar, A., & Nagar, A. K. (2020, September). A hybrid brain-computer interface for closed-loop position control of a robot arm. IEEE/CAA Journal of Automatica Sinica, 7(5).

[111] Ferrez, P. W., & Millán, J. D. (2008). Simultaneous real-time detection of motor imagery and error related potentials or improved BCI accuracy. In Proceedings of the 4th International Brain-Computer Interface Workshop and Training Course, Graz, Austria, 2008.

[112] Roberson, R., & Farrior, J. S. (Eds.). (2012). Guidance and control. Academic Press.

[113] Takagi, T., & Sugeno, M. (1992). Stability analysis and design of fuzzy control systems. Fuzzy Sets and Systems.

[114] Joh, J., Chen, Y. H., & Langari, R. (1998). On the stability issues of linear Takagi-Sugeno fuzzy models. IEEE Transactions on Fuzzy Systems, 6(3).

[115] Takagi, T., & Sugeno, M. (1985, January). Fuzzy identification to systems and its applications to modeling and control. IEEE Transactions on Systems, Man, and Cybernetics.

[116] Nagrath, I. J., & Gopal, M. (2003). Control systems engineering. Wiley

[117] Ferrez, P. W., & Millán, J. D. R. (2007). EEG-based brain-computer interaction: Improved accuracy by automatic single-trial error detection. In Proceedings of the Advances in Neural Information Processing Systems, Barcelona, Spain, 2007.

[118] Kuo, B. C. (1975). Automatic control systems. Prentice Hall.

[119] Konar, A. (2005). Computational intelligence. Springer.

[120] Sanei, S., & Chambers, J. A. (2007). EEG signal processing.Wiley.

[121] Krishnaveni, V., Jayaraman, S., Aravind, S., Hariharasudhan, V., & Ramadoss, K. (2006, November). Automatic identification and removal of ocular artifacts from EEG using wavelet transform. Measurement Science Review, 6(4).

[122] Zeng, H., Song, A. S., Yan, R. Q., & Qin, H. Y. (2013, November). EOG artifact correction from EEG recording using stationary subspace analysis and empiricalmode decomposition. Sensors, 13(11), 14839–14859. 16. Chakraborty, B., Ghosh, L., & Konar, A. (2020, July). Designing phase-sensitive common spatial pattern filter to improve brain-computer interfacing. IEEE Transactions on Biomedical Engineering, 67(7), 2064–2072. https://doi.org/10.1109/TBME.2019.2954470

[123] Lotte, F. (2012). A new feature and associated optimal spatial filter for EEG signal classification: Waveform Length. In Proceedings of the 21st International Conference on Pattern Recognition (ICPR2012), Tsukuba, Japan, 2012, pp. 1302–1305.

[124] Chakraborty, B., Ghosh, L., Konar, A. (2021, December). Optimal selection of EEG electrodes using interval Type-2 fuzzy-logic-based semi-separating signaling game. IEEE Transactions on Cybernetics, 51(12), 6200–6212. https://doi.org/10.1109/TCYB.2020.2968625

[125] Yger, F., Lotte, F., & Sugiyama, M. (2015). Averaging covariance matrices for EEG signal classification based on the CSP: An empirical study. In 23rd European Signal

Processing Conference (EUSIPCO), Nice, France, 2015, pp. 2721–2725. https://doi.org/10.1109/EUS IPCO.2015.7362879

[126] Lotte, F., & Guan, C. (2011, February). Regularizing common spatial patterns to improve BCI designs: Unified theory and new algorithms. IEEE Transactions on Biomedical Engineering, 58(2), 355–362.

[127] A. Rakshit, A. Konar and A. K. Nagar,"A Hybrid Brain-Computer Interface for Closed-Loop Position Control of a Robot Arm," *IEEE/CAA Journal of Automatica Sinica,* vol.7, no.5,September 2020.

[128] H. Pan, H. Song, Q. Zhang and W. Mi, "Review of Closed-Loop Brain-Machine Interface Systems from a Control Perspective," *IEEE Trans. Human-Machine Systems,* vol. 52, No. 5, 2022.

[129] S. Sanei and J.A Chambers, "EEG Signal Processing, Chichester, UK" *Wiley* 2007.

[130] P.W. Ferrez and J.D Mill`an, "Simultaneous real-time detection of motor imagery and error related potentials or improved BCI accuracy," in Proc. *4th International Brain-Computer Interface Workshop and Training Course,* Graz, Austria, 2008.

[131] P. W. Ferrez and J. D. R. Mill´an, "EEG-based brain-computer interaction: improved accuracy by automatic single-trial error detection," in Proc. *Advances in Neural Information Processing Systems*, Barcelona,Spain, 2007.

[132] V. Krishnaveni, S. Jayaraman, S. Aravind, V. Hariharasudhan, and K.Ramadoss, "Automatic identification and removal of ocular artifactsfrom EEG using wavelet transform," *Measur. Sci. Rev.*, vol. 6, no. 4,Nov. 2006.

[133] H. Zeng, A. S. Song, R. Q. Yan, and H. Y. Qin, "EOG artifact correction from EEG recording using stationary subspace analysis and empiricalmode decomposition," Sensors, vol. 13, no. 11, pp. 14839¡14859, Nov.2013.

[134] B. Chakraborty, L. Ghosh and A. Konar, "Designing Phase-Sensitive Common Spatial Pattern Filter to Improve Brain-Computer Interfacing," in *IEEE Transactions on Biomedical Engineering*, vol. 67, no. 7, pp. 2064-2072, July 2020, doi: 10.1109/TBME.2019.2954470

[135] B. Chakraborty, L. Ghosh and A. Konar, "Optimal Selection of EEG Electrodes Using Interval Type-2 Fuzzy-Logic-Based Semiseparating Signaling Game," in *IEEE Transactions on Cybernetics*, vol. 51, no. 12, pp. 6200-6212, Dec. 2021, doi: 10.1109/TCYB.2020.2968625

[136] F. Yger, F. Lotte and M. Sugiyama, "Averaging covariancematrices for EEG signal classification based on the CSP: An empirical study," *23rd European Signal Processing Conference (EUSIPCO), Nice, France*, 2015, pp. 2721-2725, doi: 10.1109/EUSIPCO.2015.7362879.

[137] F. Lotte and C. Guan, "Regularizing Common Spatial Patterns to Improve BCI Designs: Unified Theory and New Algorithms," in *IEEE Transactions on Biomedical*

Engineering, vol. 58, no. 2, pp. 355-362, Feb. 2011, doi: 10.1109/TBME.2010.2082539.

[138] F. Lotte, "A new feature and associated optimal spatial filter for EEG signal classification: Waveform Length," Proceedings of *the 21st International Conference on Pattern Recognition (ICPR2012)*,Tsukuba, Japan, 2012, pp. 1302-1305.

[139] I. J. Nagrath and M. Gopal, Control Systems Engineering, *Wiley*, 2003.

[140] J. R. Wolpaw and E. W. Wolpaw, Brain-Computer Interfaces: Principles and Practice. Oxford, UK: Oxford University Press, 2012.

[141] J. Zhao, W. Li, and M. F. Li, "Comparative study of SSVEP- and P300 based models for the telepresence control of humanoid robots," PLoS One, vol. 10, no. 11, pp. e0142168, Nov. 2015.

[142] X. Q. Mao, W. Li, C. W. Lei, J. Jin, F. Duan, and S. Chen, "A brain robot interaction system by fusing human and machine intelligence," IEEE Trans. Neural Syst. Rehabil. Eng., vol. 27, no. 3, pp. 533–542, Mar. 2019.

[143] T. Bastos-Filho, A. Floriano, E. Couto, and R. J. M. Godinez-Tello, "Towards a system to command a robotic wheelchair based on independent SSVEP-BCI, " in Smart Wheelchairs and Brain-Computer Interfaces, P. Diez, Ed. London, UK: Academic Press, 2018, pp. 369–379.

[144] A. F. Salazar-Gomez, J. DelPreto, S. Gil, F. H. Guenther, and D. Rus, "Correcting robot mistakes in real time using EEG signals, " in Proc. IEEE Int. Conf. Robotics and Automation, Singapore, 2017, pp. 6570–6577.

[145] A. Lopes, J. Rodrigues, J. Perdigao, G. Pires, and U. Nunes, "A new hybrid motion planner: Applied in a brain-actuated robotic wheelchair," IEEE Robot. Autom. Mag., vol. 23, no. 4, pp. 82–93, Dec. 2016.

[146] F. Arrichiello, P. Di Lillo, D. Di Vito, G. Antonelli, and S. Chiaverini, "Assistive robot operated via P300-based brain computer interface, " in Proc. IEEE Int. Conf. Robotics and Automation, Singapore, 2017, pp. 6032–6037.

[147] S. L. Sheng, P. P. Song, L. Y. Xie, Z. D. Luo, W. N. Chang, S. R. Jiang, H. Y. Yu, C. Zhu, J. T. C. Tan, and F. Duan, "Design of an SSVEP based BCI system with visual servo module for a service robot to execute multiple tasks, " in Proc. IEEE Int. Conf. Robotics and Automation, Singapore, 2017, pp. 2267–2272.

[148] L. M. Alonso-Valerdi, R. A. Salido-Ruiz, and R. A. Ramirez-Mendoza, “Motor imagery based brain-computer interfaces: An emerging technology to rehabilitate motor deficits,” Neuropsychologia, vol. 79, pp. 354–363, Dec. 2015.

[149] S. Bhattacharyya, S. Shimoda, and M. Hayashibe, “A synergetic brain machine interfacing paradigm for multi-DOF robot control,” IEEE Trans. Syst. Man Cybern.: Syst., vol. 46, no. 7, pp. 957–968, Jul. 2016.

[150] S. Bhattacharyya, A. Konar, and D. N. Tibarewala, “Motor imagery and error related potential induced position control of a robotic arm,” IEEE/CAA J. Autom. Sinica, vol. 4, no. 4, pp. 639–650, Sept. 2017.

[151] Y. S. Zhang, P. Xu, T. J. Liu, J. Hu, R. Zhang, and D. Z. Yao, “Multiple frequencies sequential coding for SSVEP-based brain-computer interface,” PLoS One, vol. 7, no. 3, pp. e29519, Mar. 2012.

[152] R. G. Muller-Putz, R. Scherer, C. Brauneis, and G. Pfurtscheller, “Steady-state visual evoked potential (SSVEP)-based communication: Impact of harmonic frequency components,” J. Neural Eng., vol. 2, no. 4, pp. 123–130, Dec. 2005.